



**12th International Workshop on Greenhouse Gas
Measurements from Space (IWGGMS-12)**

June 7 (Tue) - 9 (Thu), 2016, Kyoto University, Kyoto, Japan

East Asia Regional CO₂ Concentrations Observed by GOSAT - Spatial and Seasonal Variations

Ke-Sheng Cheng

Department of Bioenvironmental Systems Engineering

National Taiwan University

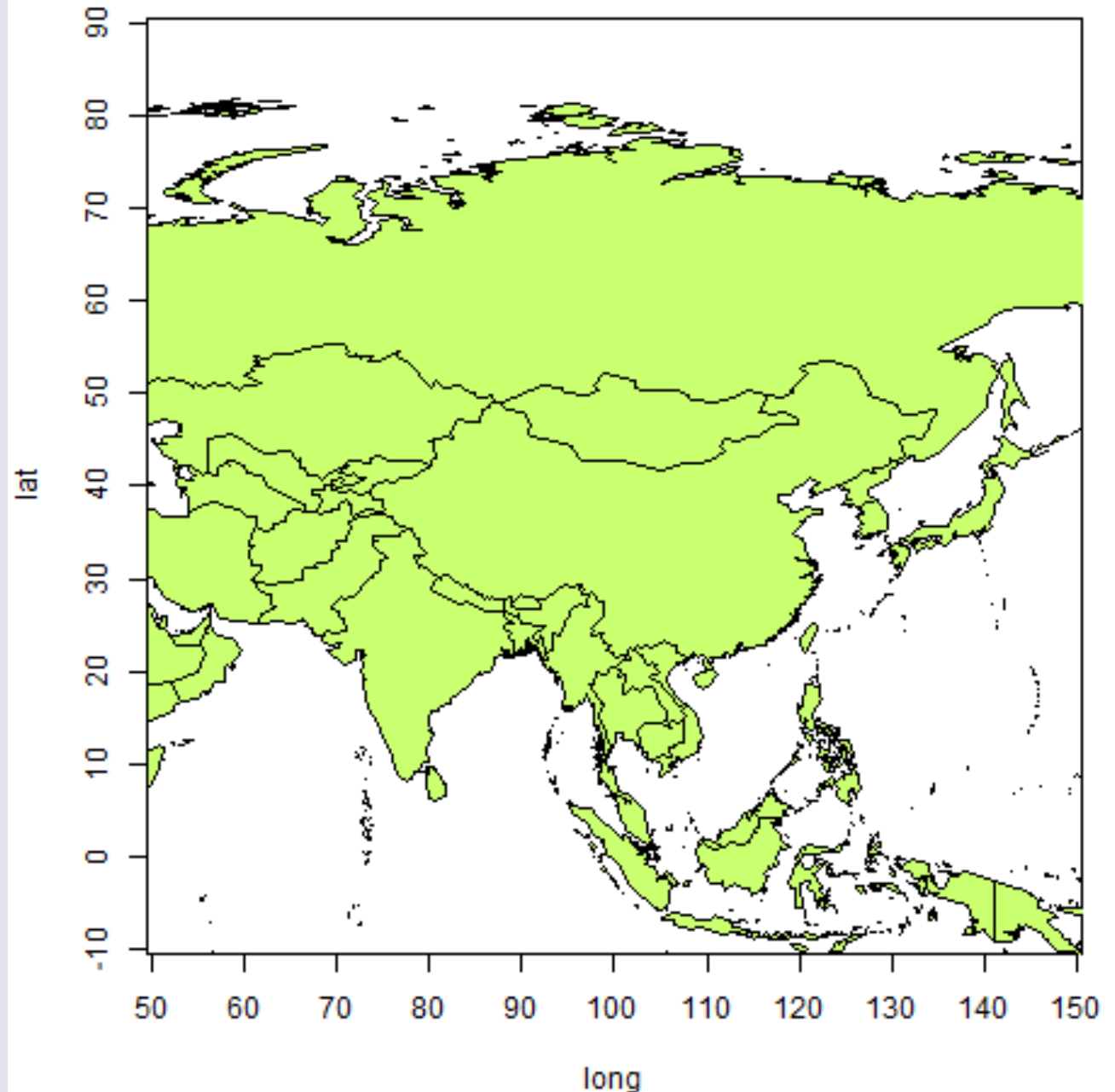
Introduction

- **CO₂ concentration estimated by GOSAT FTS (XCO₂) were collected for the period of 2009 – 2015.**
- **We focus on analyzing the spatial and seasonal variations of CO₂ concentrations in East Asia Region (Longitude E50 – E150, Latitude N90 – S10).**



Study Area

- East Asia
 - China
 - Japan
 - Korean Peninsula
 - Mongolia
 - Taiwan
- Period of data collection: 2009 - 2016



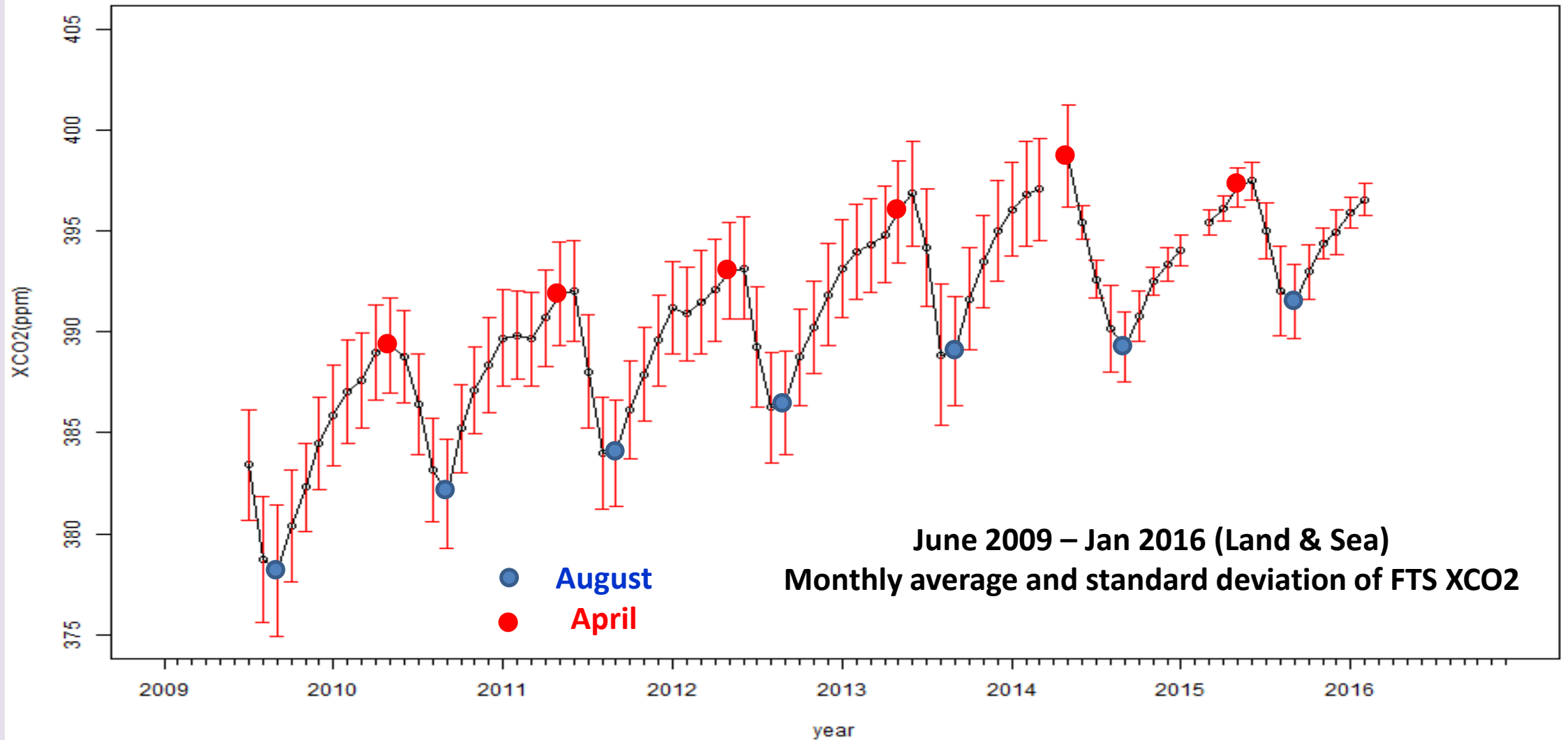
- Spatial resolution of the FTS CO₂ concentration (XCO₂) is 1.5 km by 1.5 km.
- Grid cells of 1° × 1° were used in this study. A total of 10201 cells in the study area. (GCO₂: Grid average CO₂ concentration)

FTS XCO2 data availability

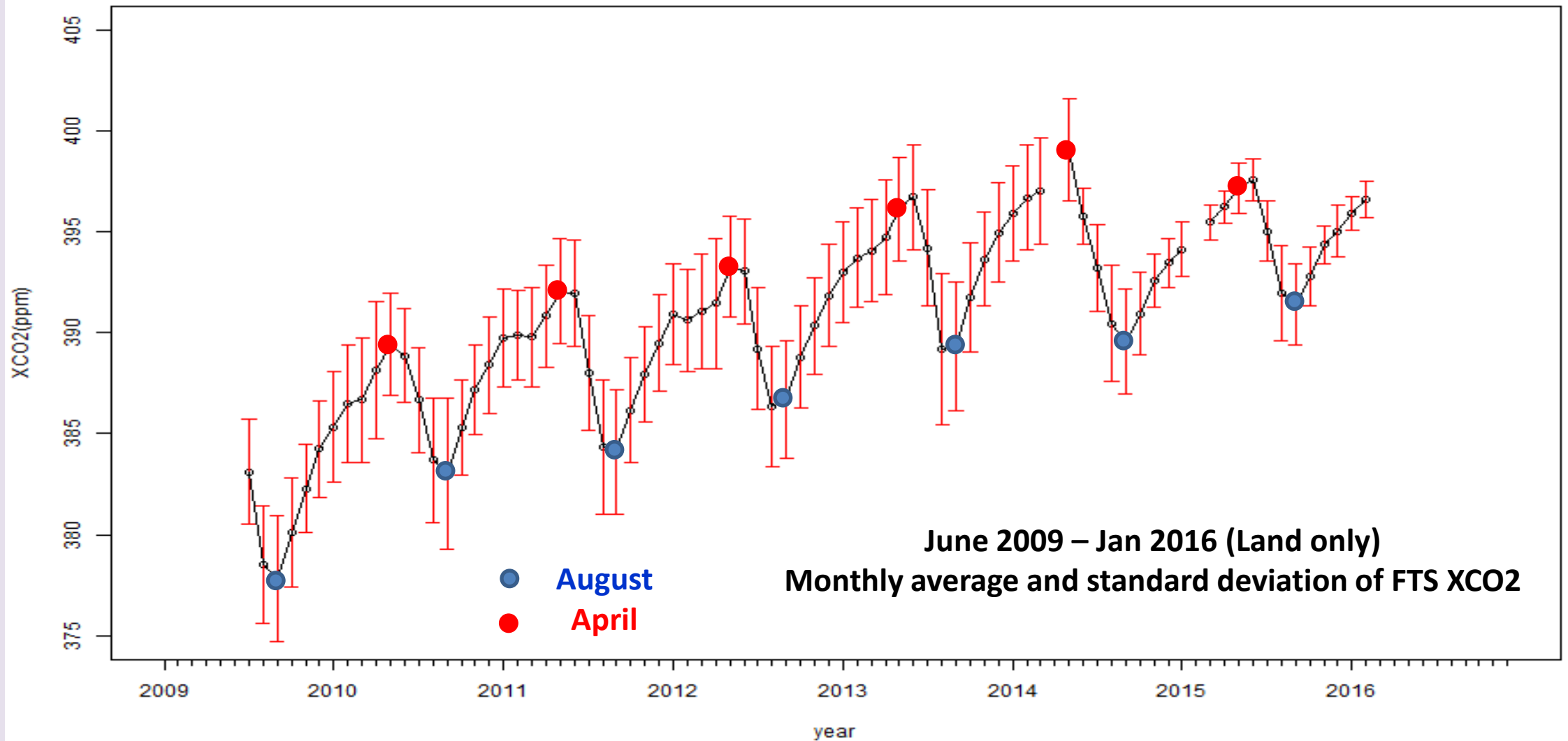
Time period	Cells with data	Percentage	Avg # of measurements per cell	Avg CO2 concentration (ppm)	Stdev of CO2 concentration (ppm)	Time period	Cells with data	Percentage	Avg # of measurements per cell	Avg CO2 concentration (ppm)	Stdev of CO2 concentration (ppm)
2009_6,7,8	821	8.05	5	383.3	1	2011_12,1,2	769	7.54	5.6	388.9	1.4
2009_9,10,11	1426	13.98	4.1	381.8	1.7	2012_3,4,5	299	2.93	5.1	392.3	0.9
2009_12,1,2	1211	11.87	4.5	384.5	1.3	2012_6,7,8	556	5.45	3.4	393	0.8
2010_3,4,5	545	5.34	4.2	388.7	1	2012_9,10,11	559	5.48	4.5	387.9	1.5
2010_6,7,8	851	8.34	3.4	389.2	0.7	2012_12,1,2	838	8.21	5	392.2	1.4
2010_9,10,11	984	9.65	3.4	384.5	1.2	2013_3,4,5	331	3.24	5.2	395.2	1
2010_12,1,2	791	7.75	5.9	387.7	1.3	2013_6,7,8	754	7.39	3.6	396	0.8
2011_3,4,5	373	3.66	5.6	390.5	1	2013_9,10,11	653	6.4	4.1	391	1.6
2011_6,7,8	741	7.26	3.7	391.6	0.9	2013_12,1,2	729	7.15	4.5	394.4	1.1
2011_9,10,11	581	5.7	3.8	385.7	1.3	2014_3,4,5	538	5.27	3.3	398.7	0.6

Trend and Seasonal Variation of XCO₂ in the East Asia Region

trend of XCO₂



trend of XCO2 on land



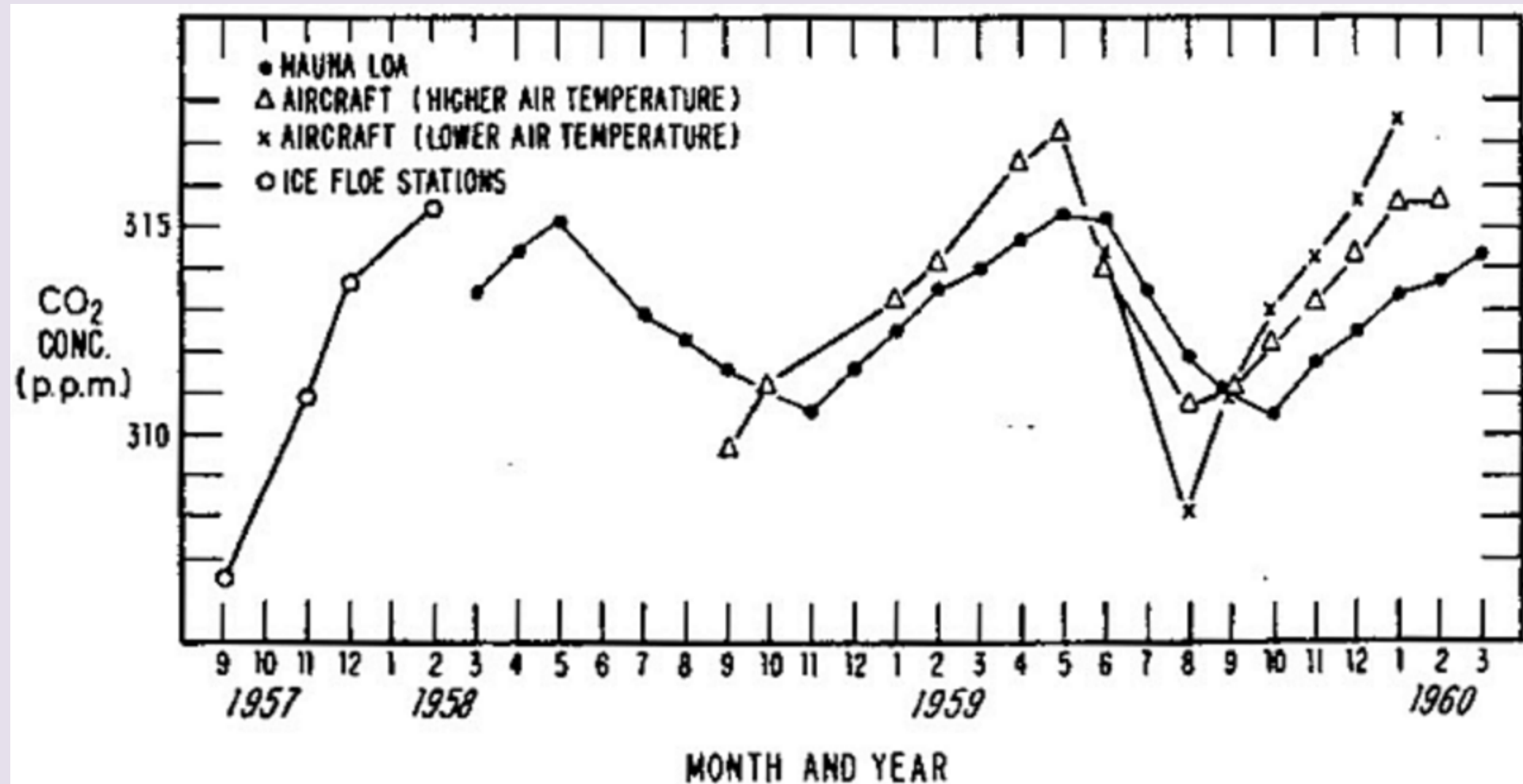
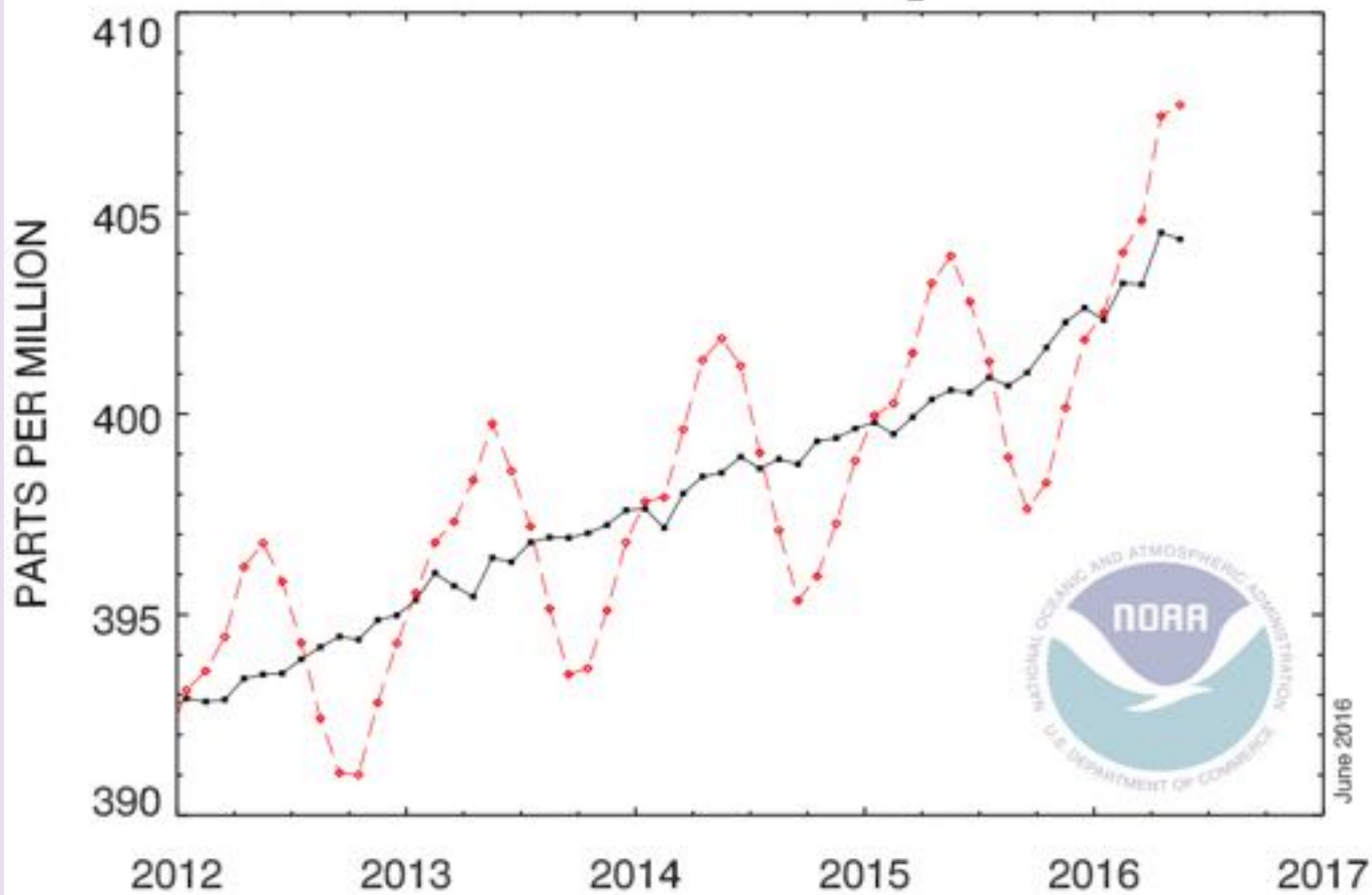
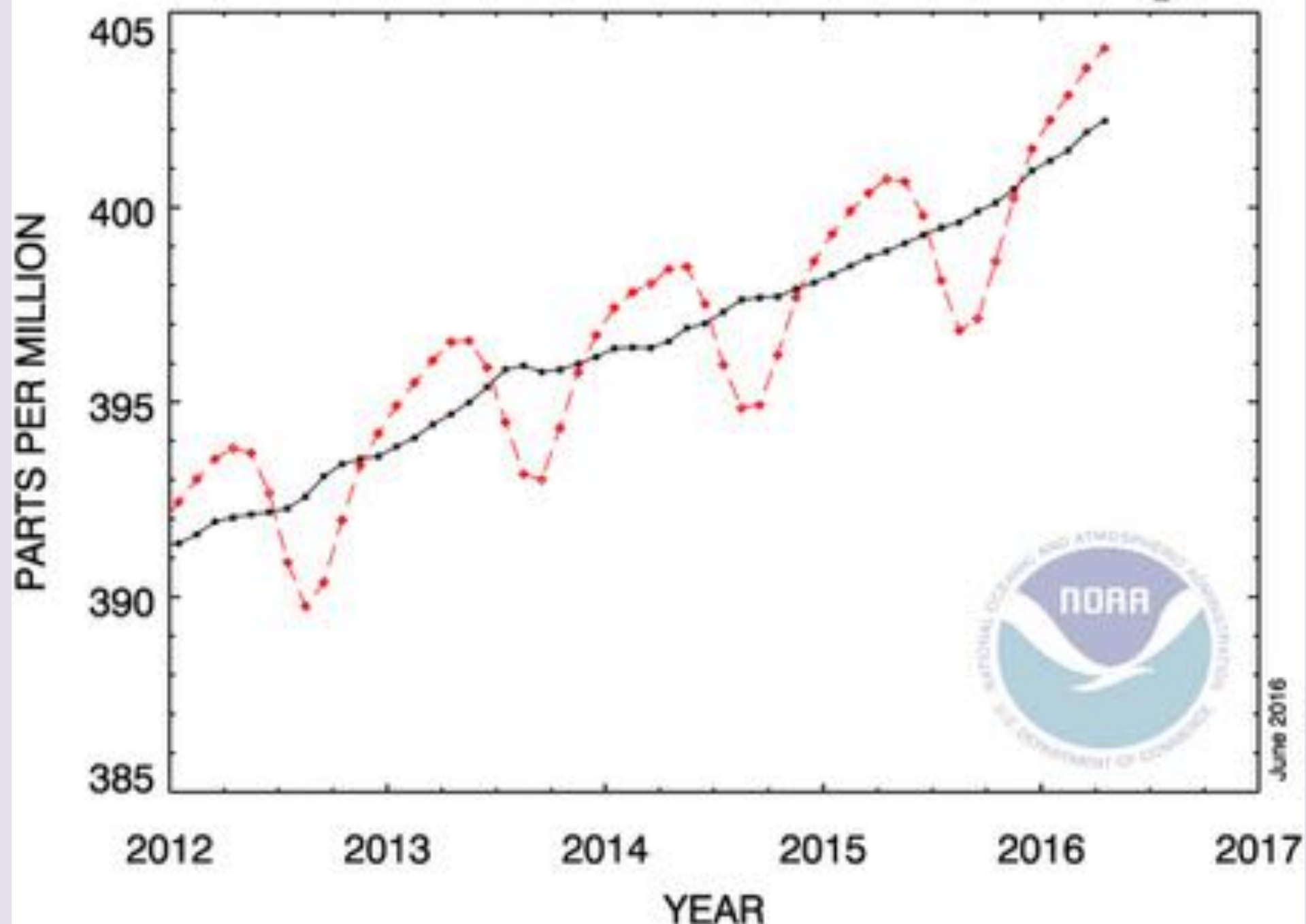


Fig. 1. Variation in concentration of atmospheric carbon dioxide in the Northern Hemisphere.

RECENT MONTHLY MEAN CO₂ AT MAUNA LOA



RECENT GLOBAL MONTHLY MEAN CO₂



Seasonal Variation of FTS XCO₂

season	mean	sd
spring	392.4977	4.360145
summer	385.8039	4.903655
autumn	388.1570	4.458877
winter	392.6235	4.055581

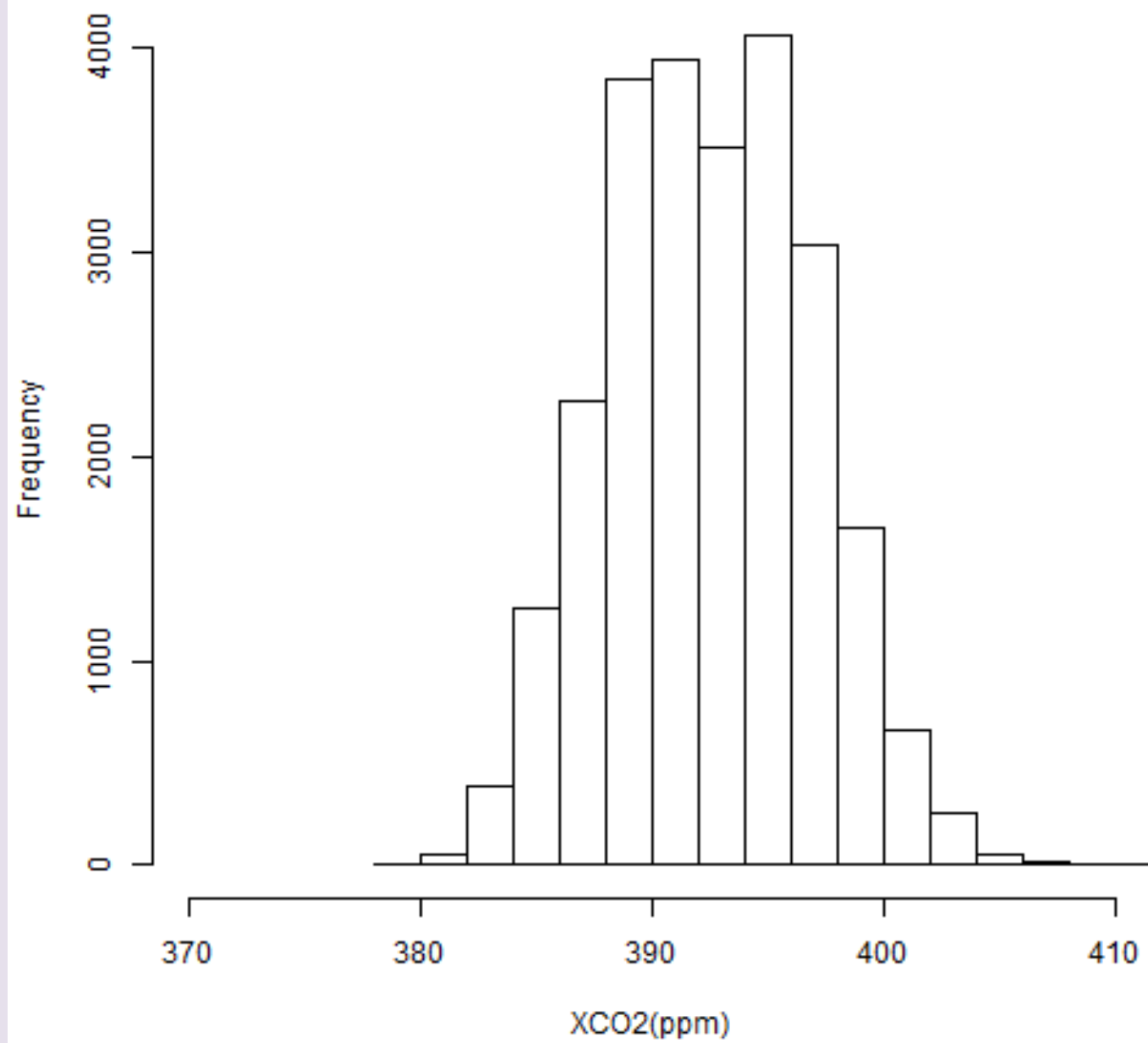
Spring: March – May

Summer: June – August

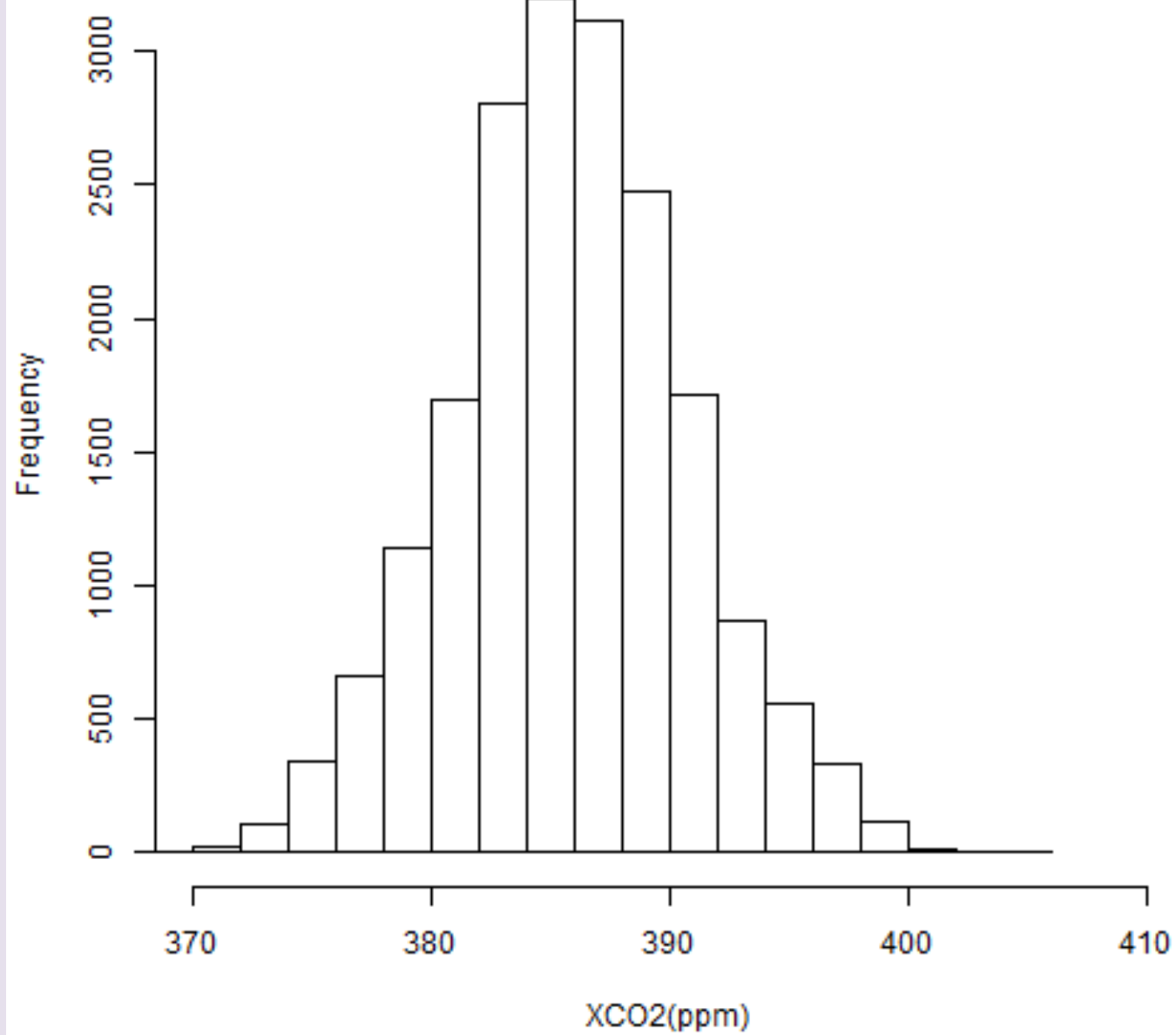
Autumn: September – November

Winter: December - February

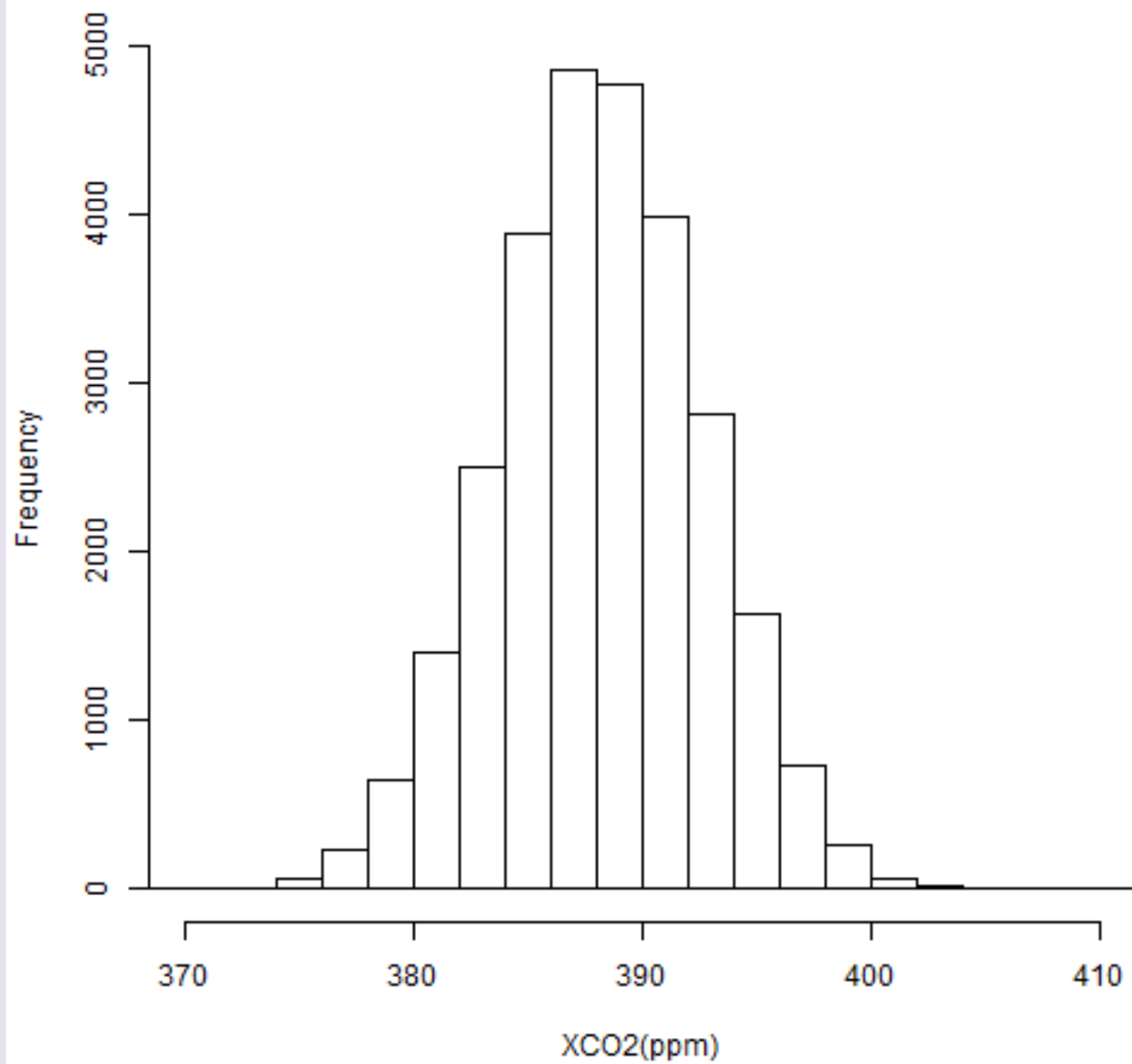
spring



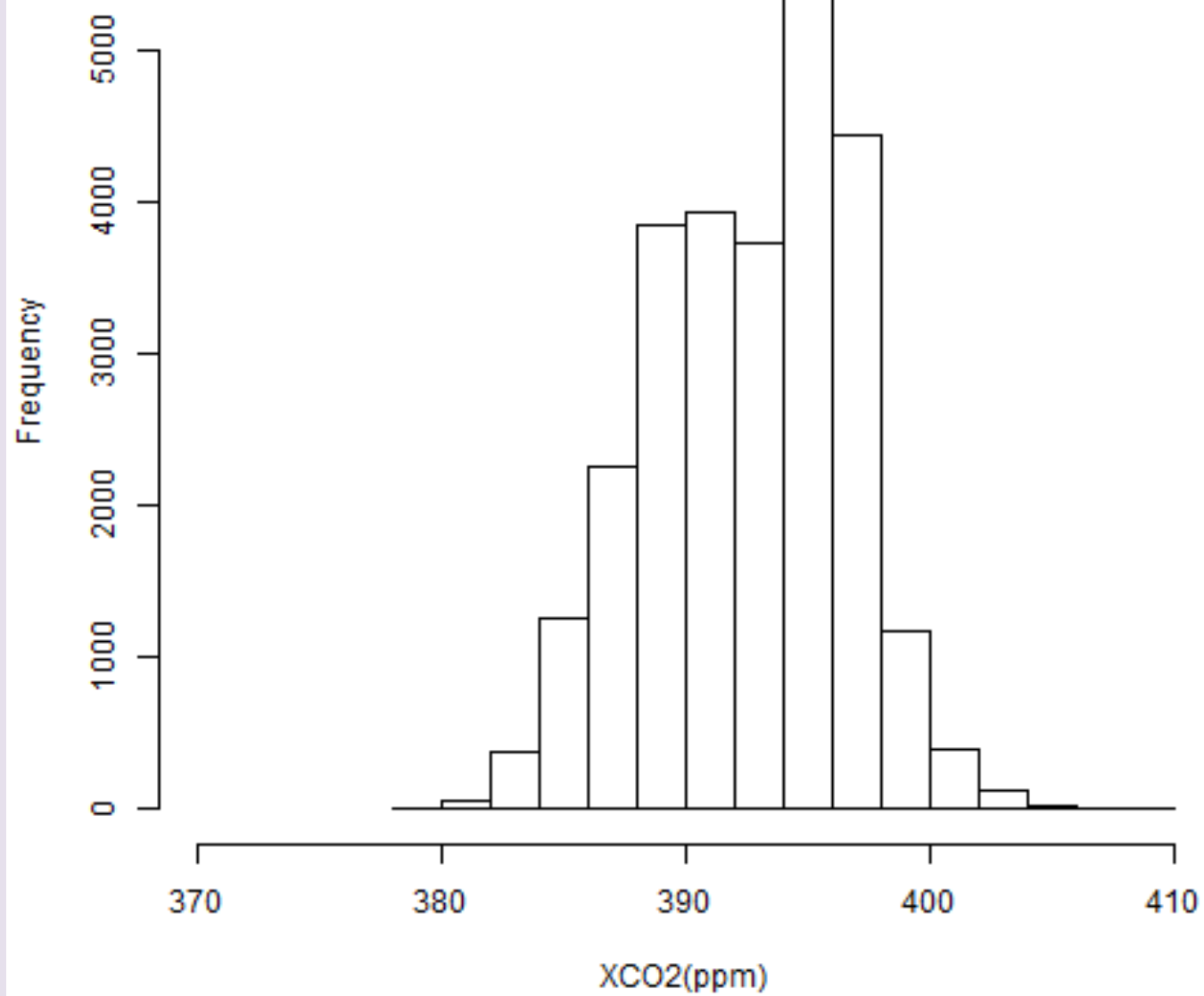
summer

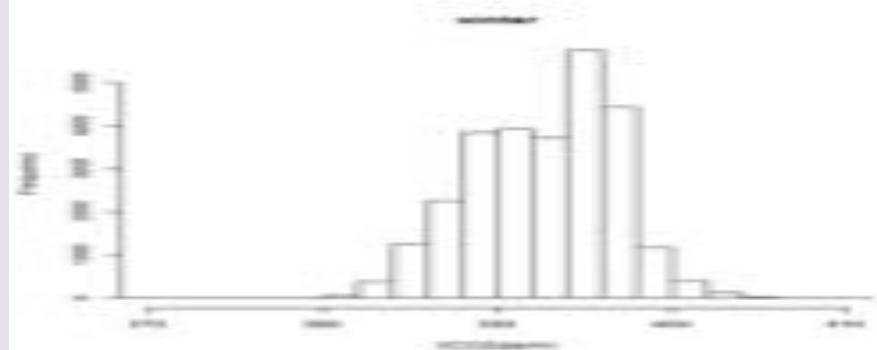
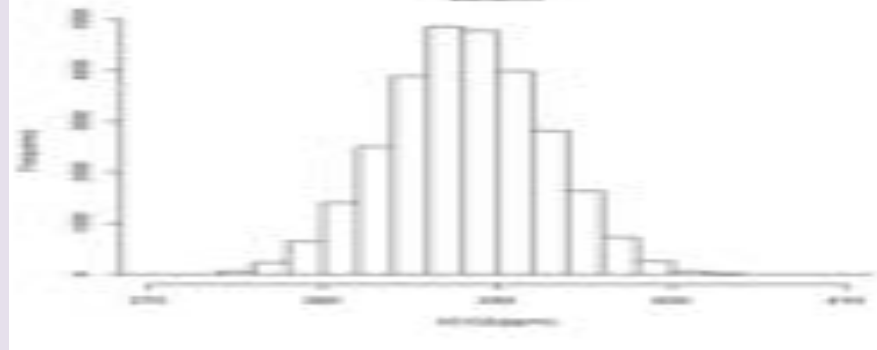
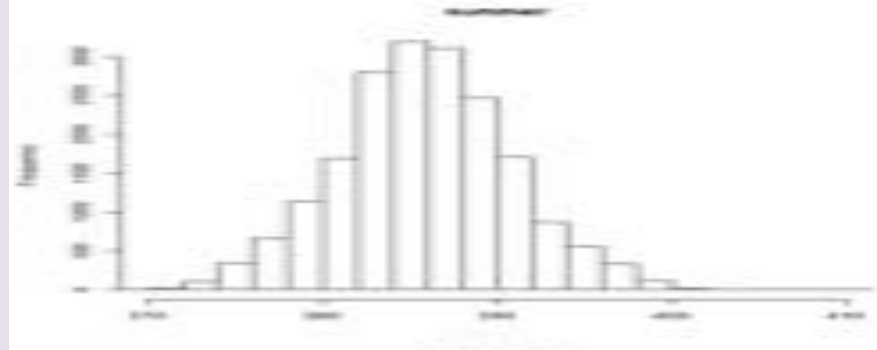
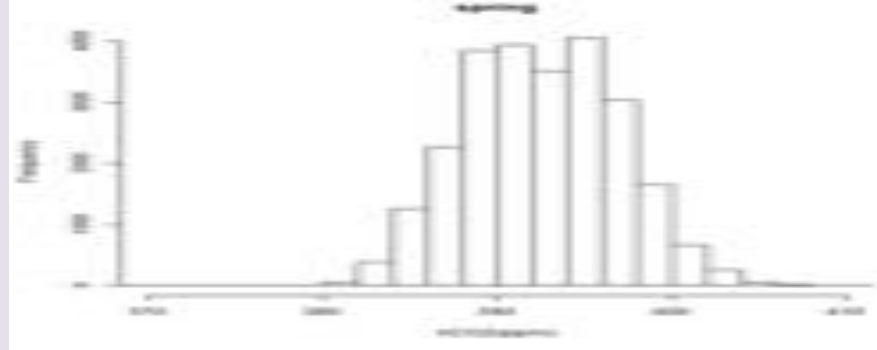


autumn

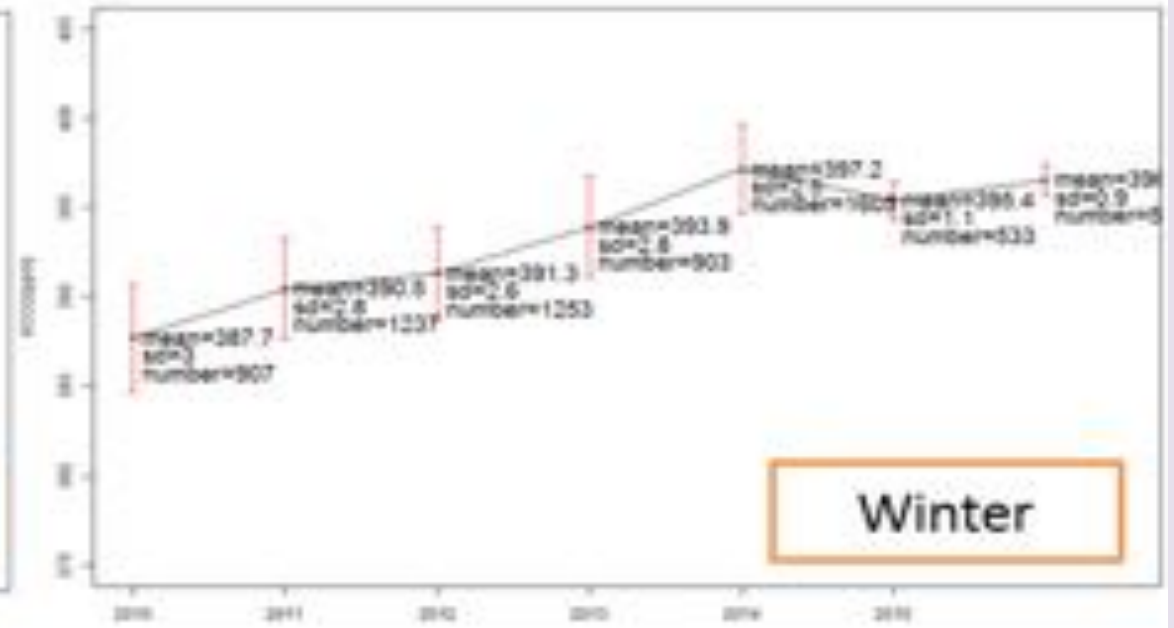
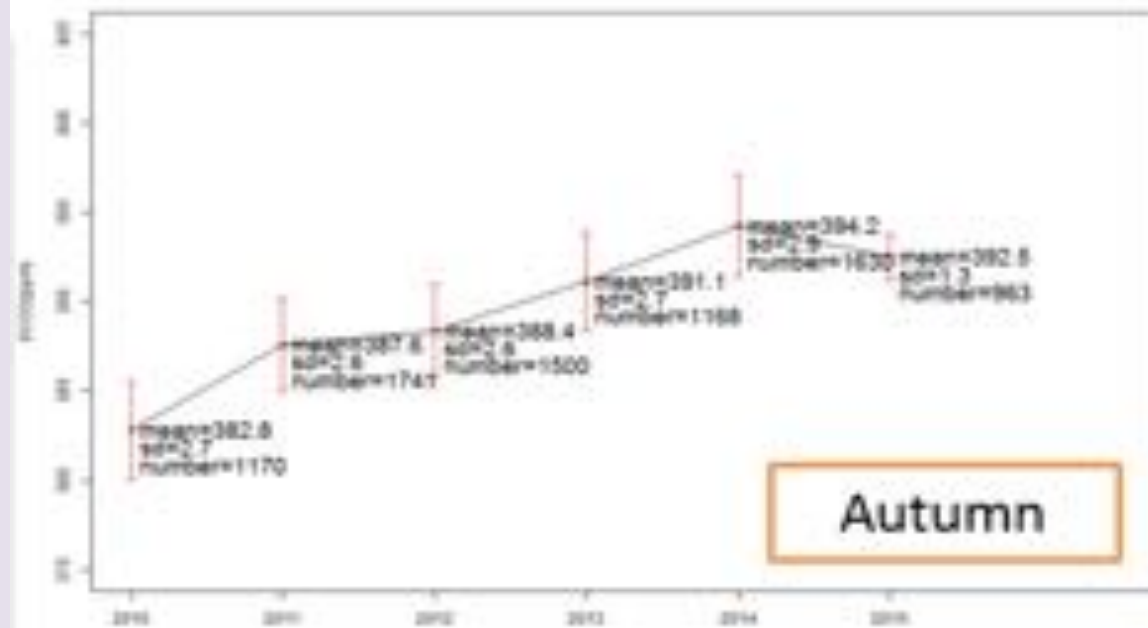
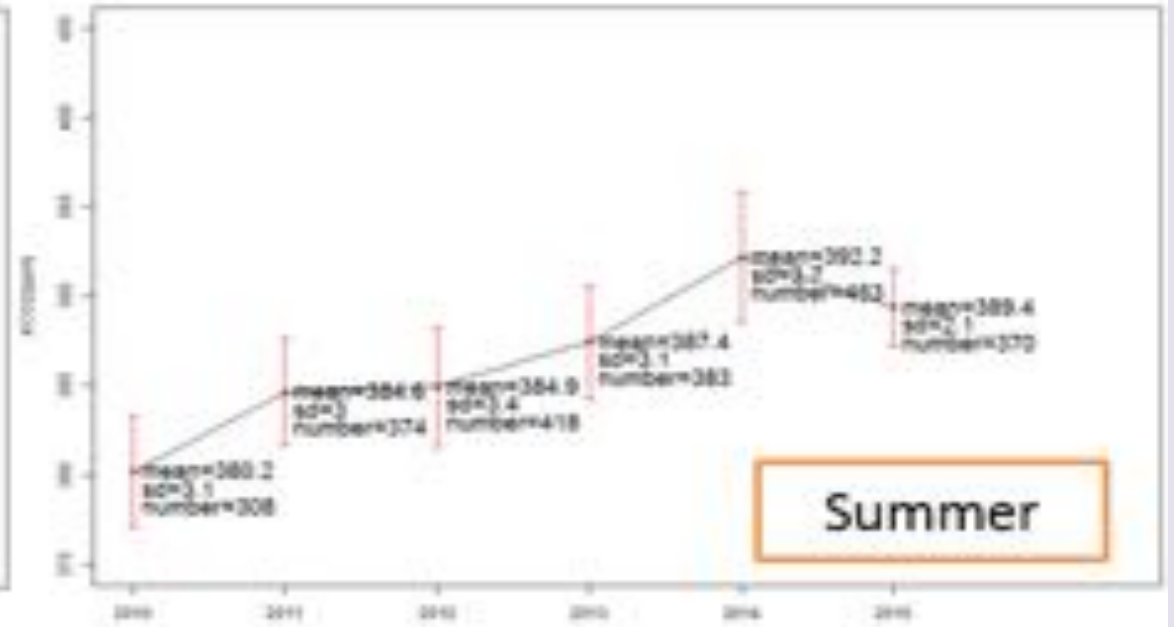
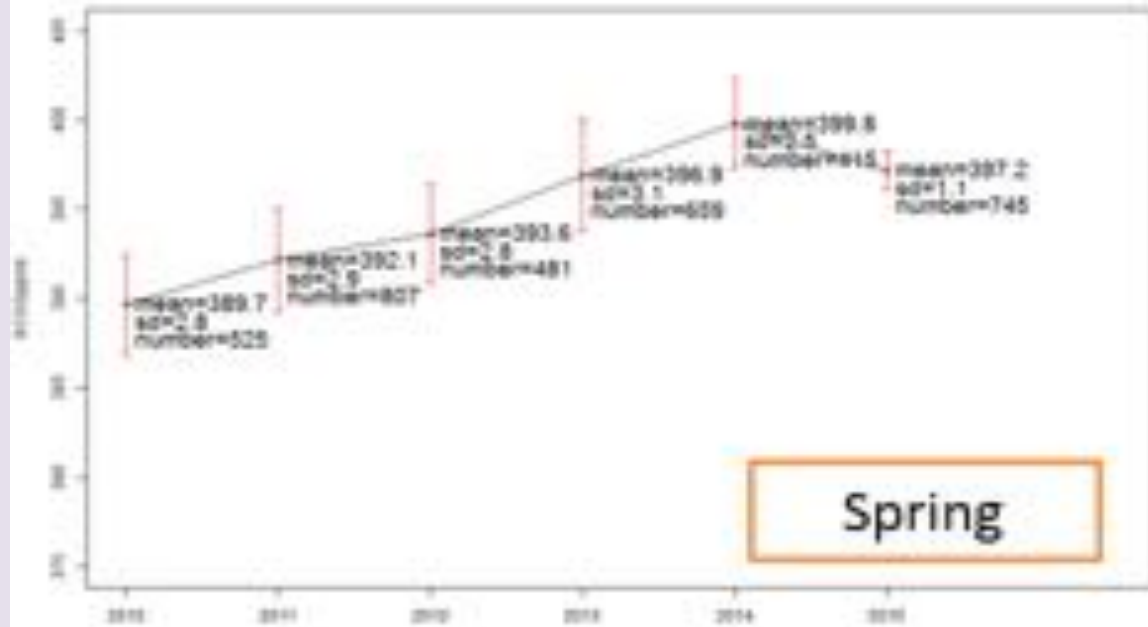


winter





Increasing trend of seasonal XCO2



- These latitudinal differences in fluctuation are the result of photosynthetic activity by plants. As plants begin to photosynthesize in the [spring](#) and summer, they consume CO₂ from the atmosphere and eventually use it as a carbon source for growth and reproduction. This causes the decrease in CO₂ levels that begins every year in May. Once winter arrives, plants save energy by decreasing photosynthesis. Without photosynthesis, the dominant process is the exhalation of CO₂ by the total ecosystem, including bacteria, plants, and animals.

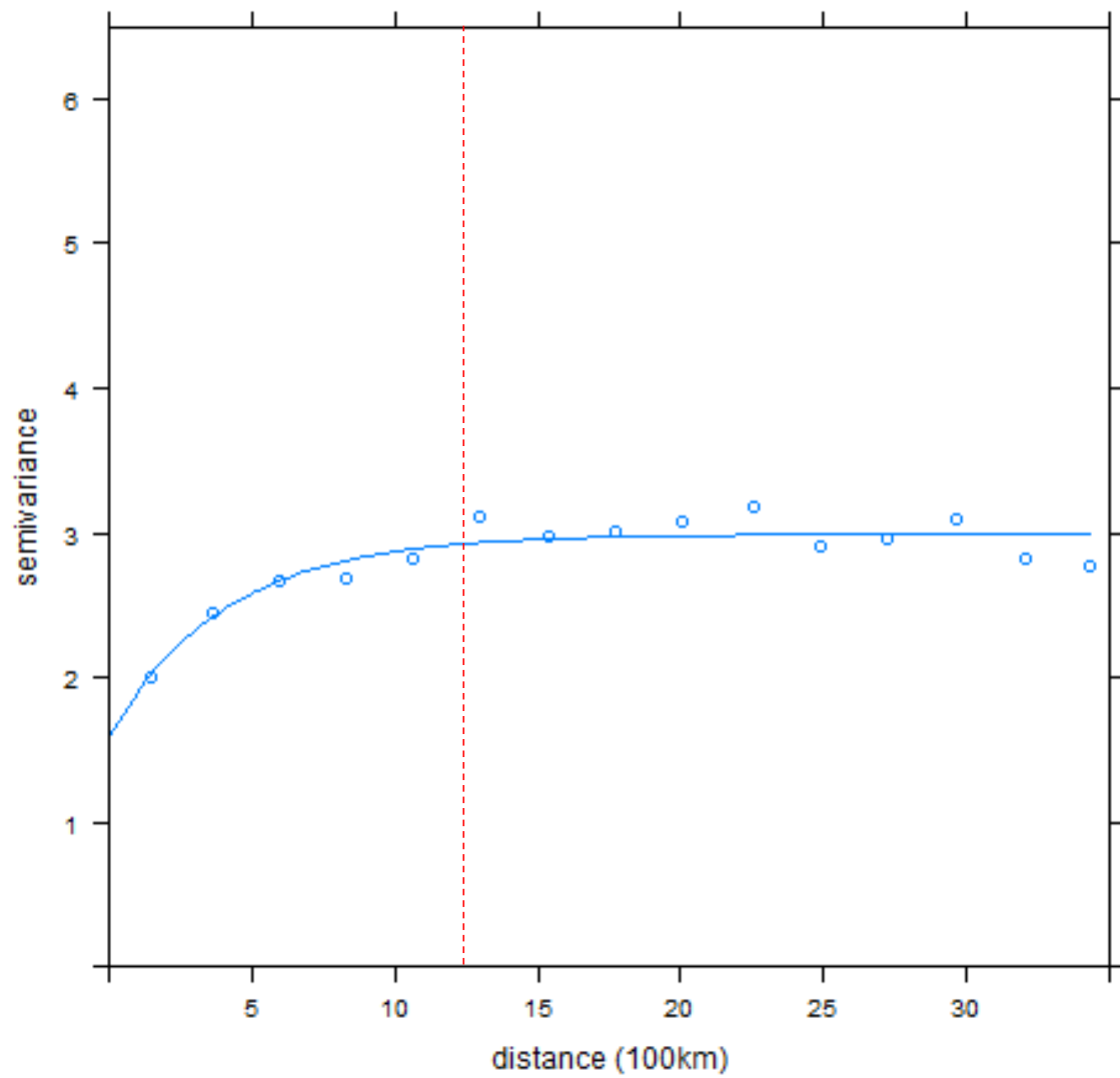
Modeling Spatial Variability of XCO₂

- Spatial variability modeling (semivariogram)
- Spatial interpolation (Kriging method)
- Preliminary results and analyses

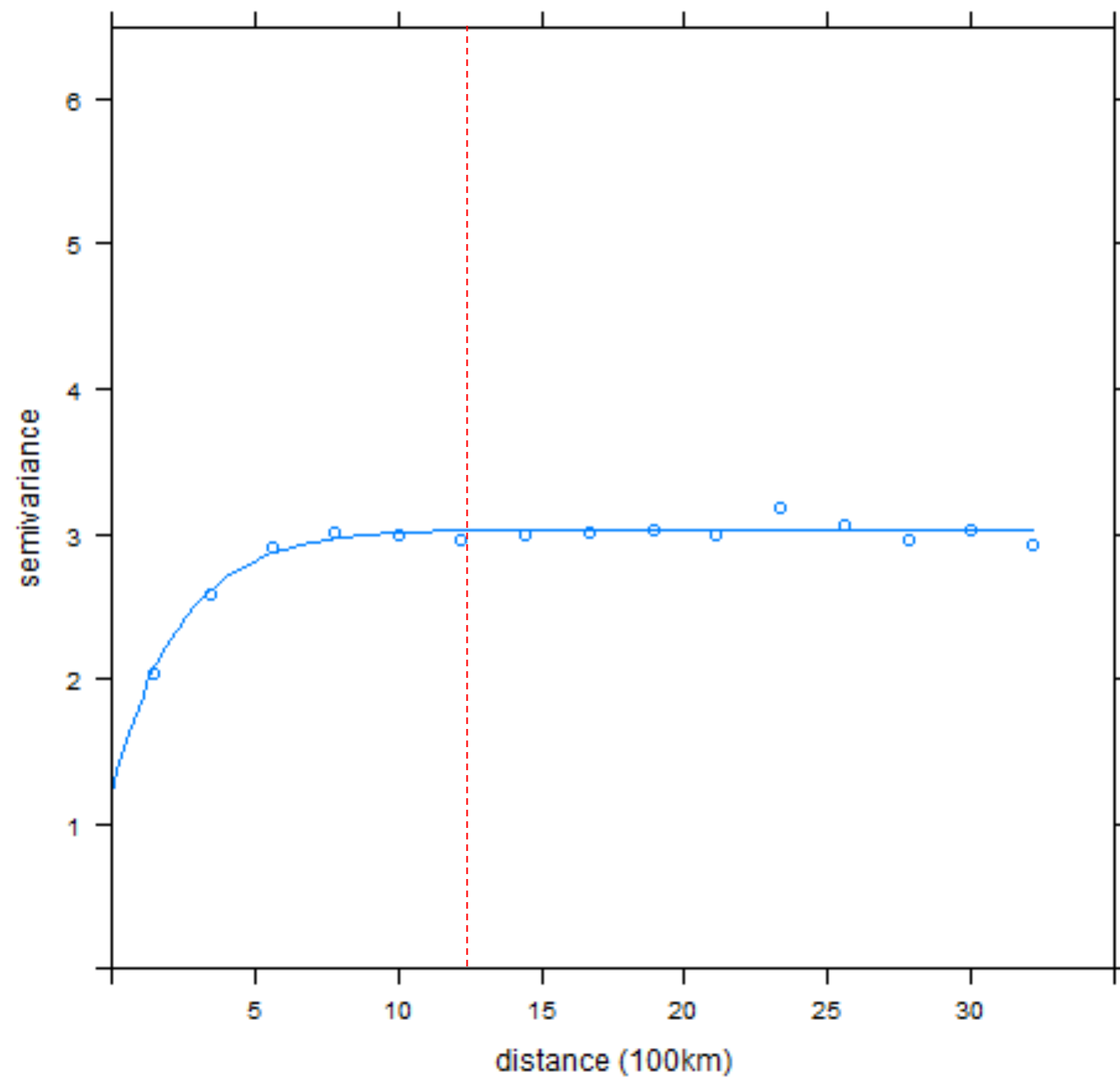
Semivariogram Modeling of XCO₂

- Seasonal semivariograms
 - Ranges are approximately 12°.
 - Sills (variance of XCO₂) mostly vary in a range from 2.5 to 5 ppm.
 - Semivariograms of the Dec - Feb and March - May periods have higher sills than the June - August and September - November periods.

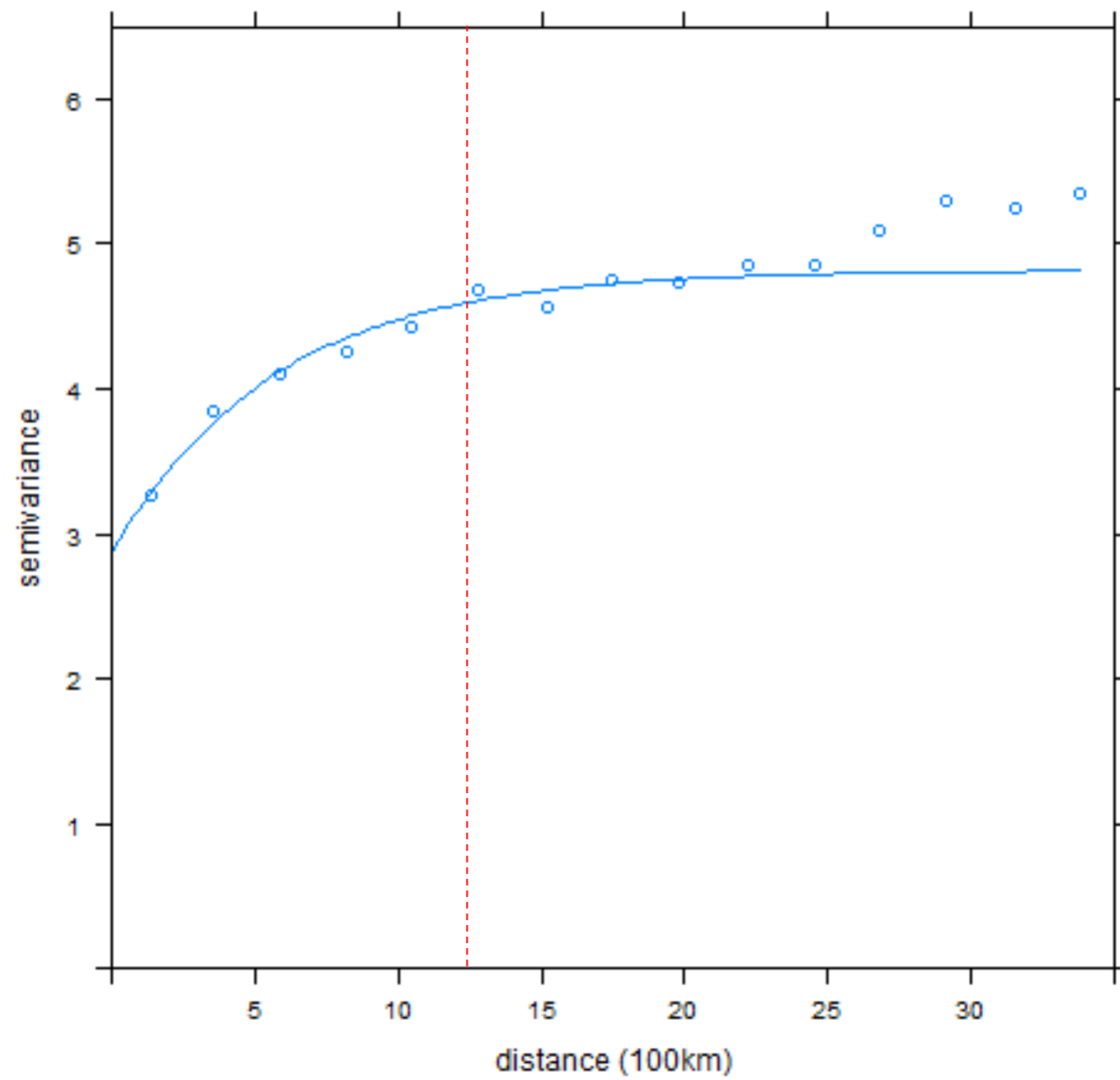
2009_6,7,8



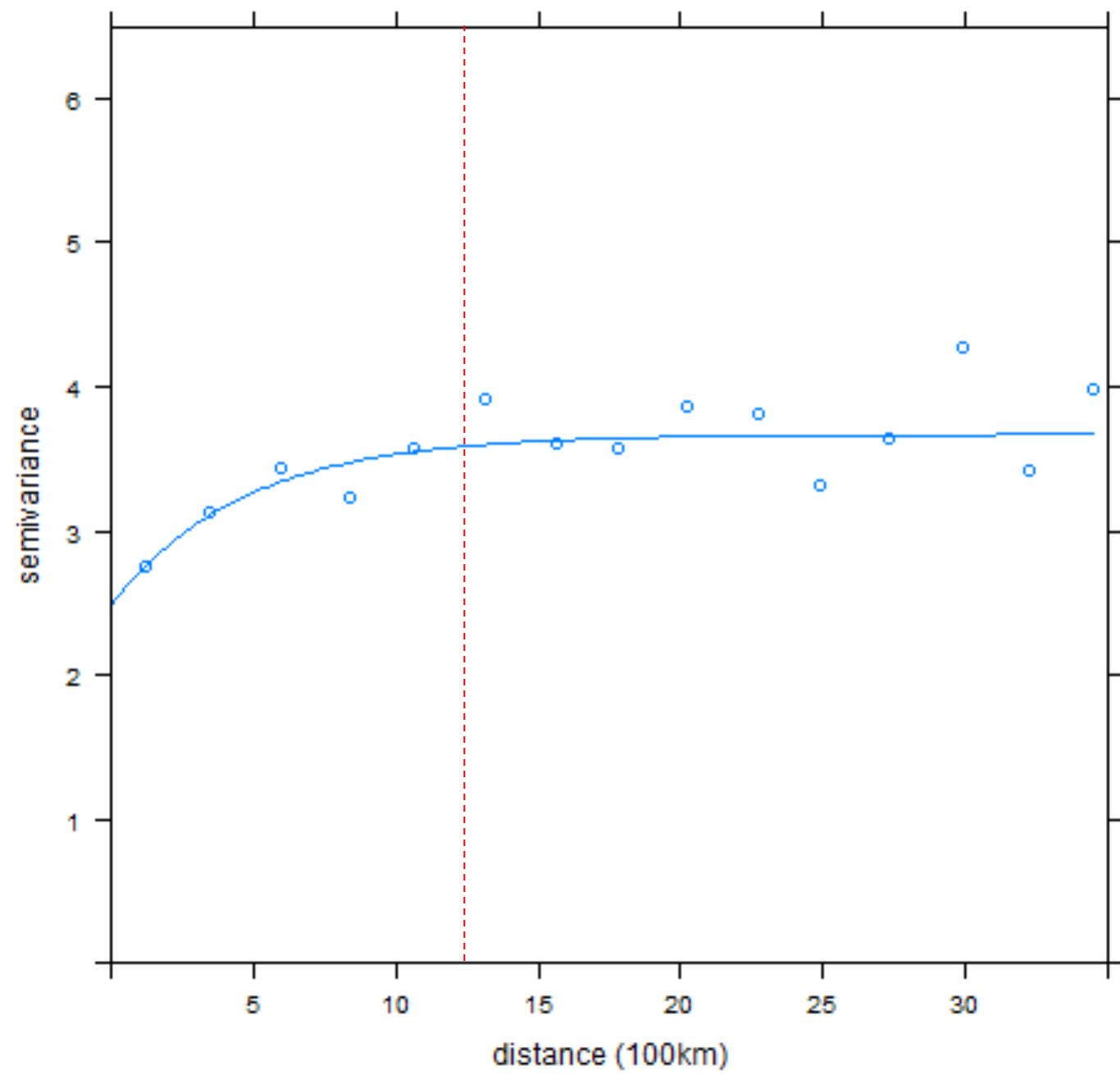
2009_9,10,11



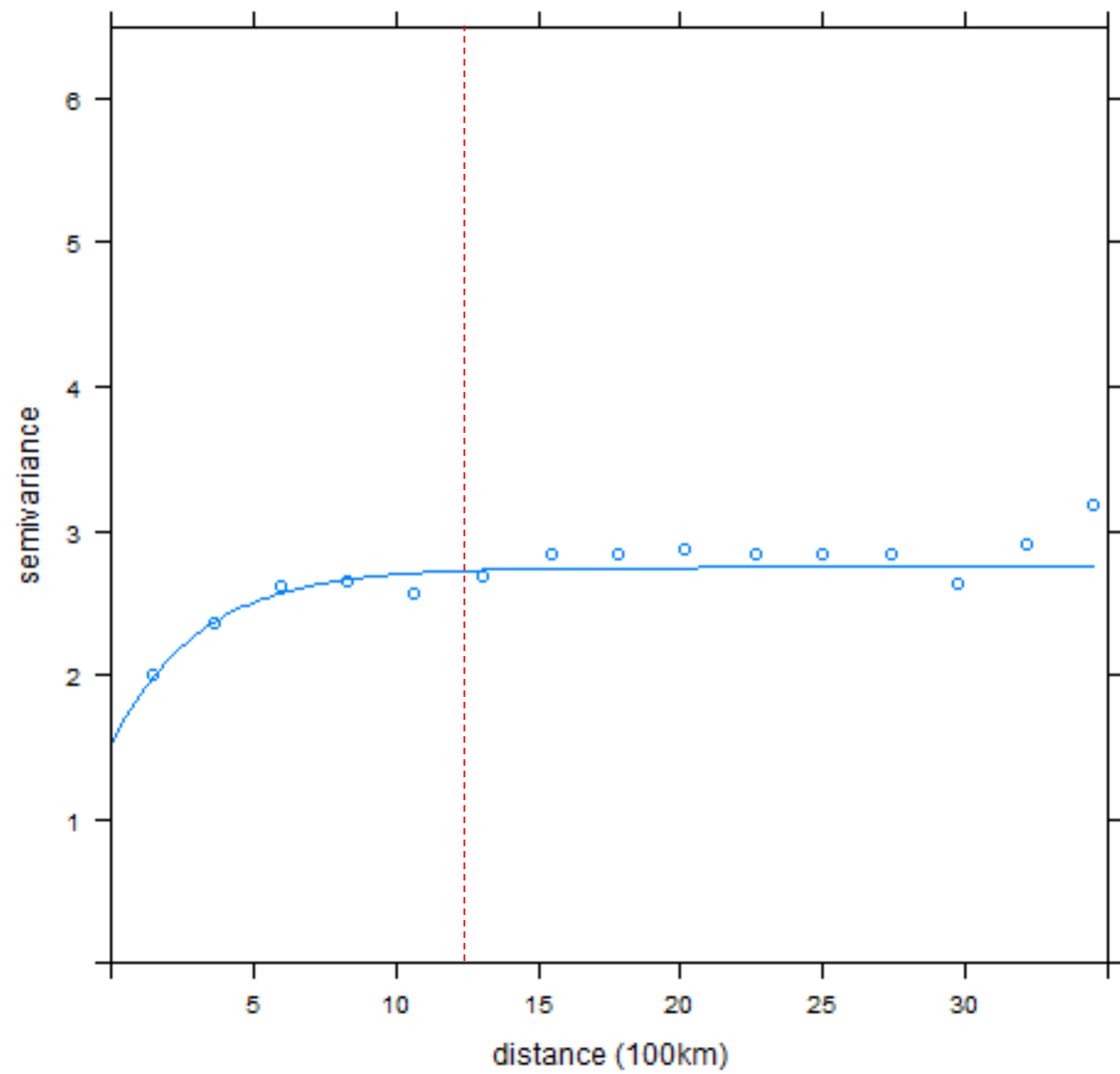
2009_12,1,2



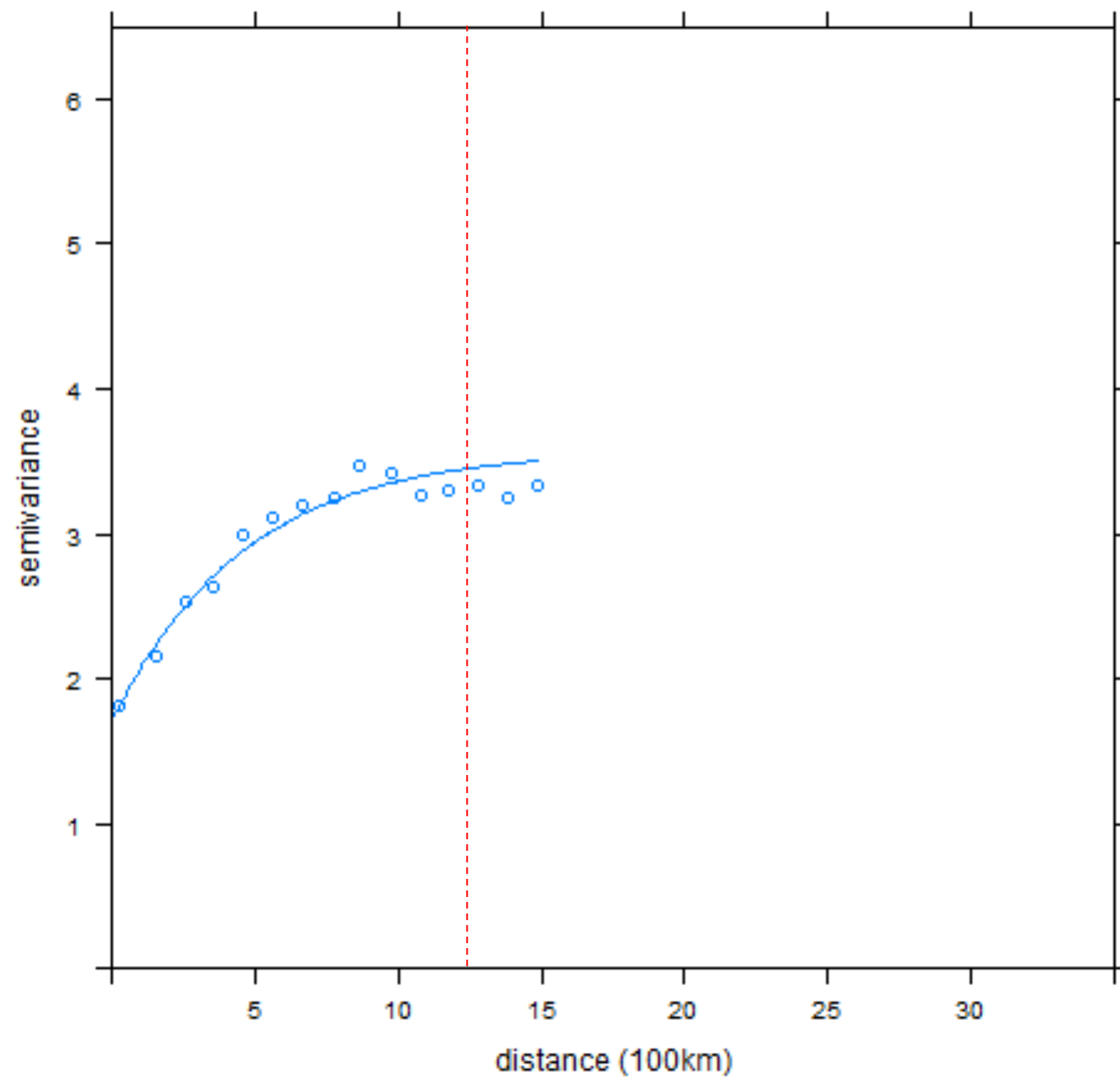
2010_3,4,5



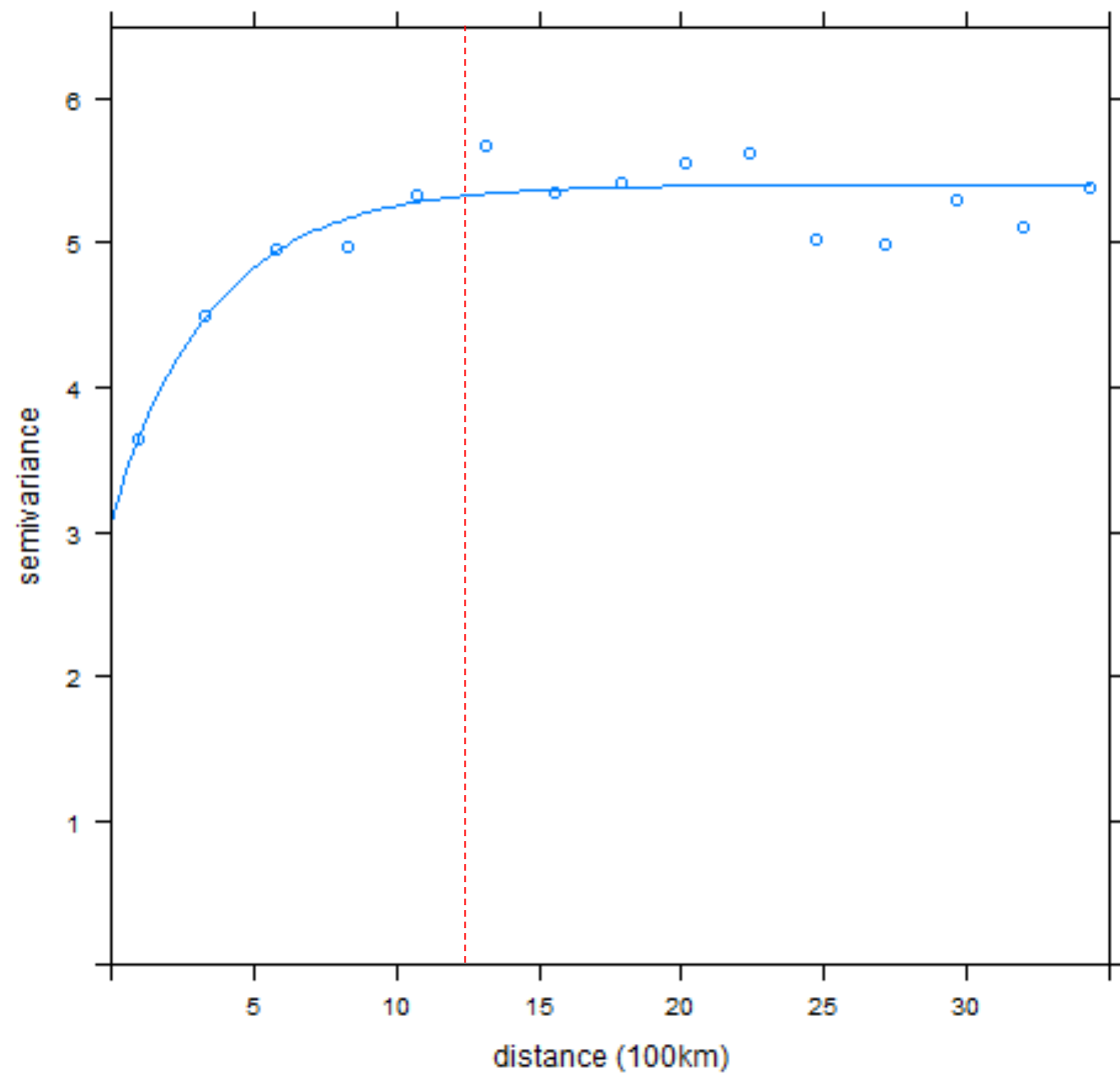
2010_6,7,8



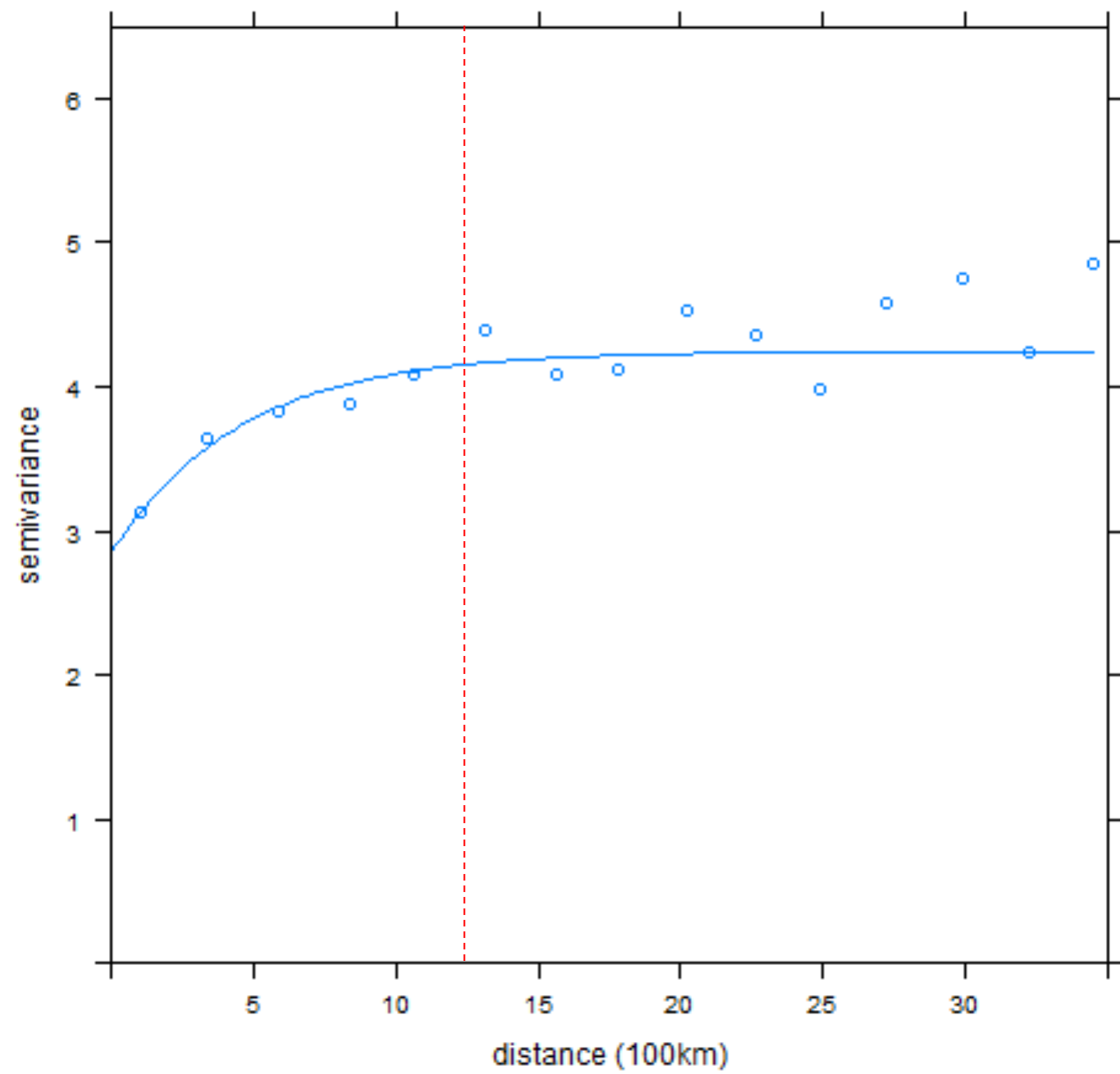
2010_9,10,11



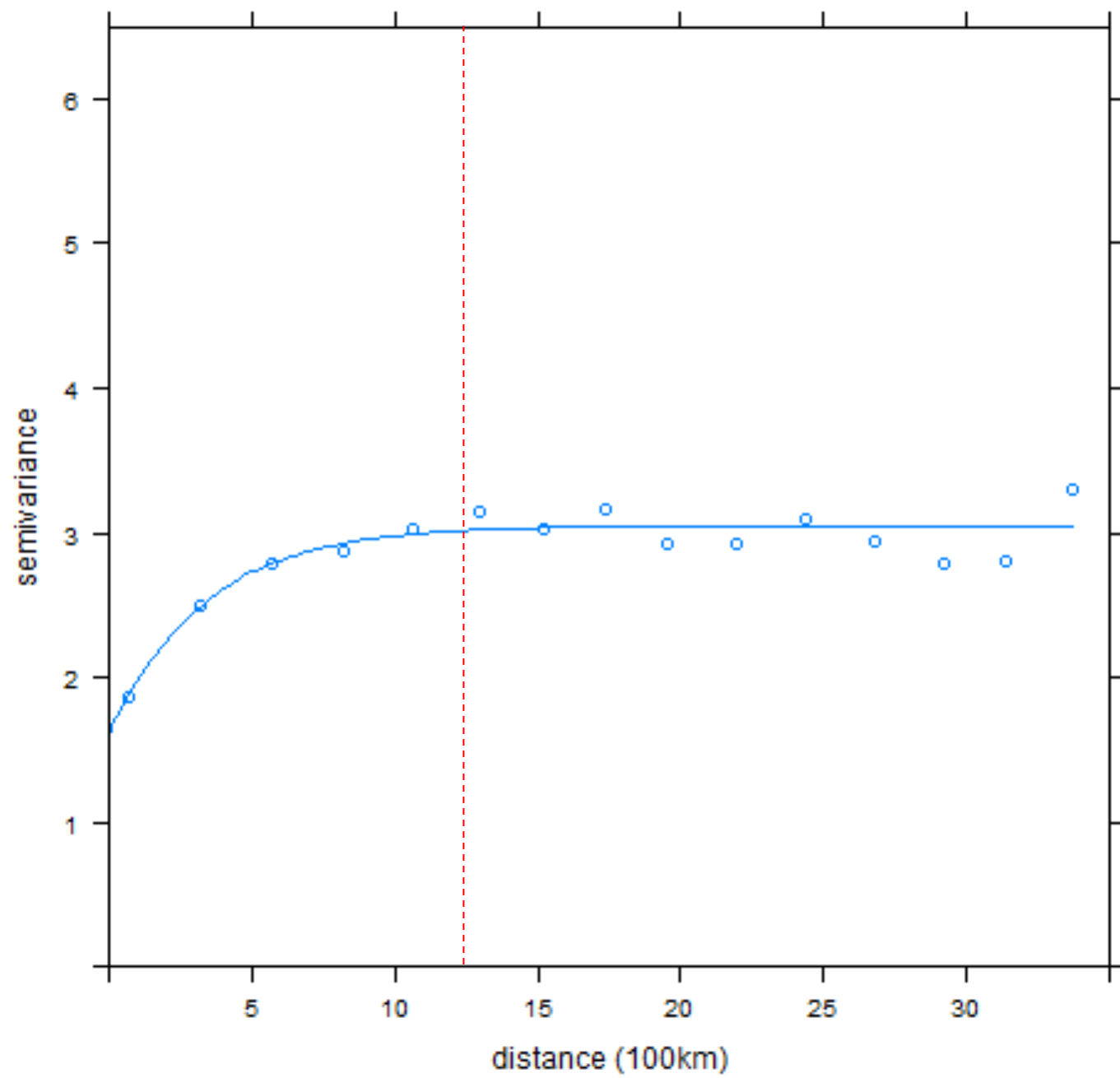
2010_12,1,2



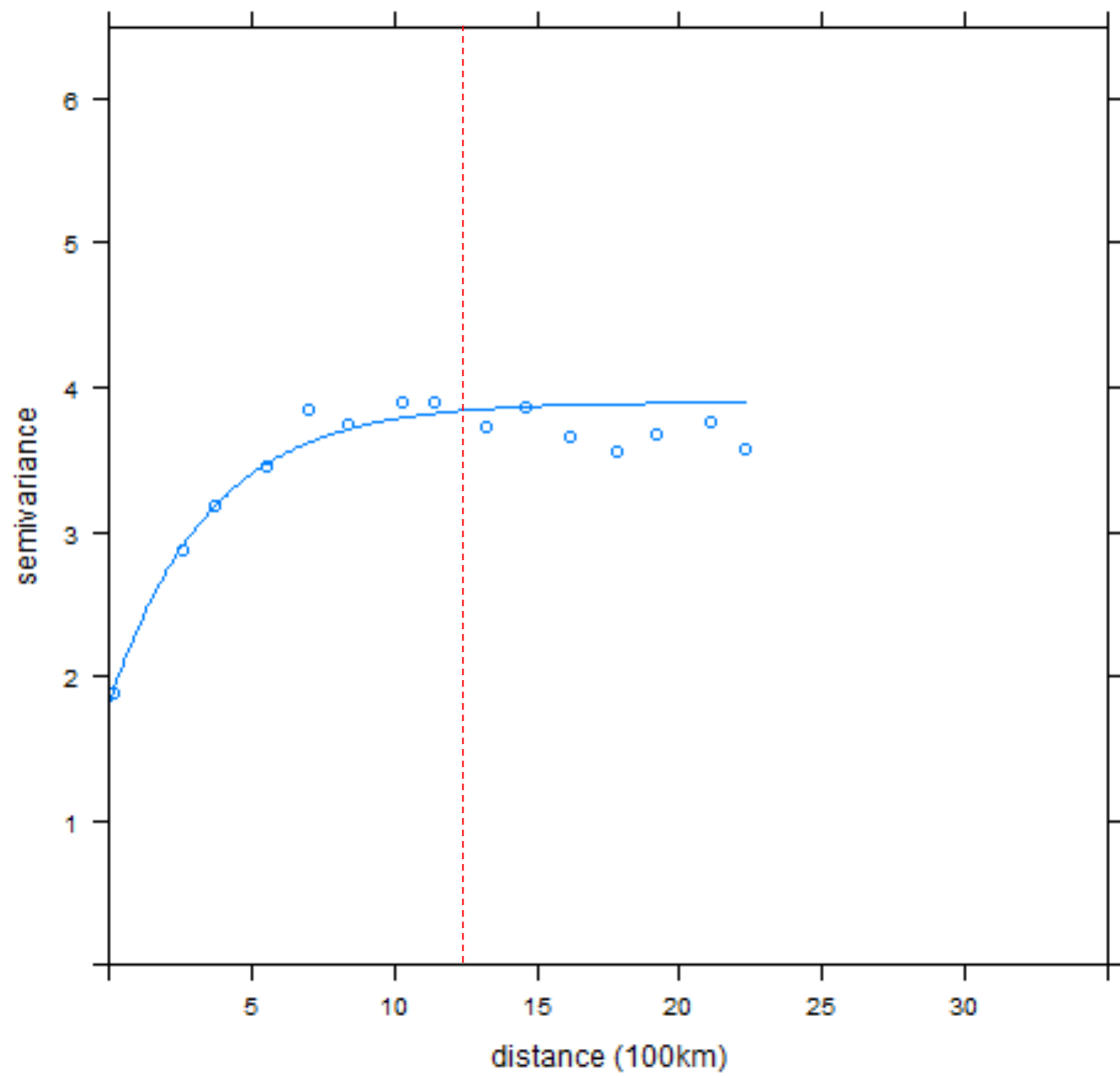
2011_3,4,5



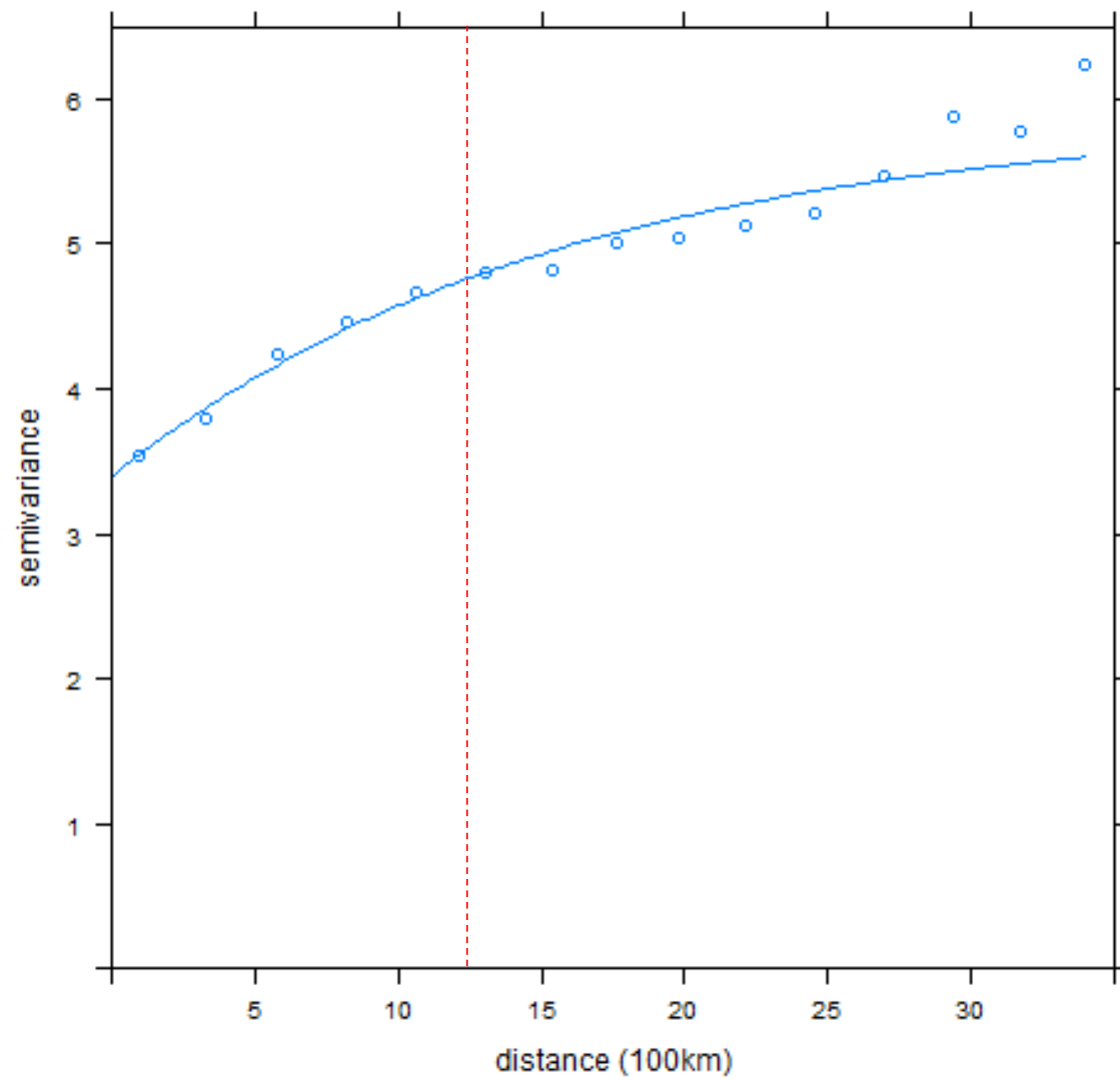
2011_6,7,8



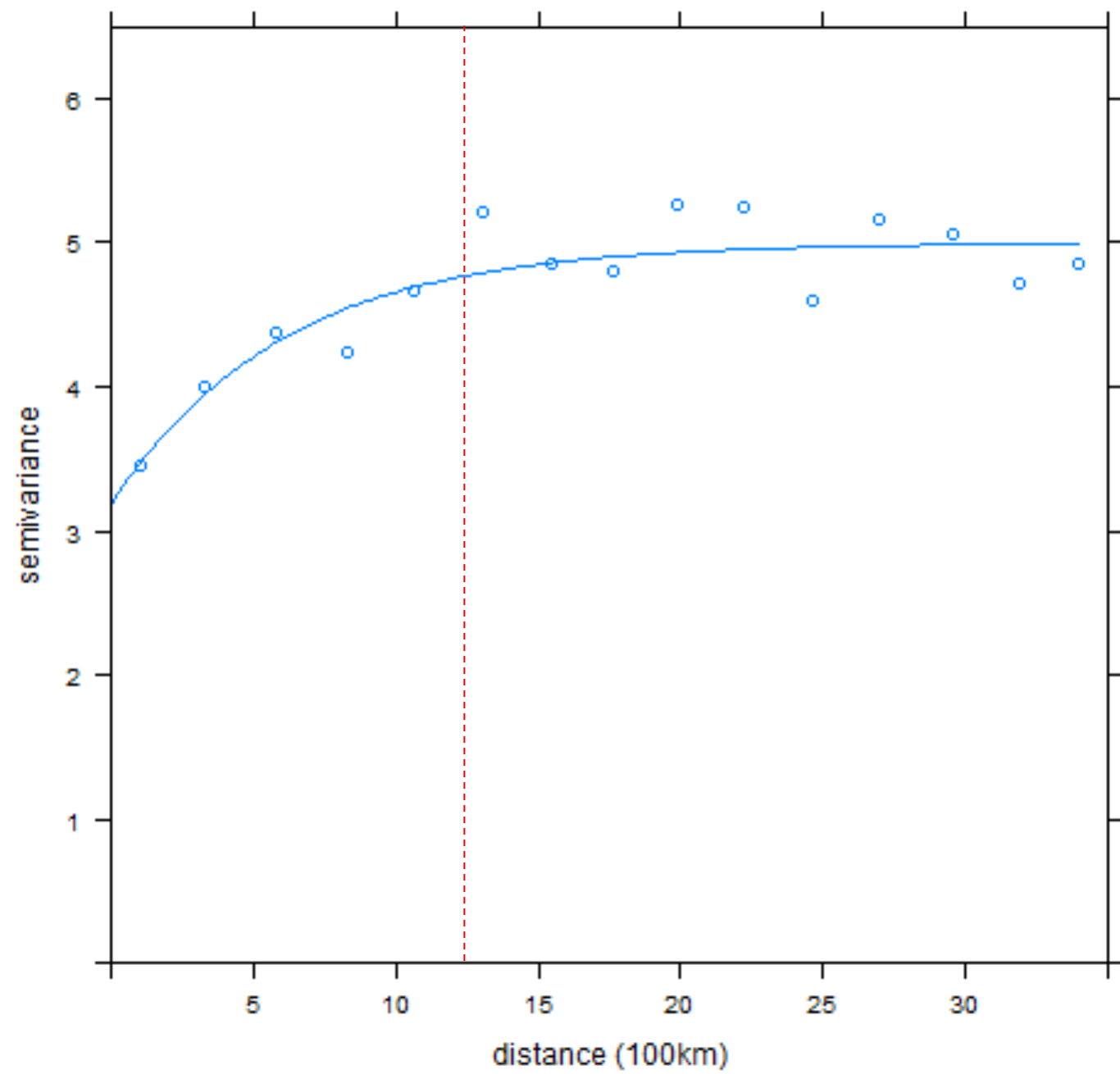
2011_9,10,11



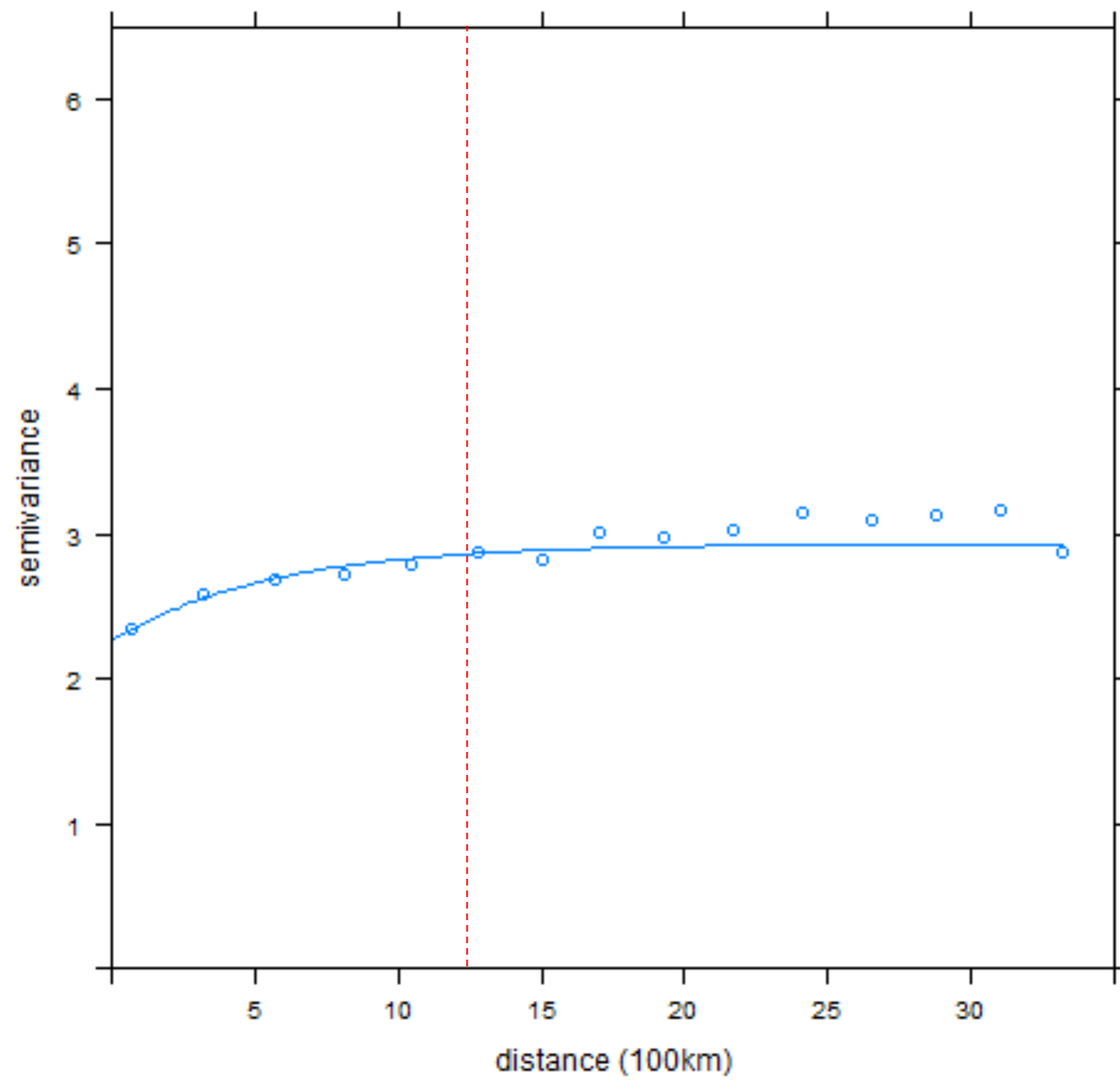
2011_12,1,2



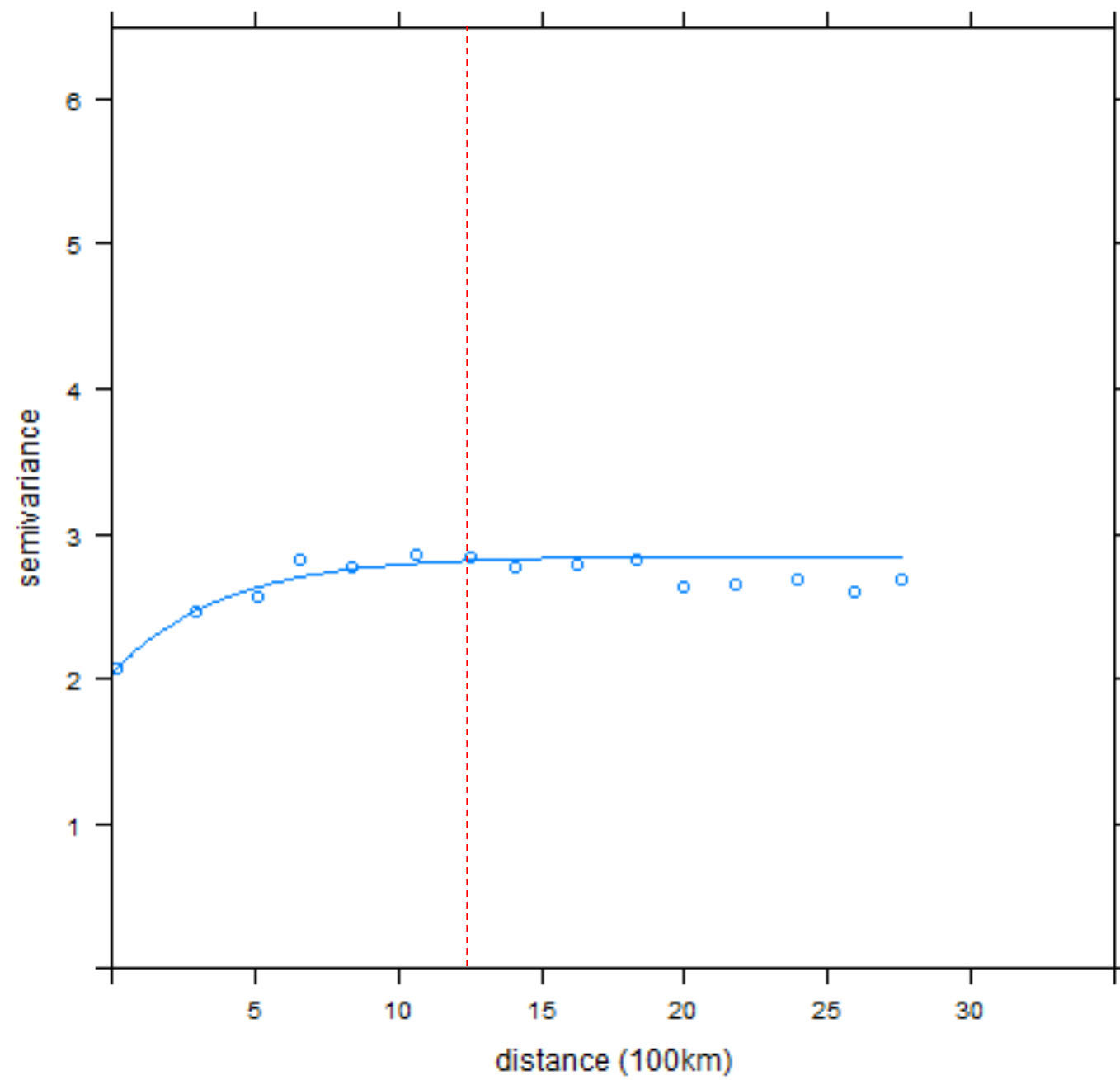
2012_3,4,5



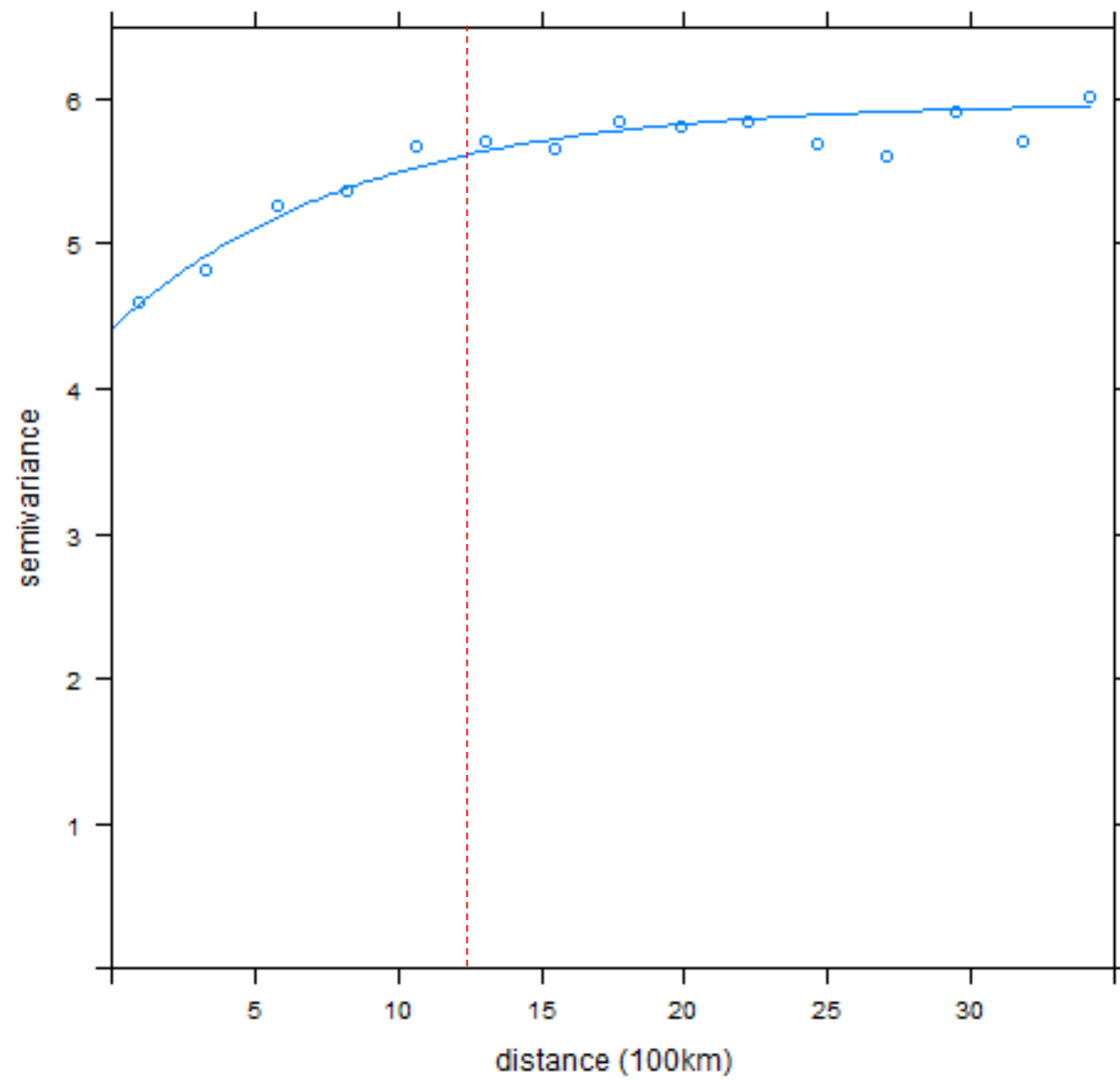
2012_6,7,8



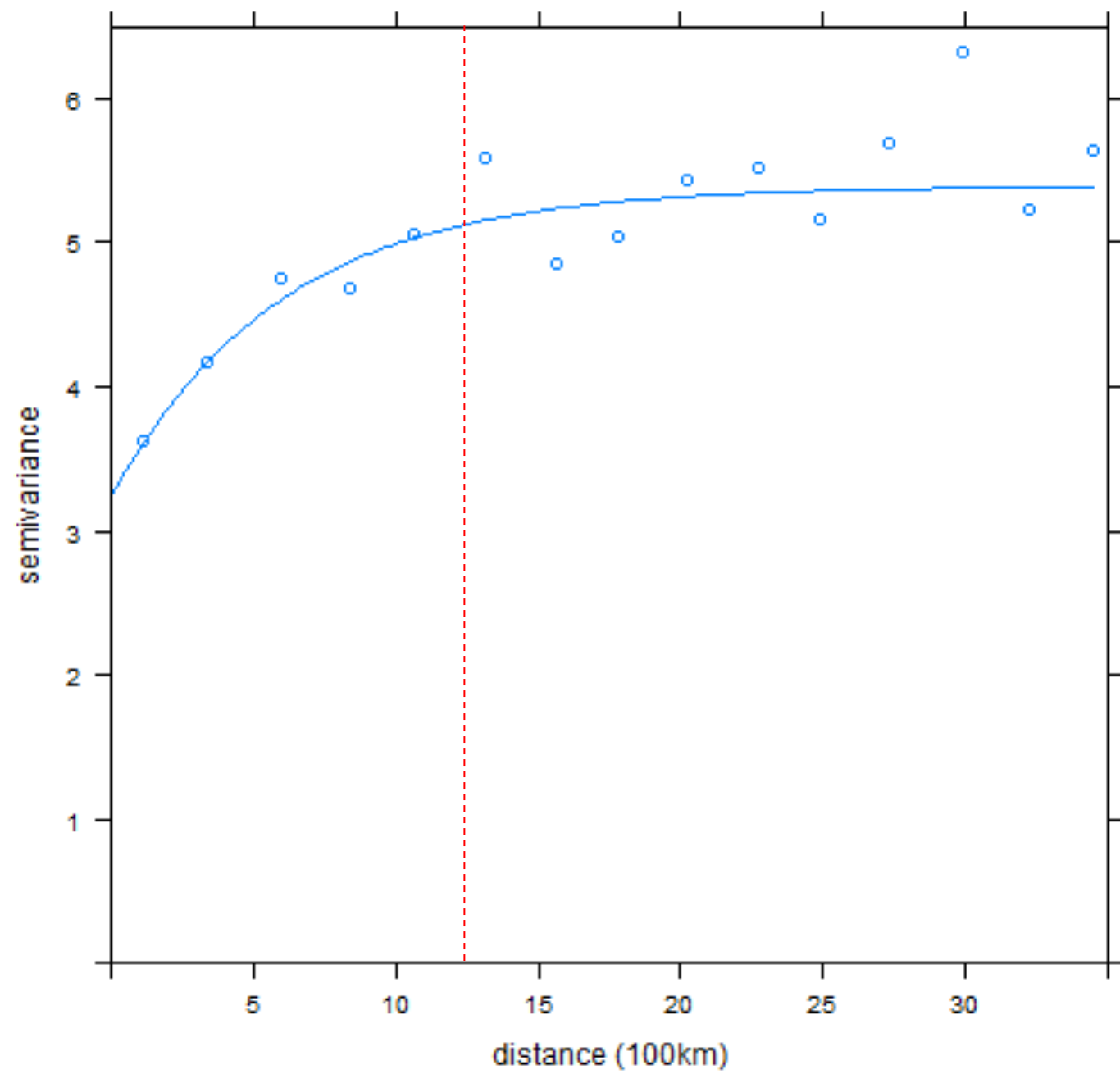
2012_9,10,11



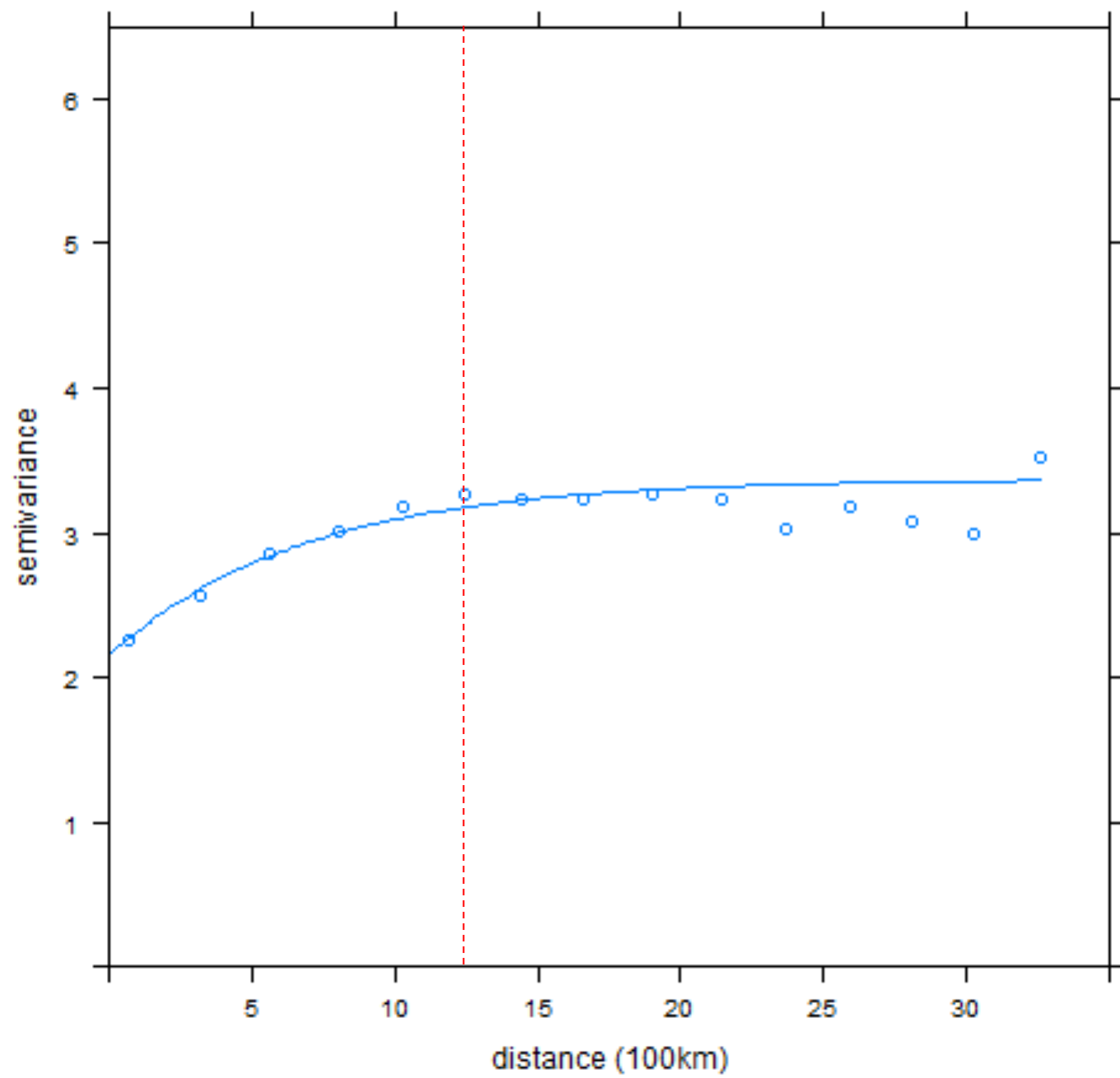
2012_12,1,2



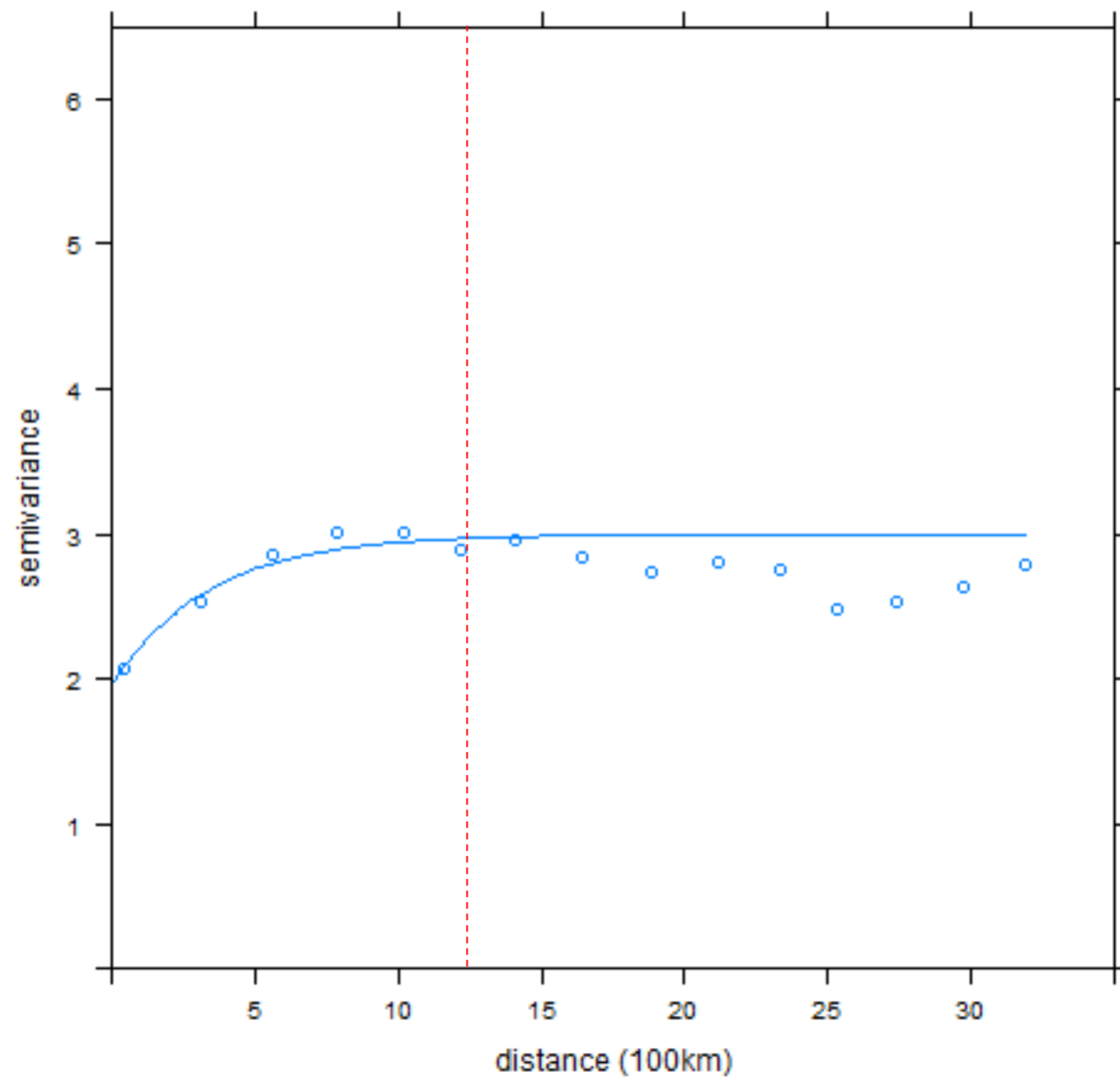
2013_3,4,5



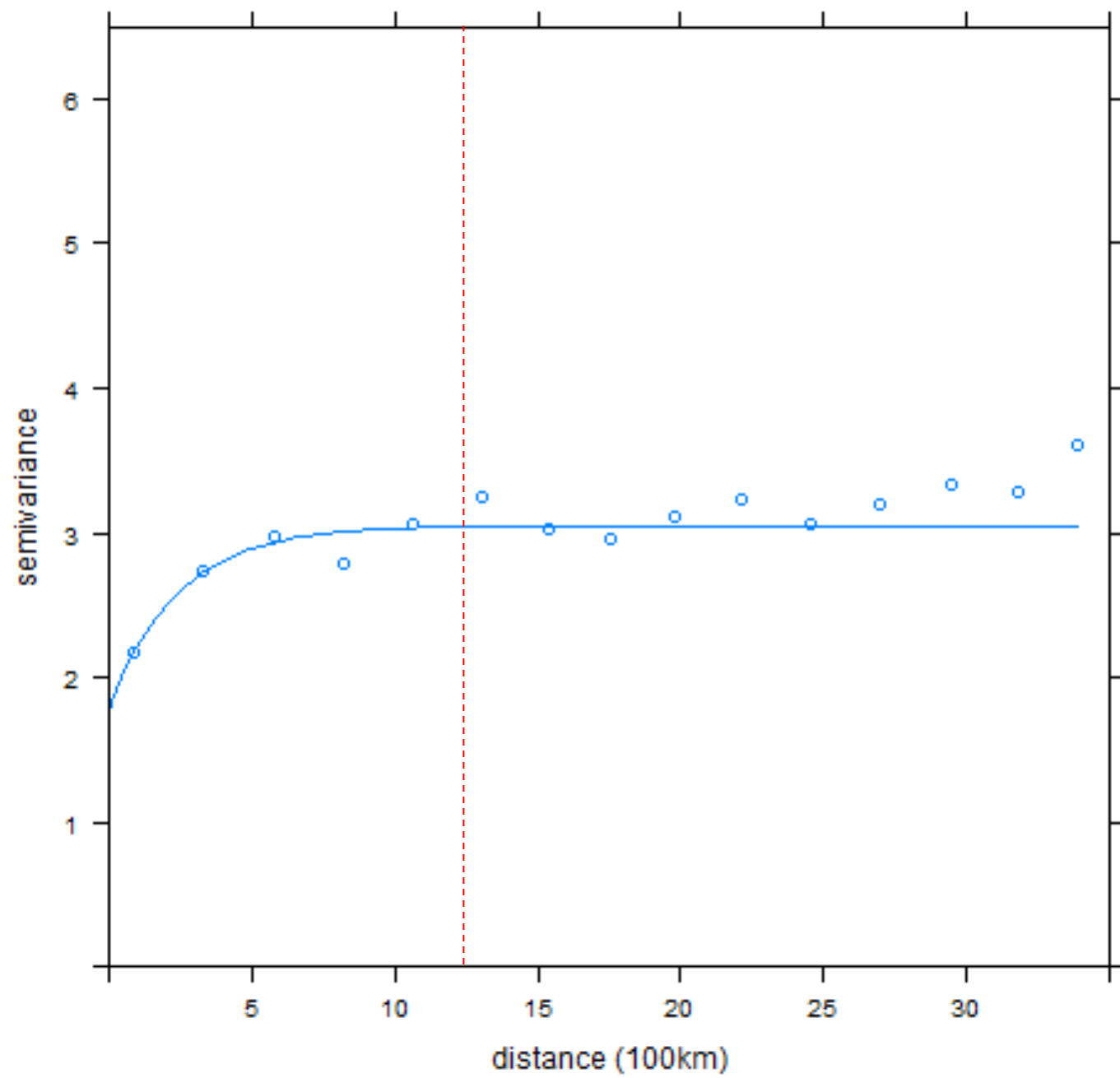
2013_6,7,8



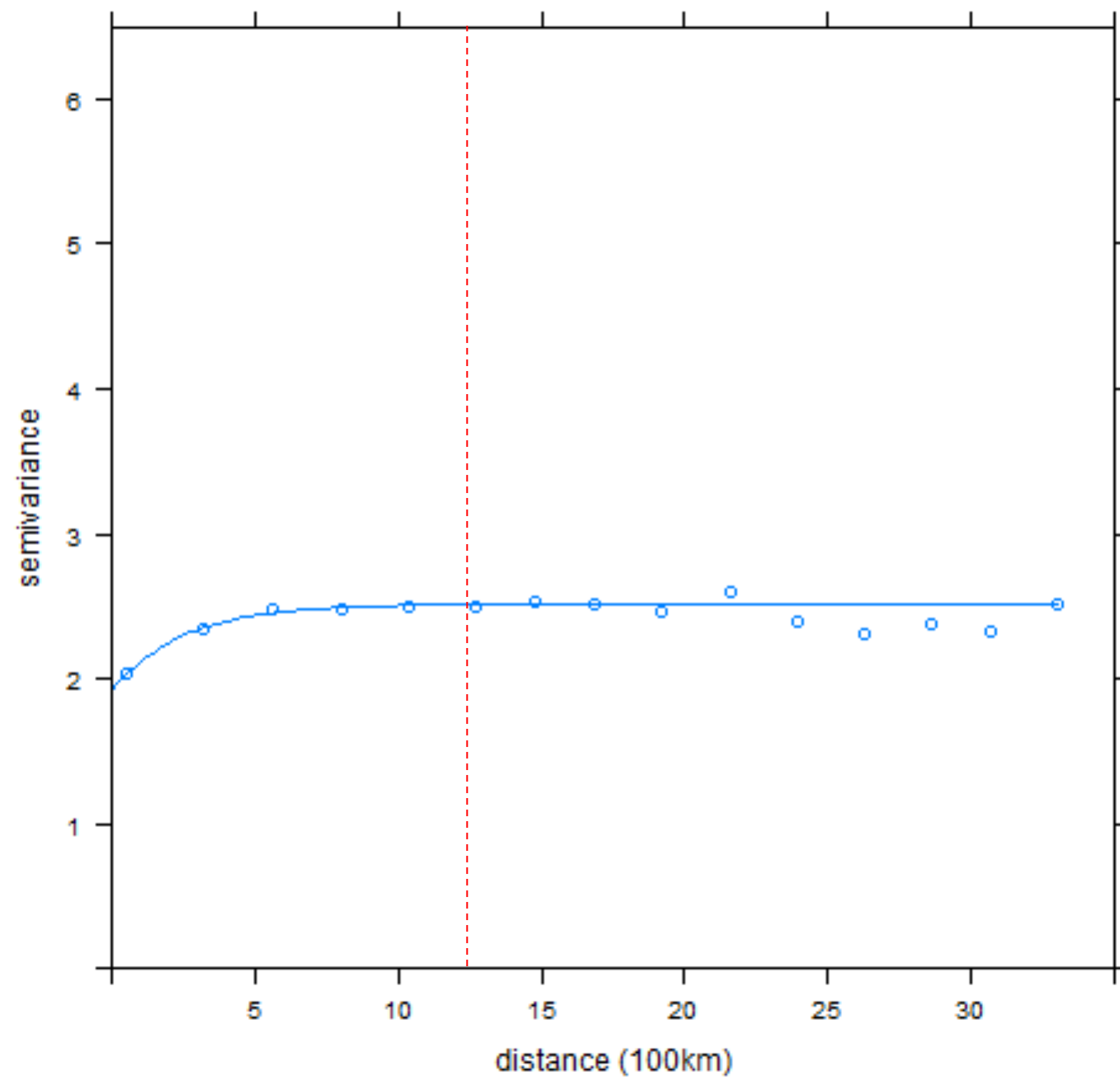
2013_9,10,11



2013_12,1,2

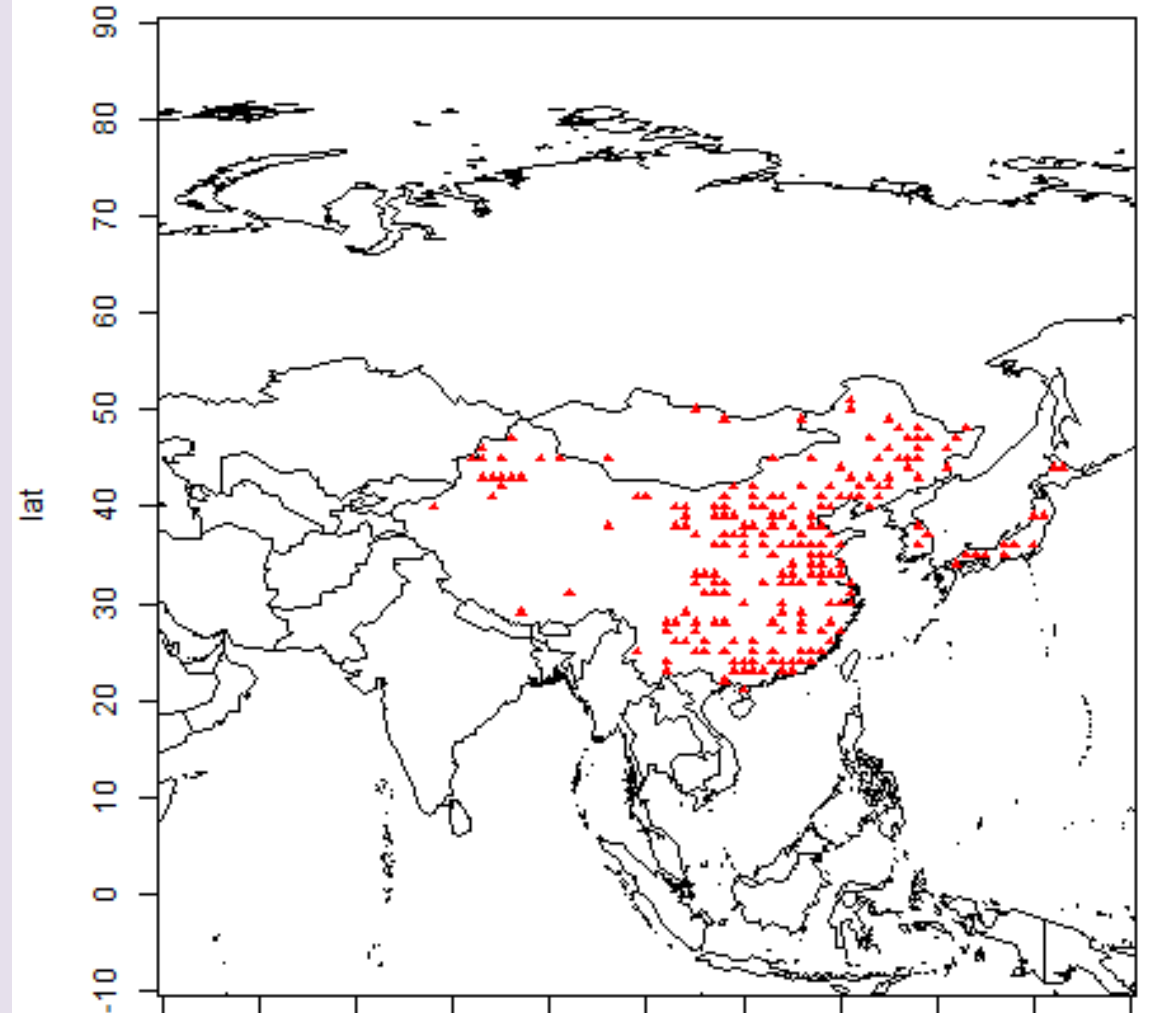


2014_3,4,5

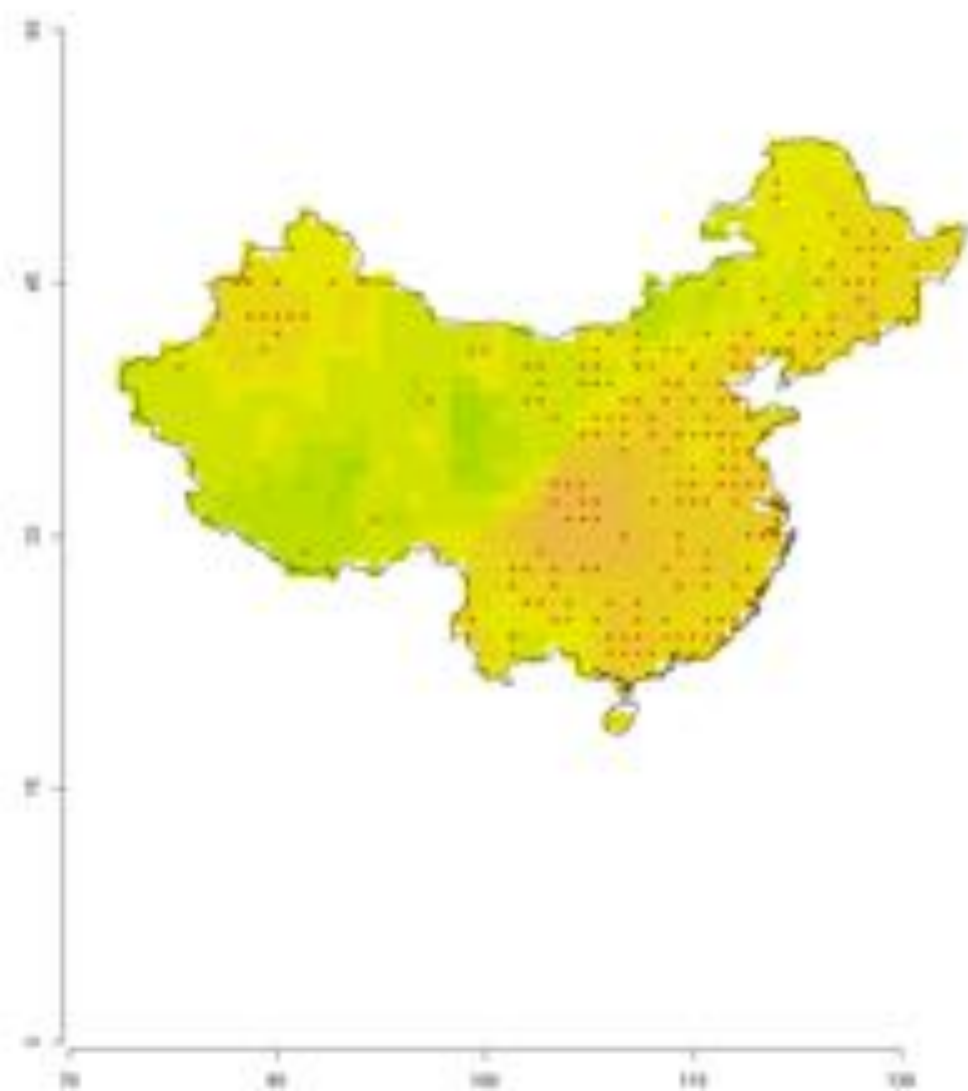


Spatial distribution of XCO₂ estimates and kriging variance

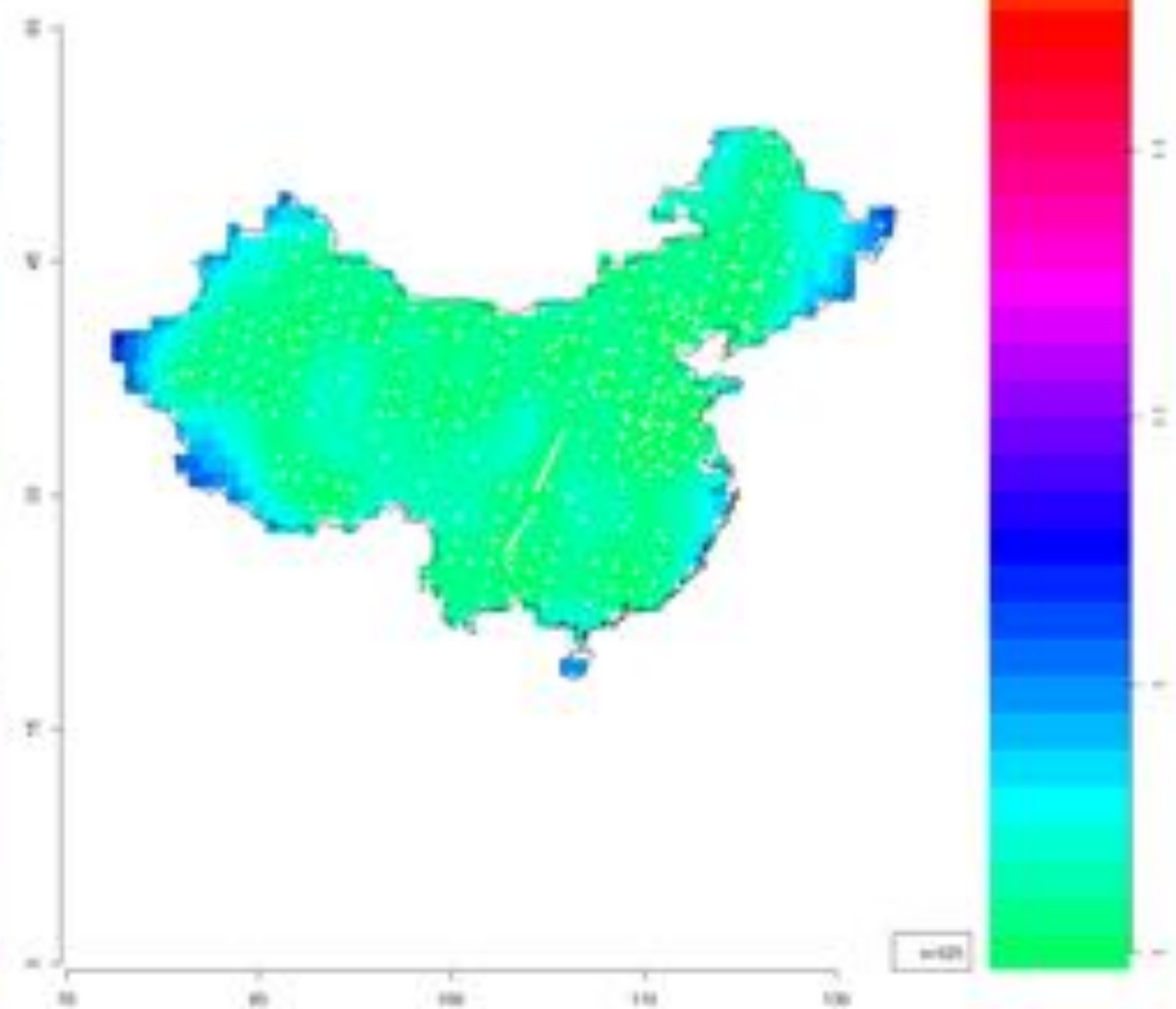
Night-time image of the Suomi NPP satellite



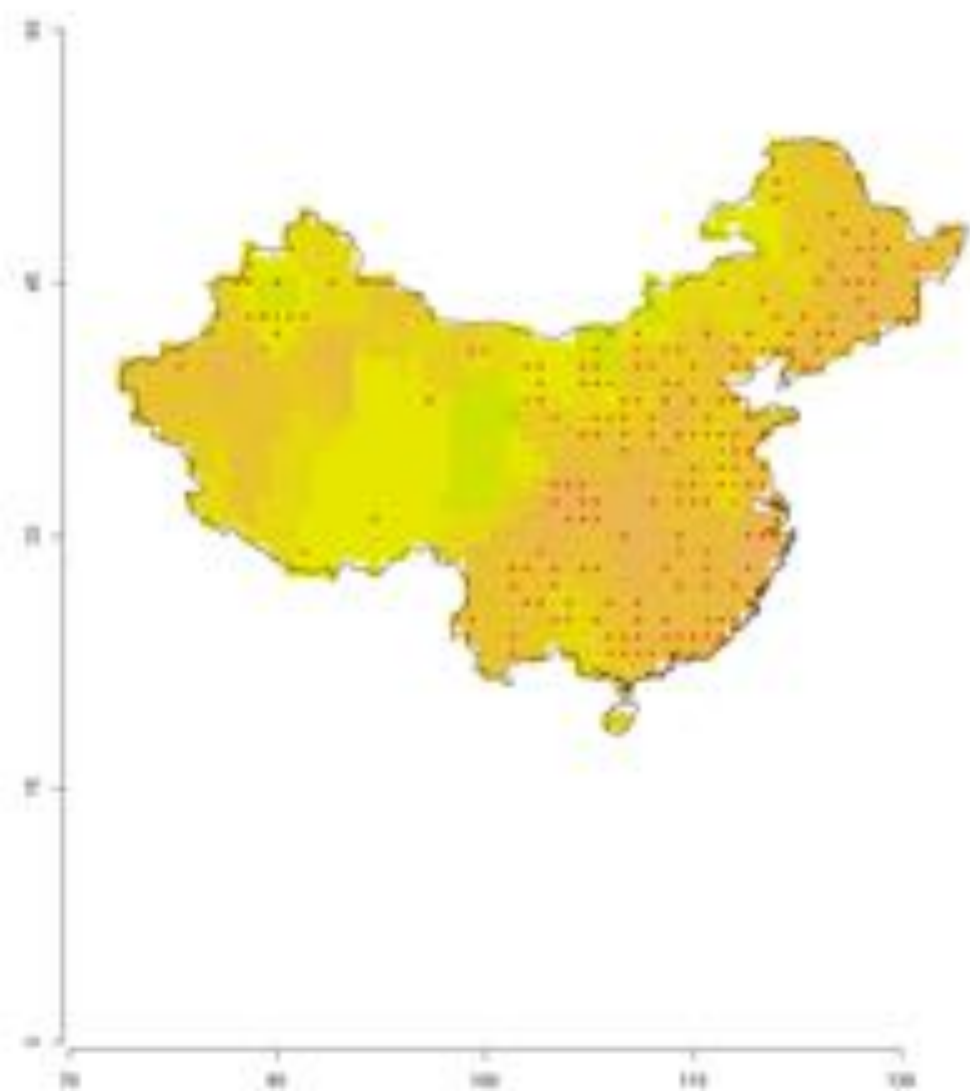
Pred_sst_130_2008



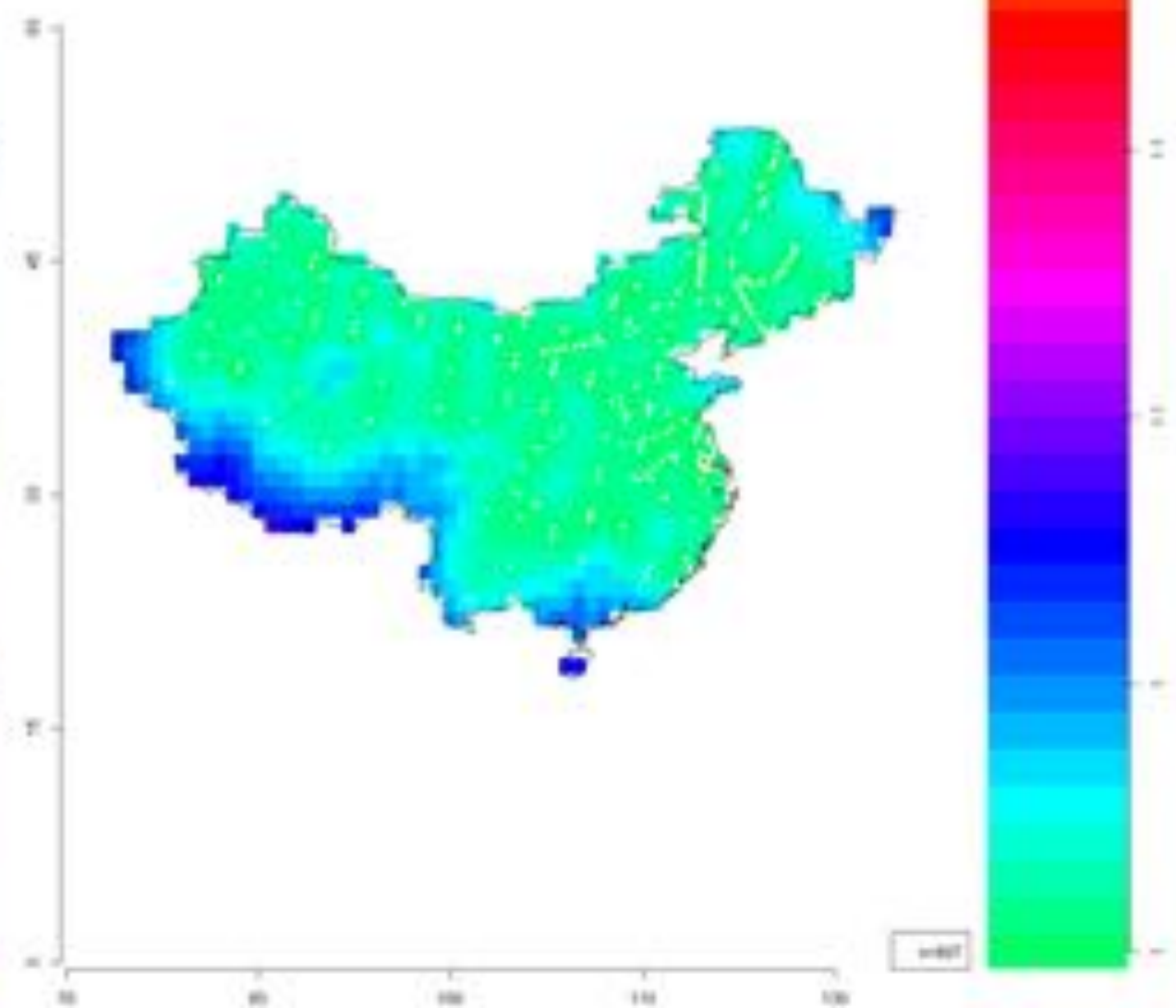
Vw_sst_130_2008



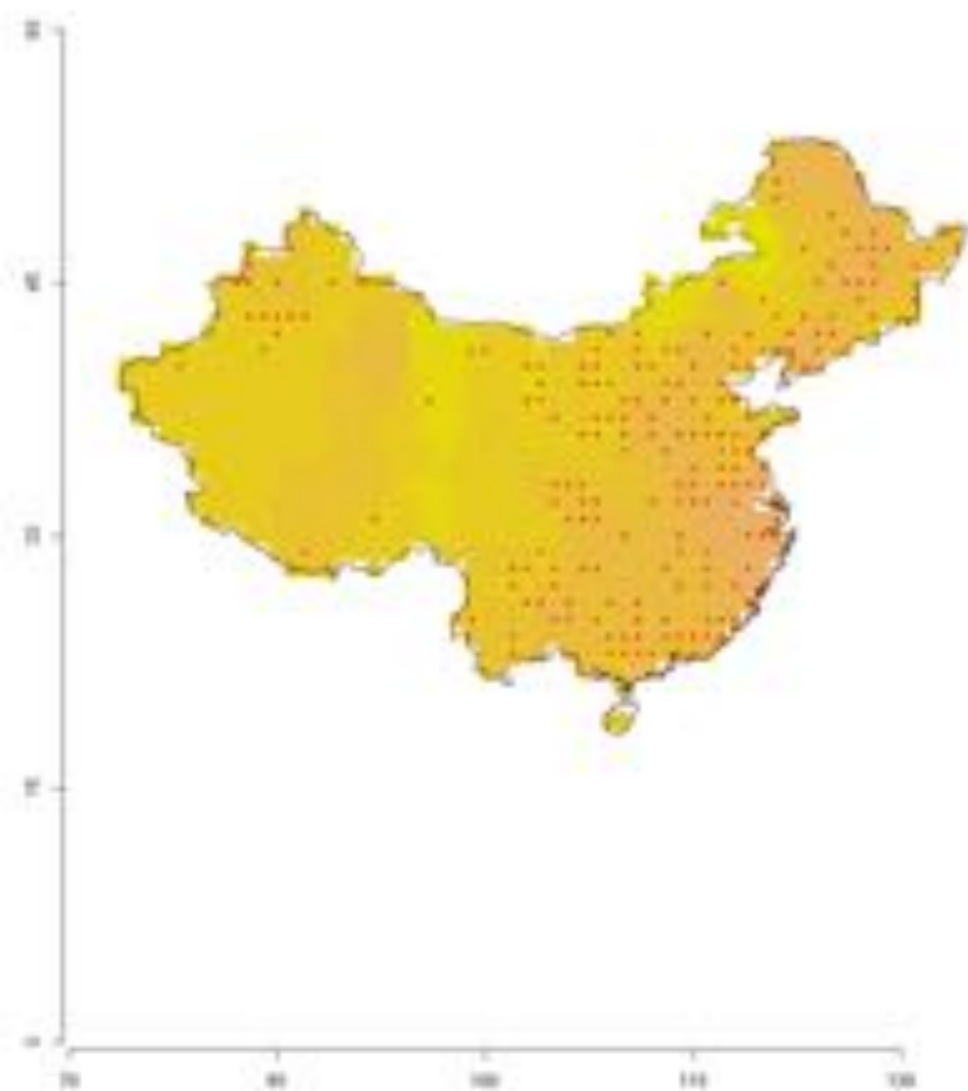
Pred_sar1_s30_2010



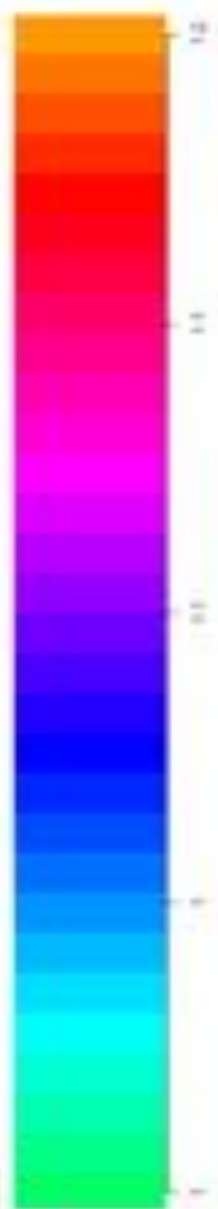
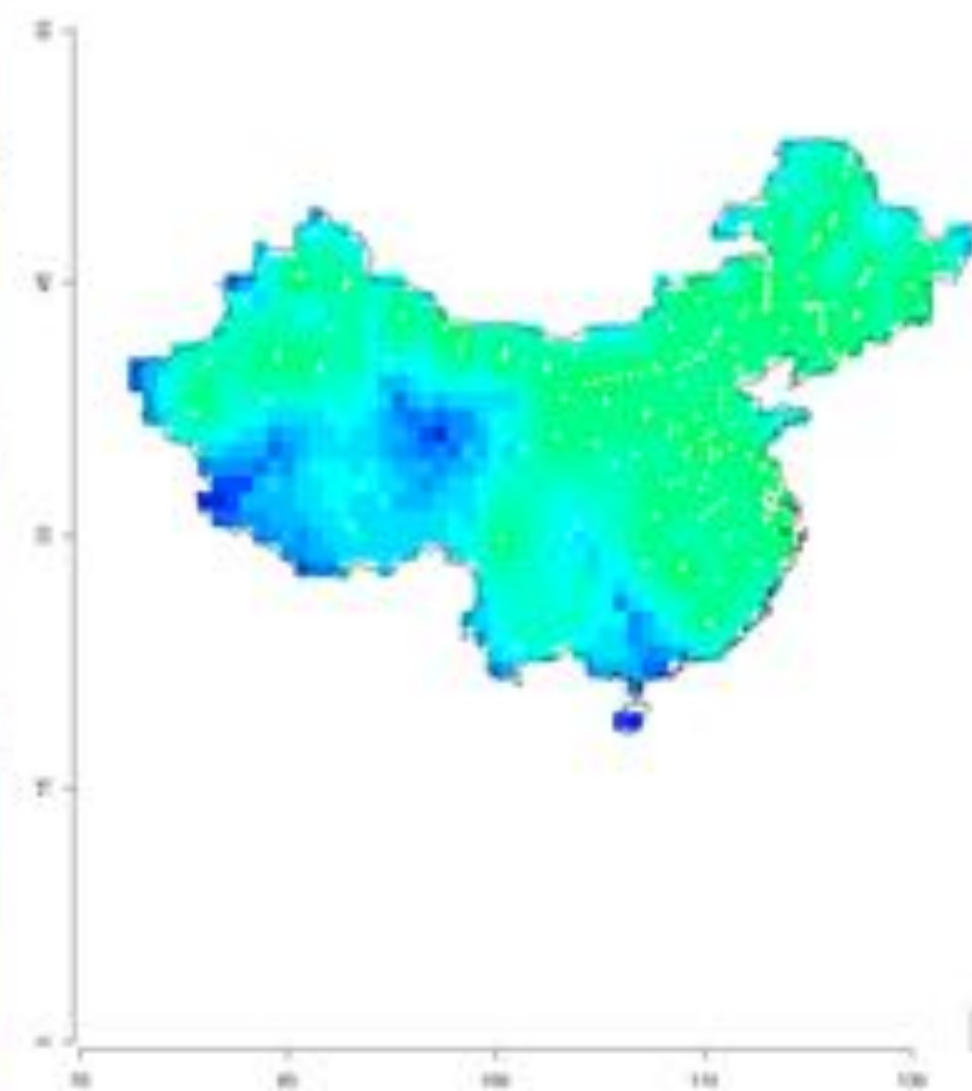
Vw_sar1_s30_2010



Pre0_sst_100_2011

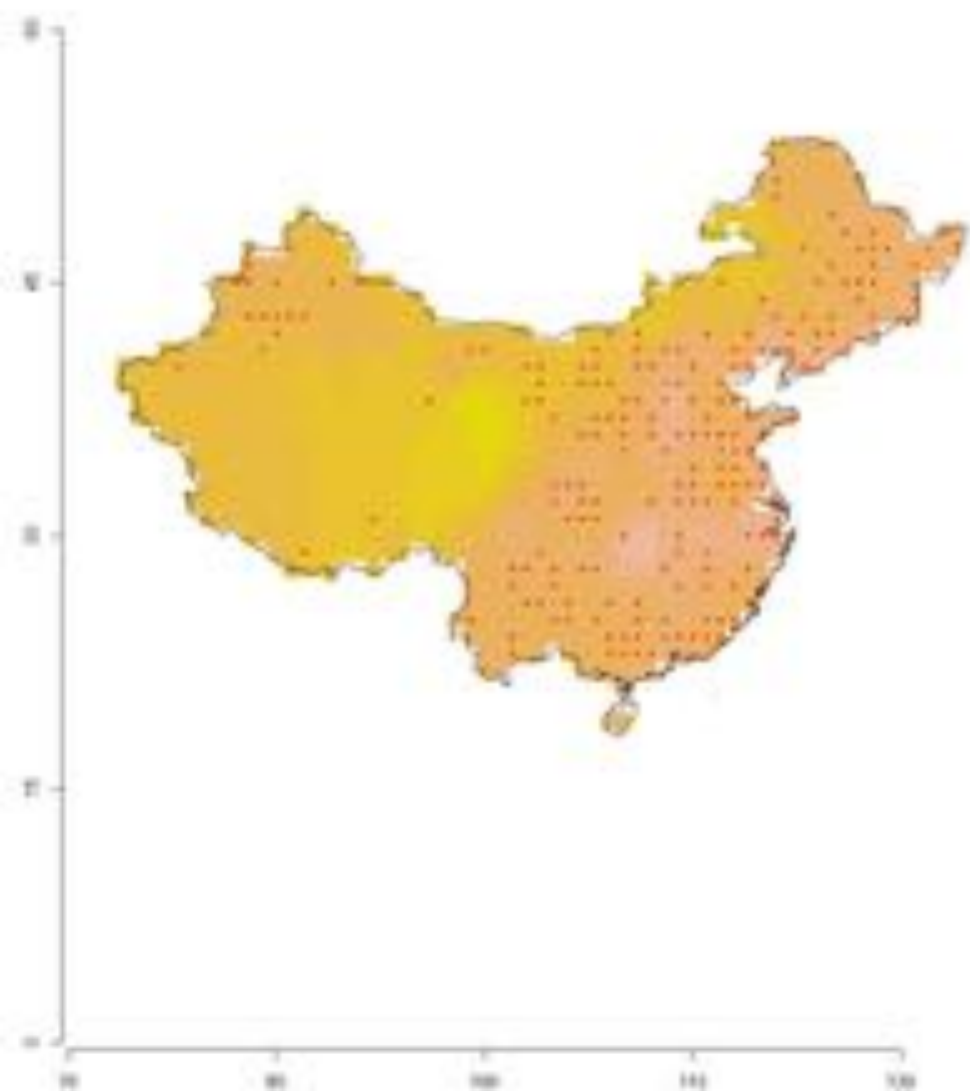


Nw_sst_100_2011

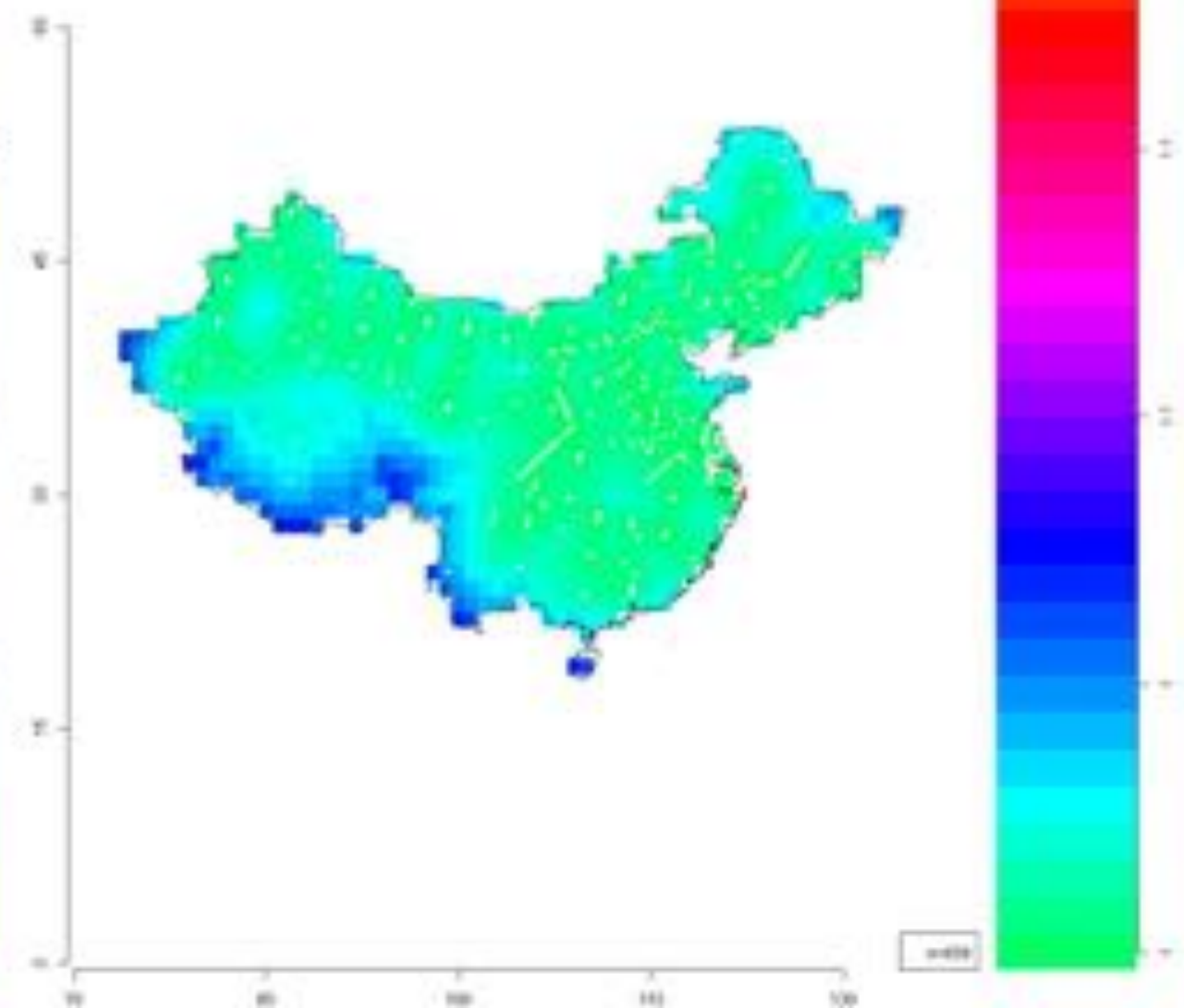


0.001

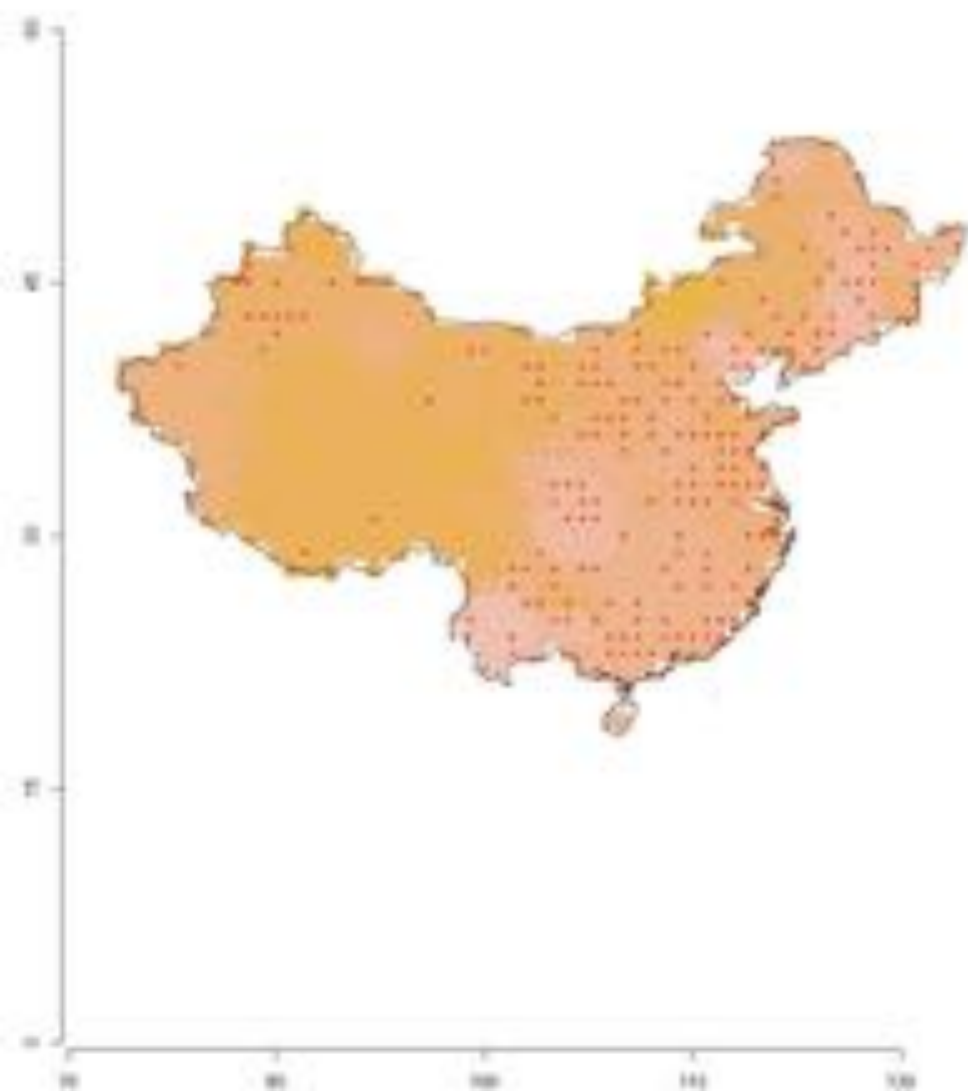
Pind_ghg_c30_2012



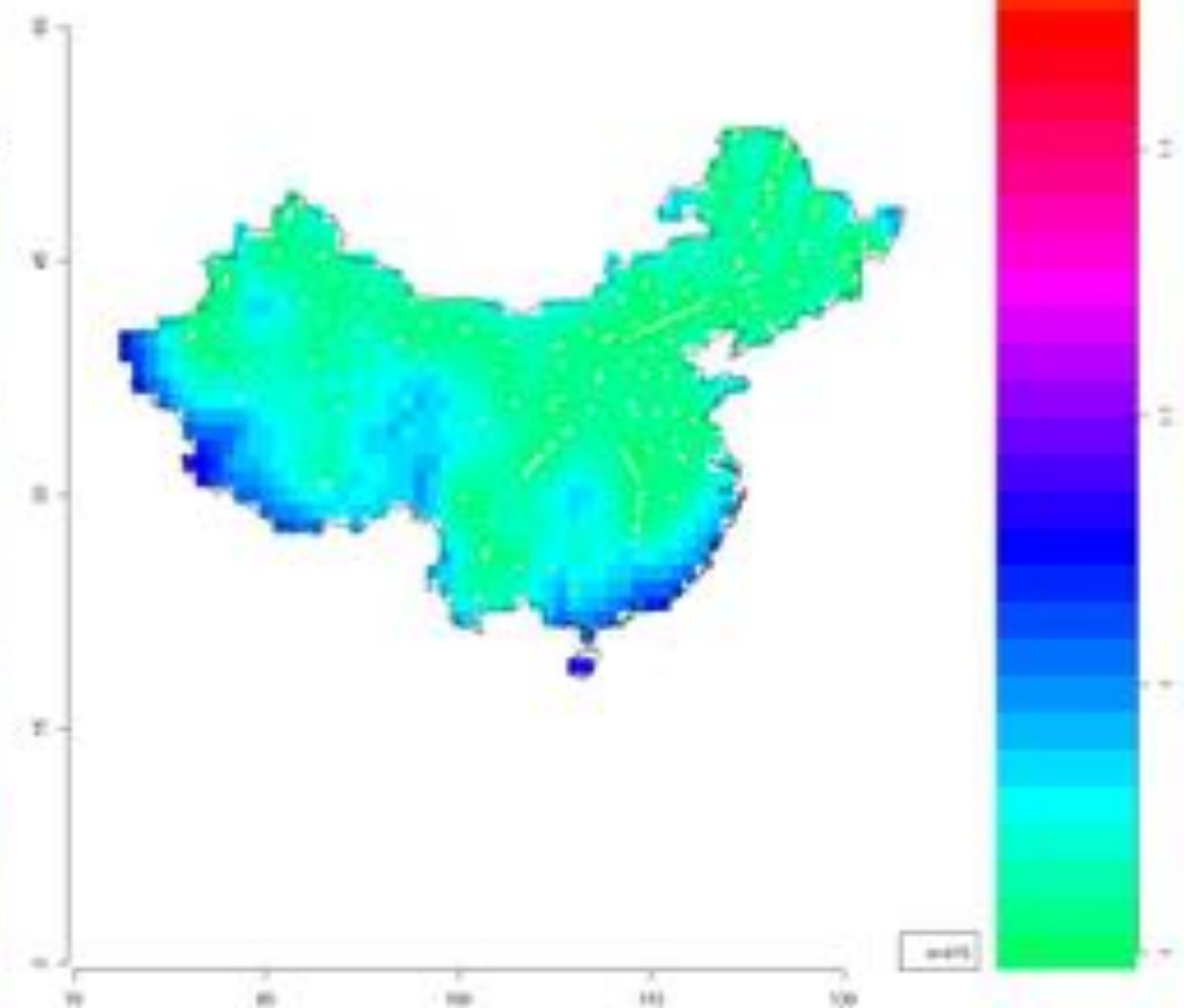
Vw_ghg_c30_2012



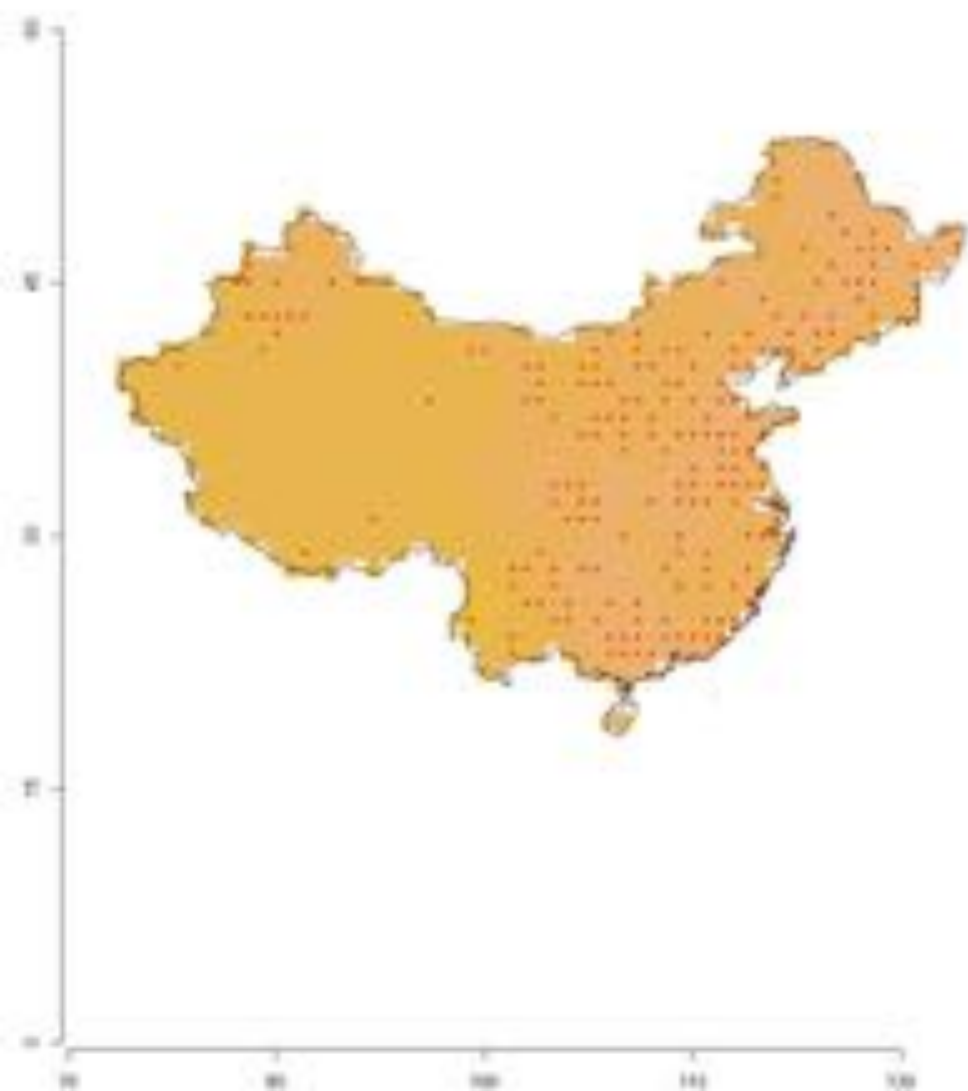
Pind_smt_c30_2013



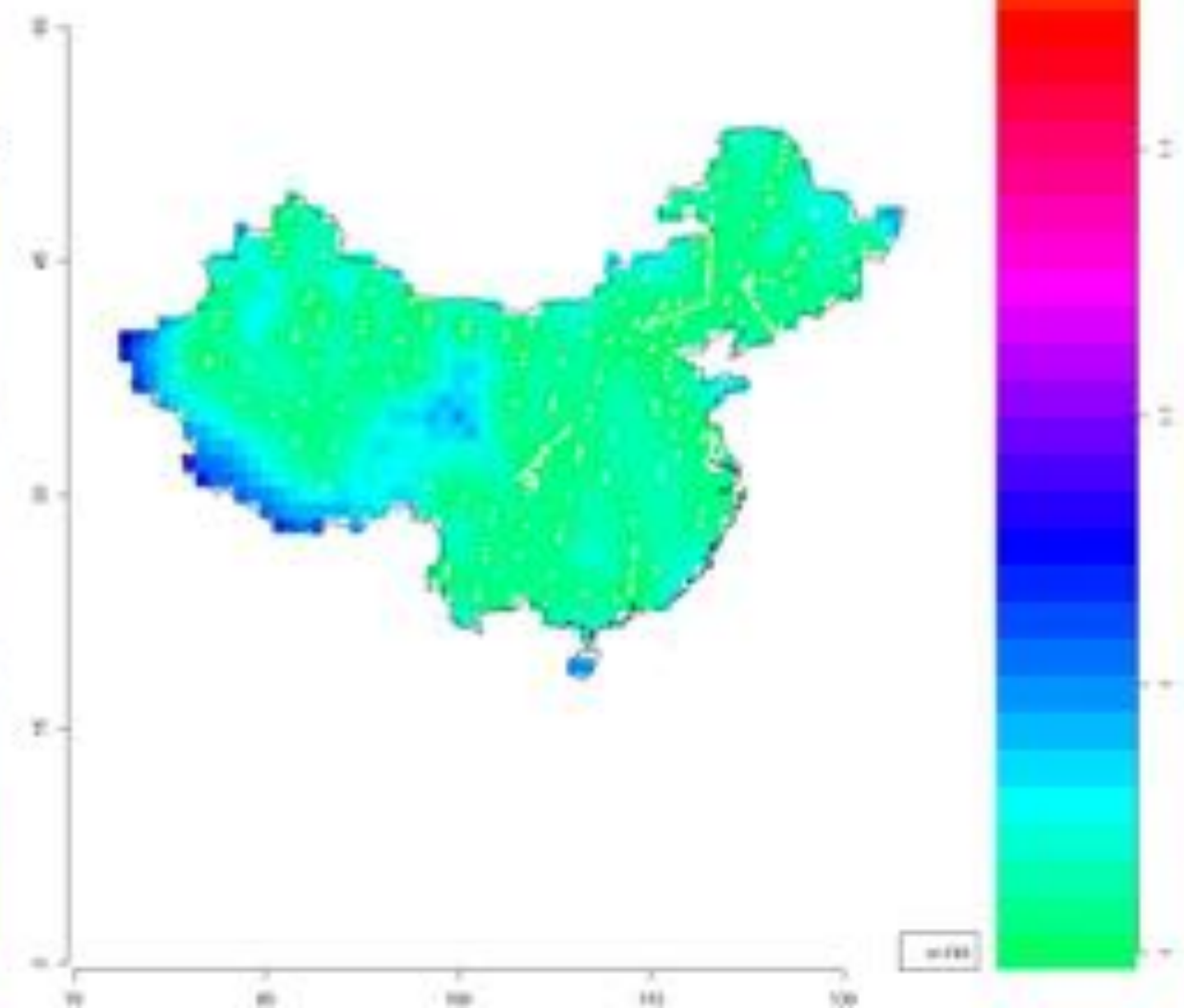
Vw_smt_c30_2013



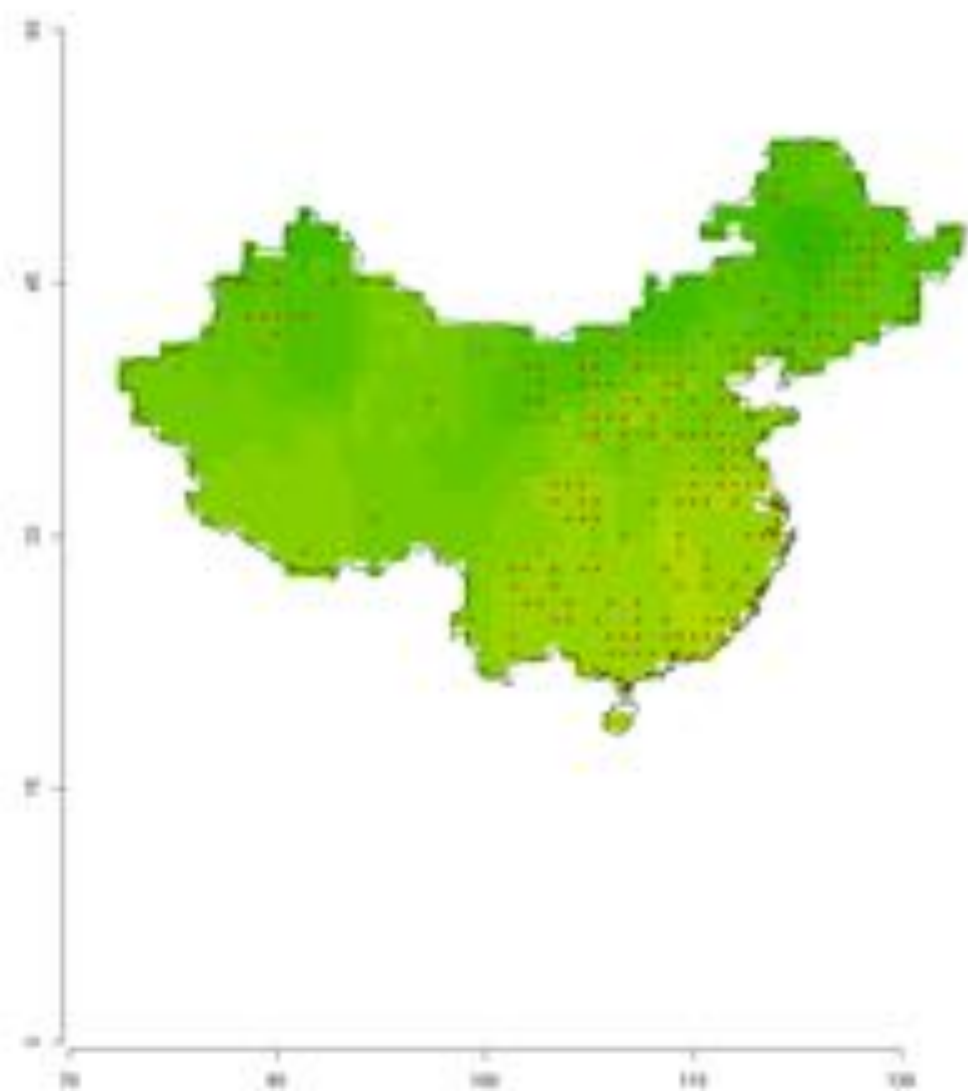
PM_{2.5}_aht_c30_2014



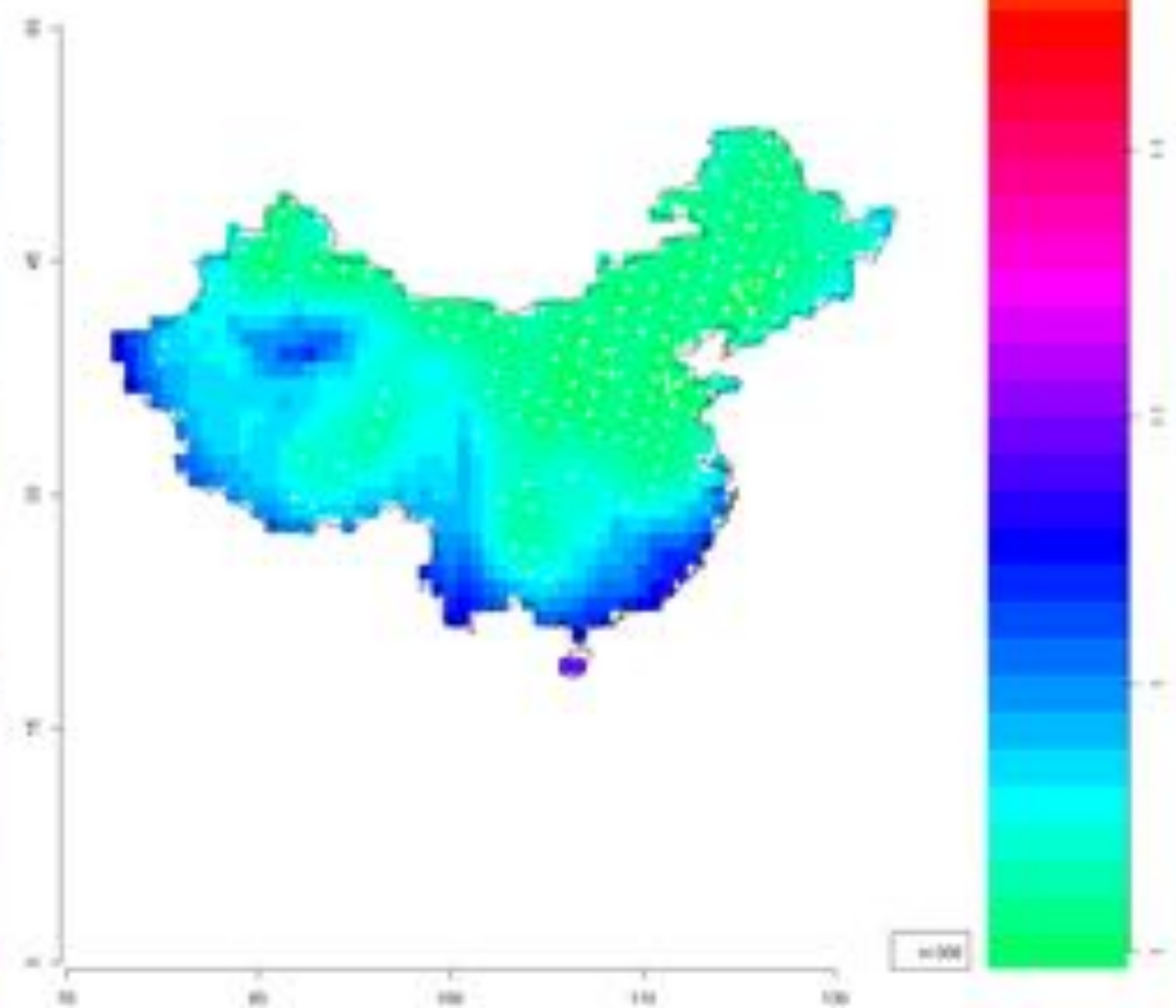
VW_aht_c30_2014



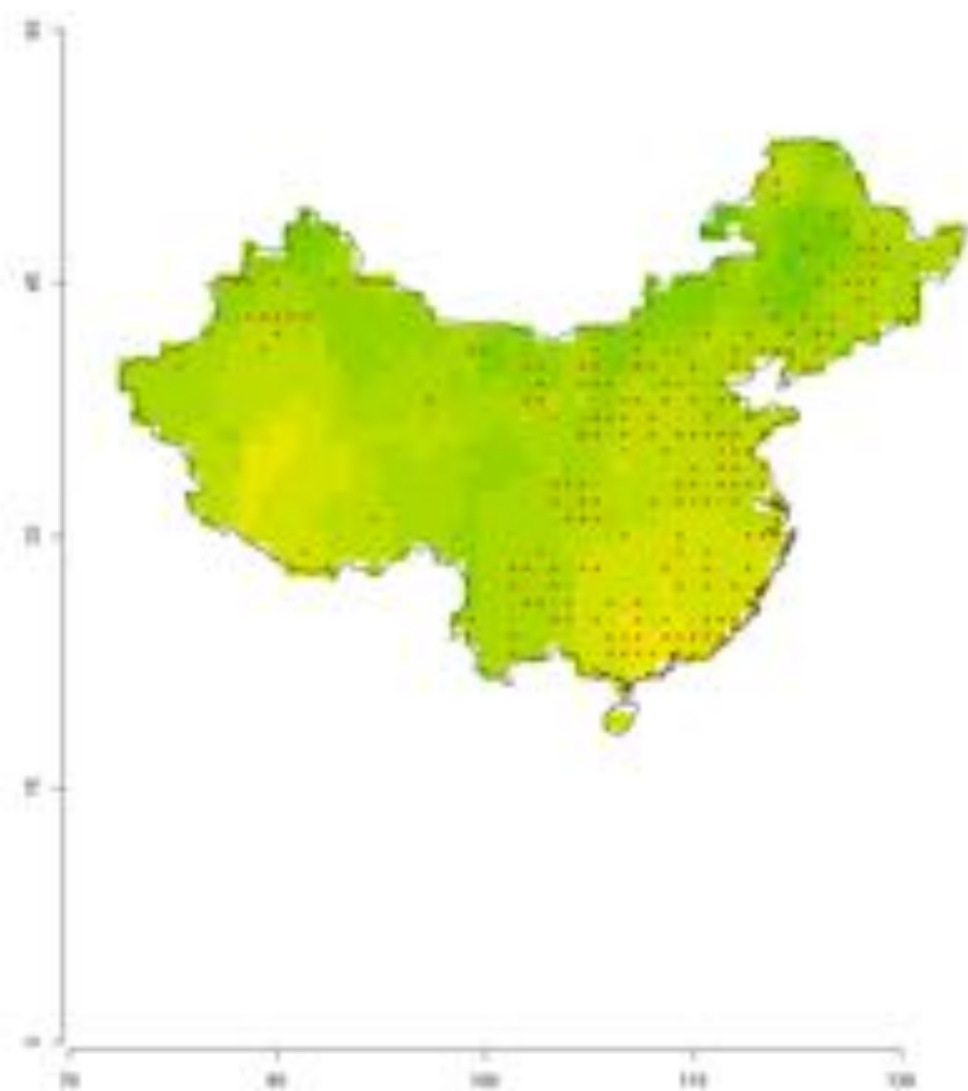
Pred_ao2_130_2008



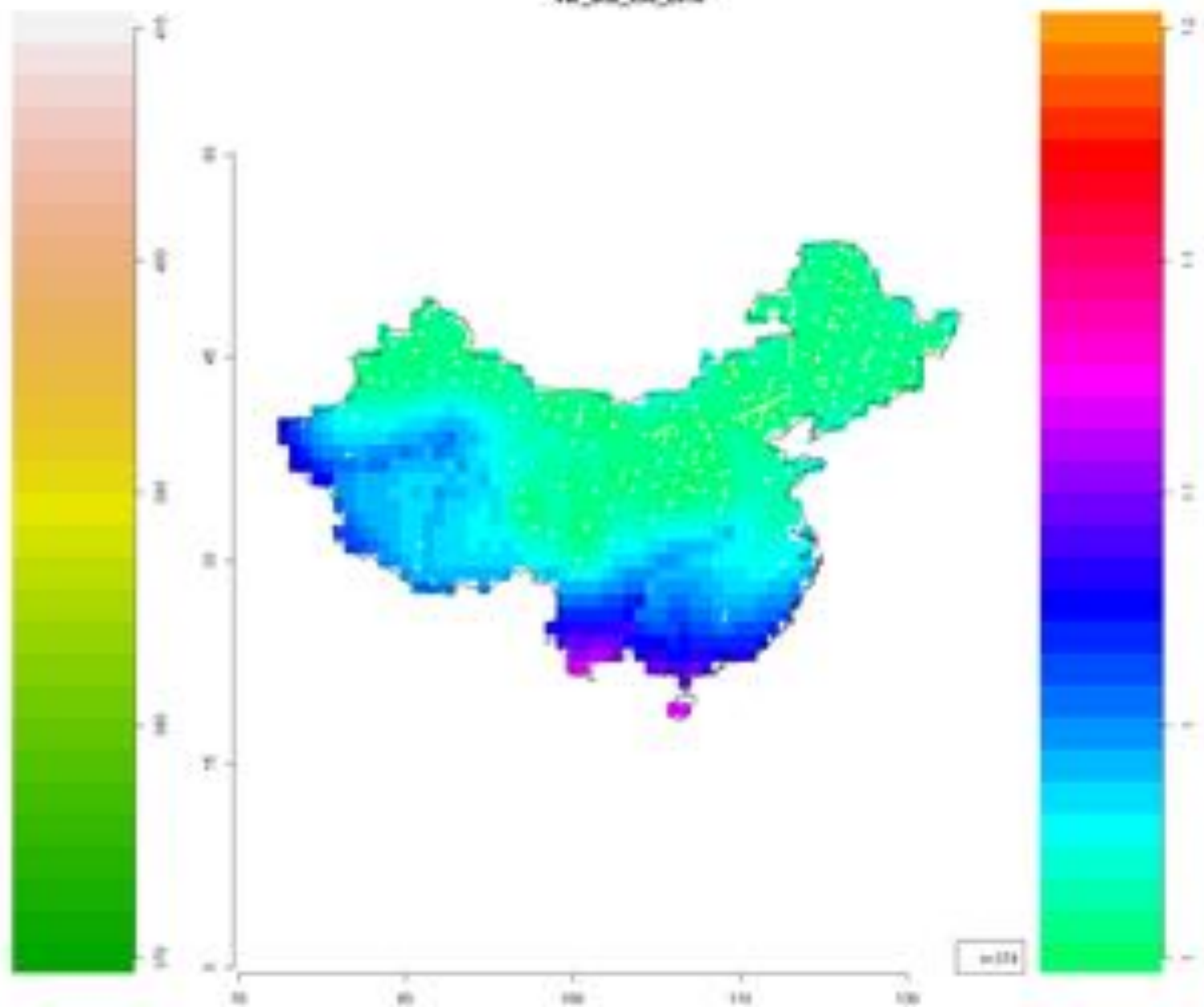
Vw_ao2_130_2008



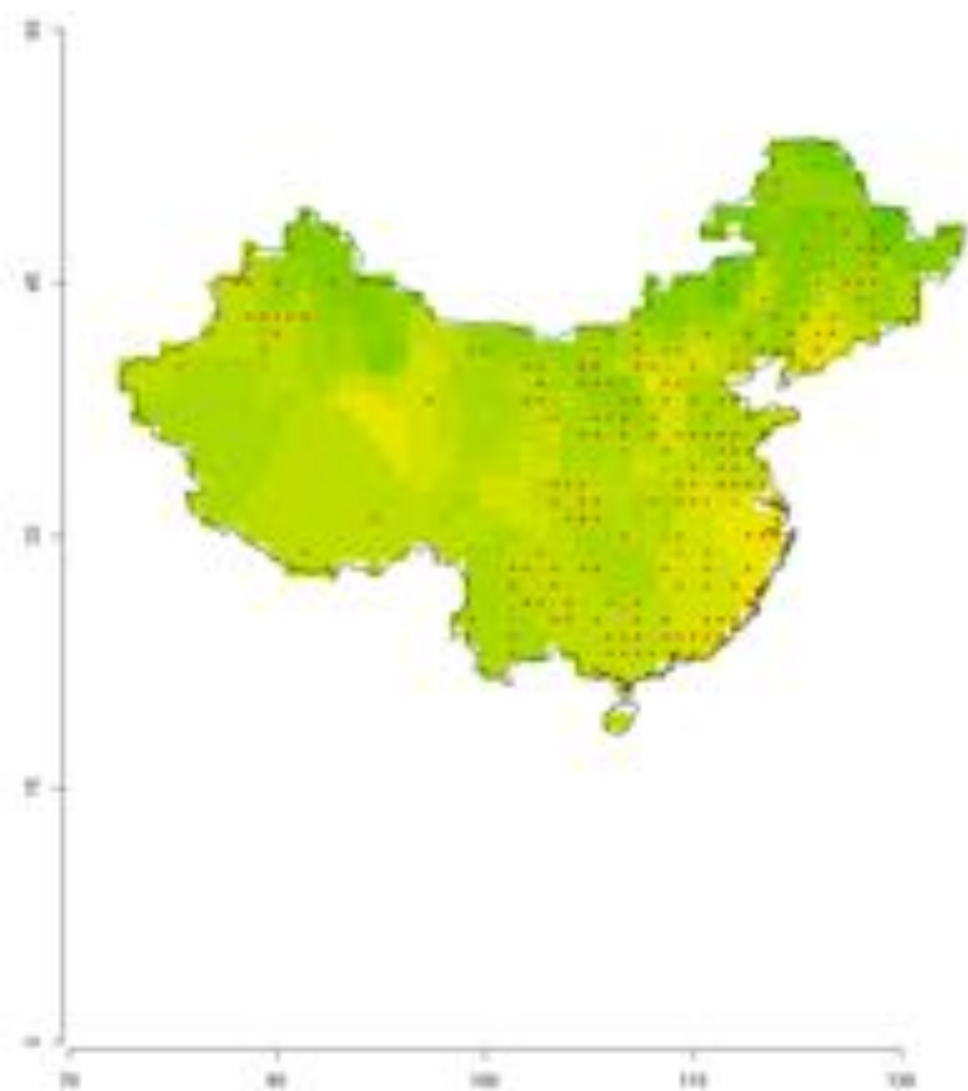
Pre0_ao2_100_2010



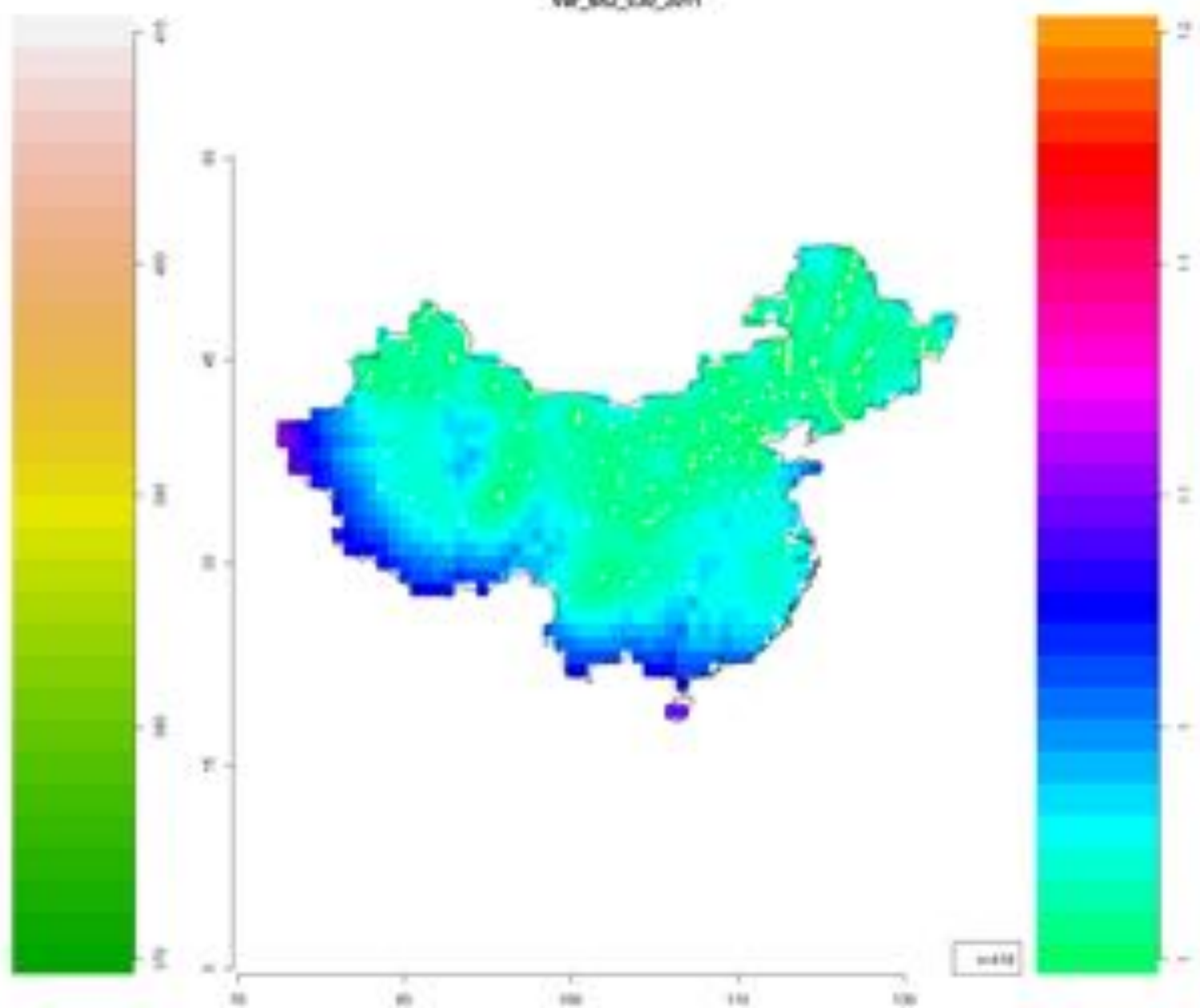
Nw_ao2_100_2010



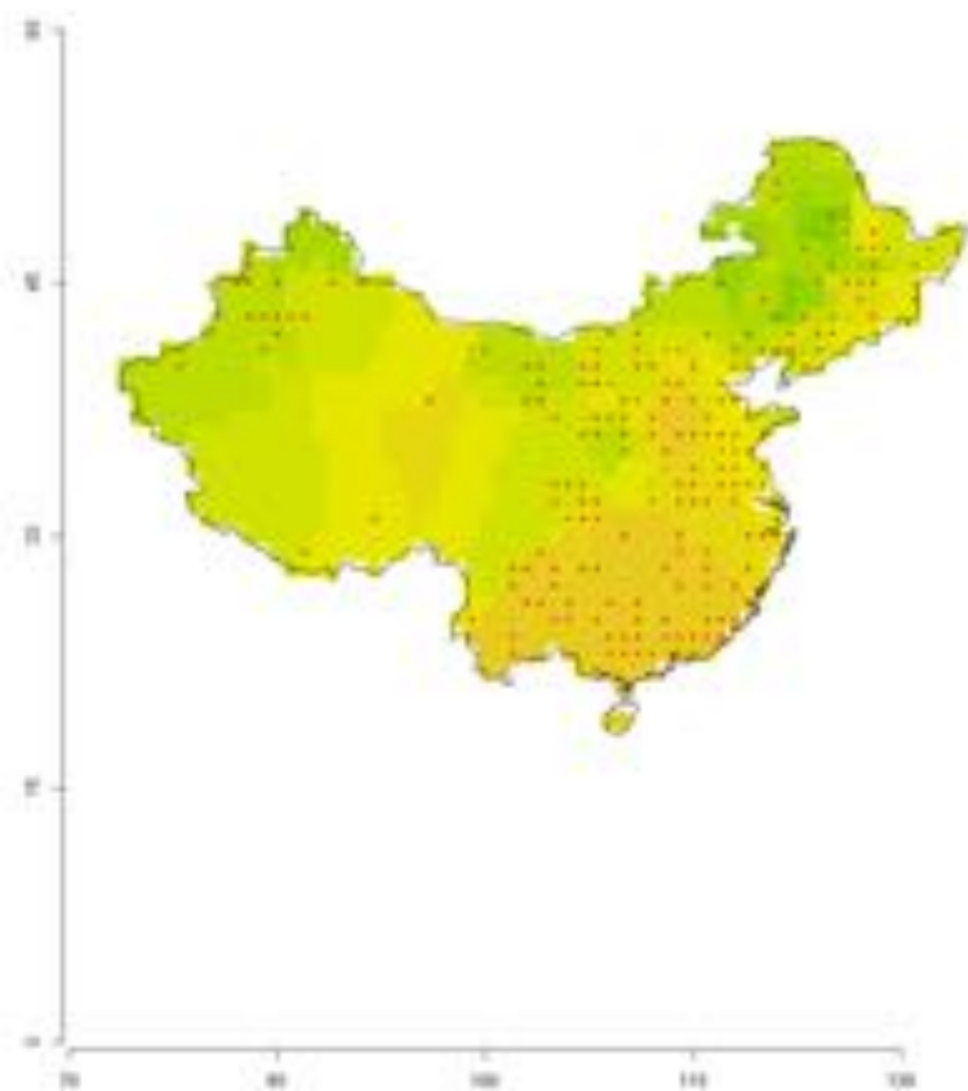
Pred_ao2_100_2011



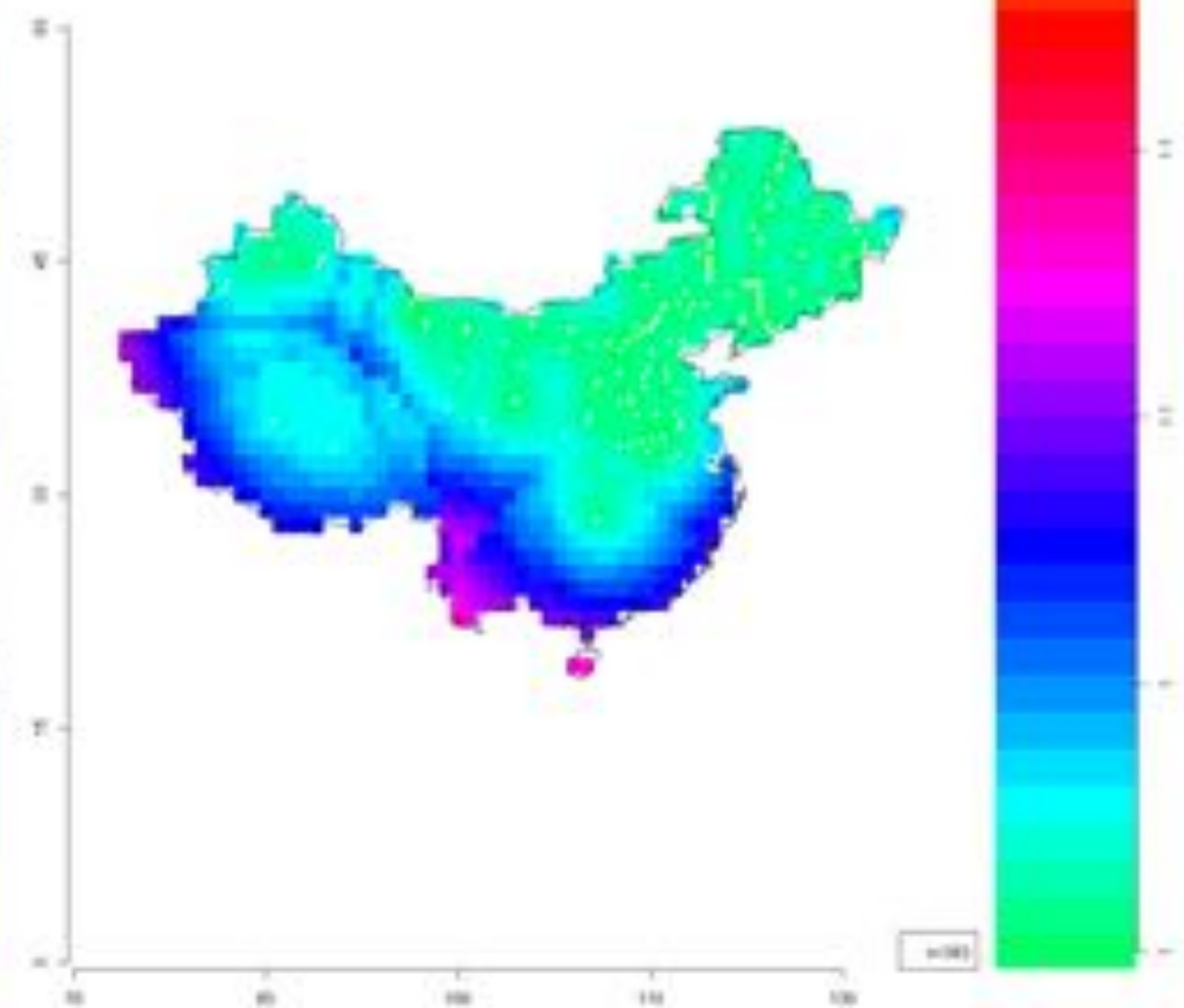
Nw_ao2_100_2011



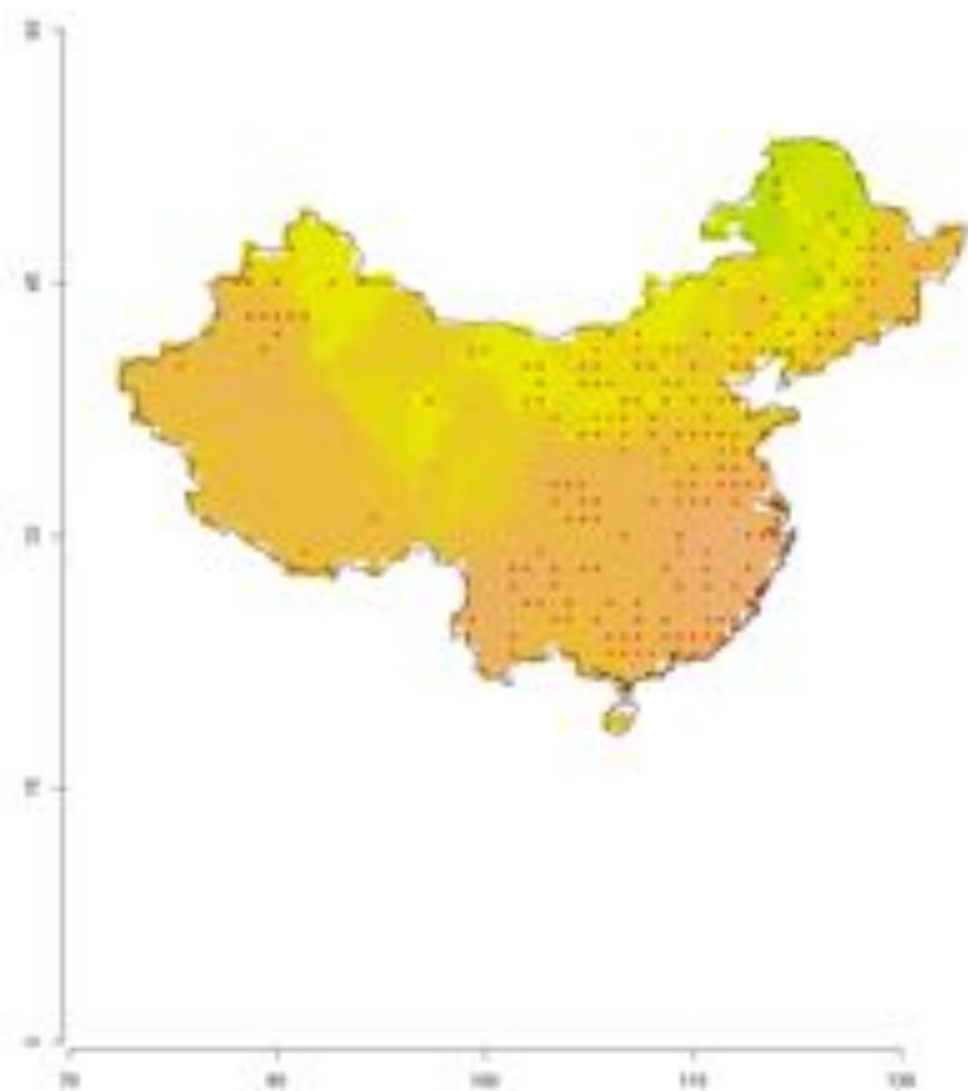
Pre0_ao2_100_2012



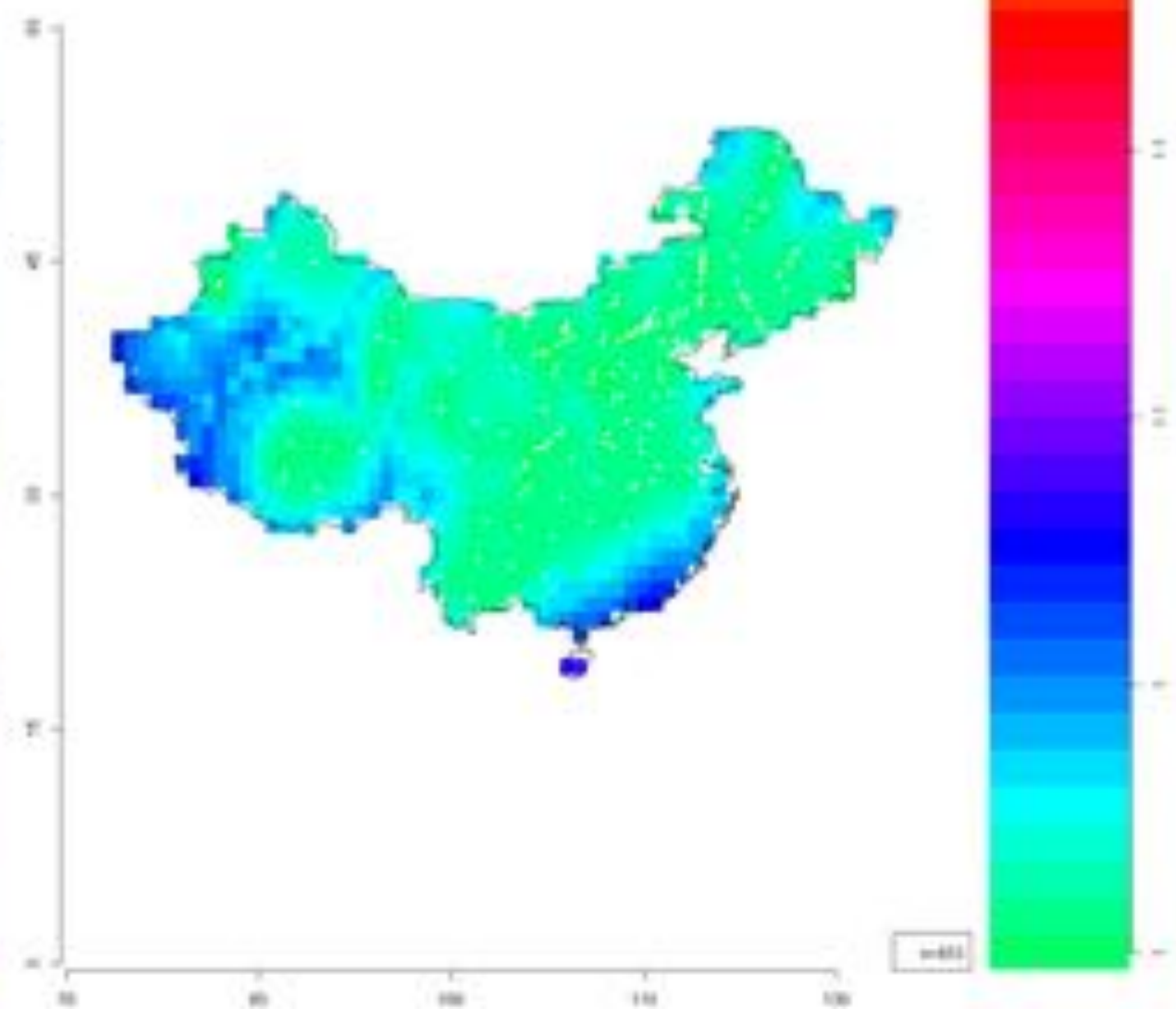
Nw_ao2_100_2012



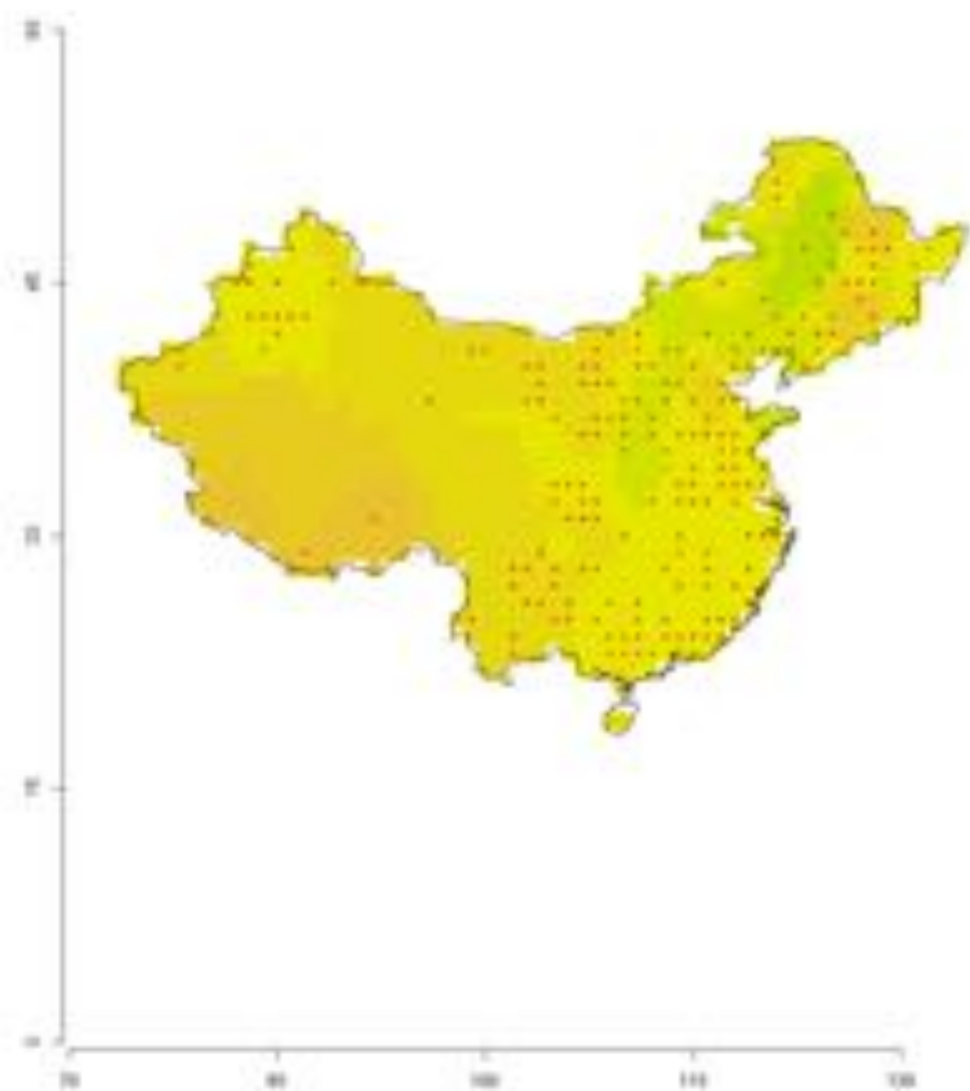
Pred_m02_100_2013



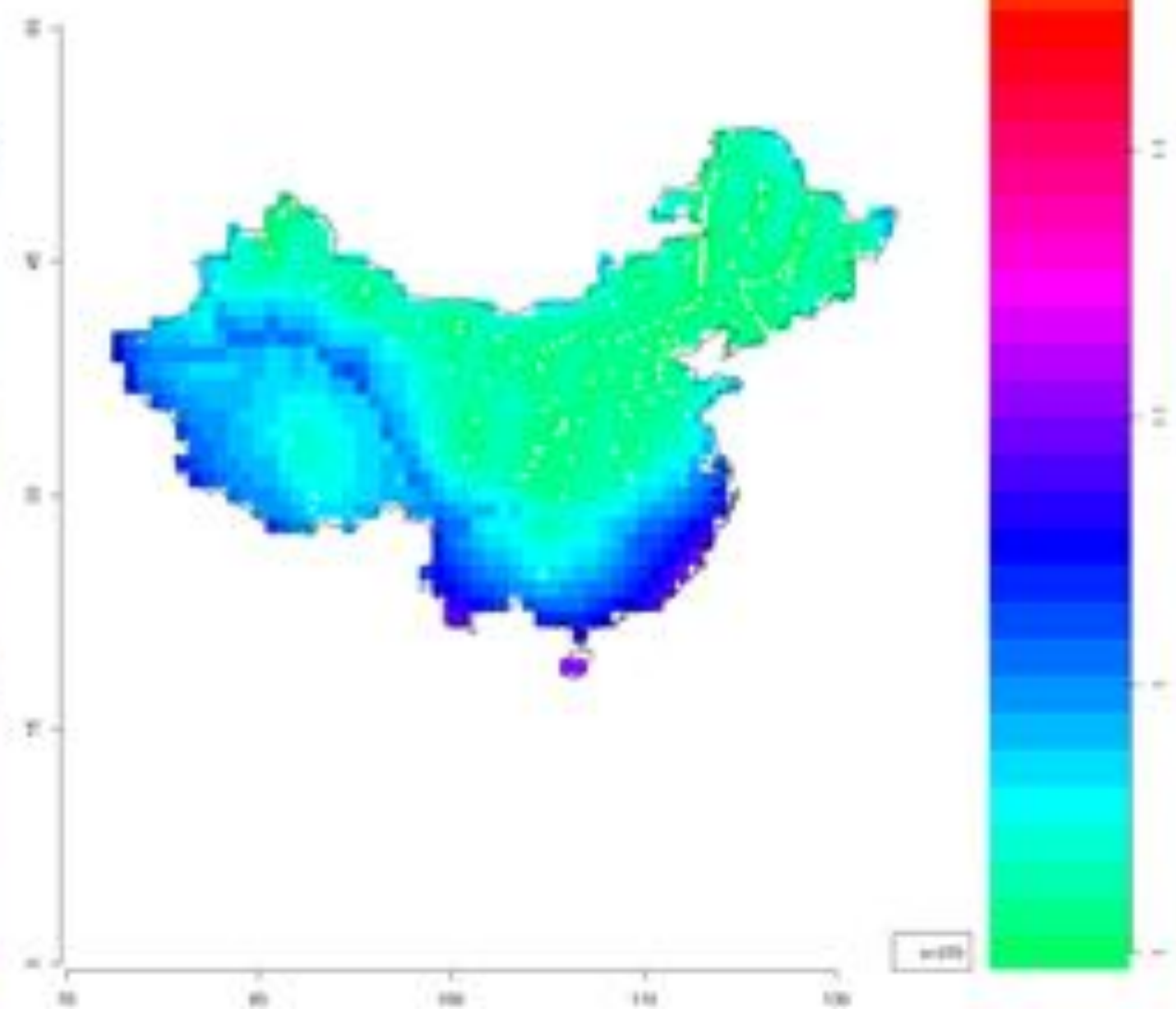
Nw_m02_100_2013



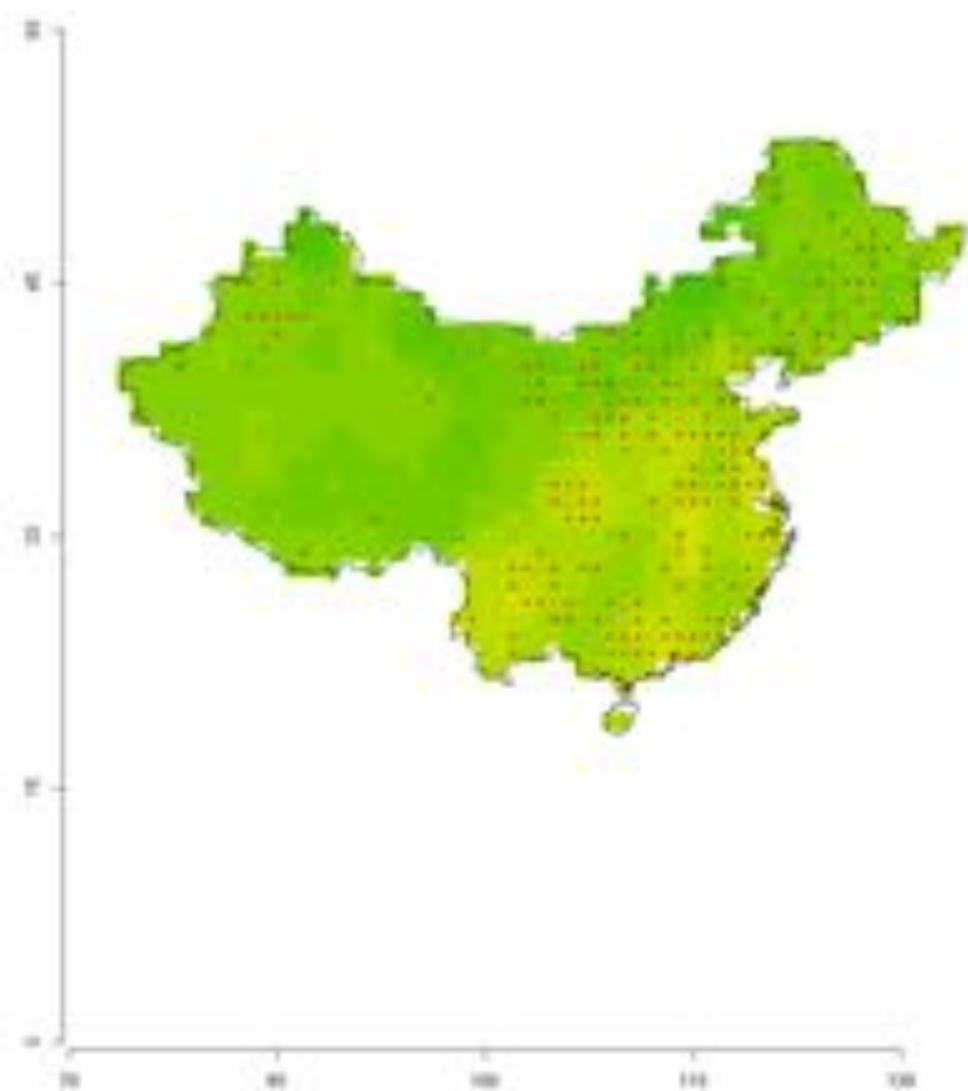
Pred_ao2_100_2014



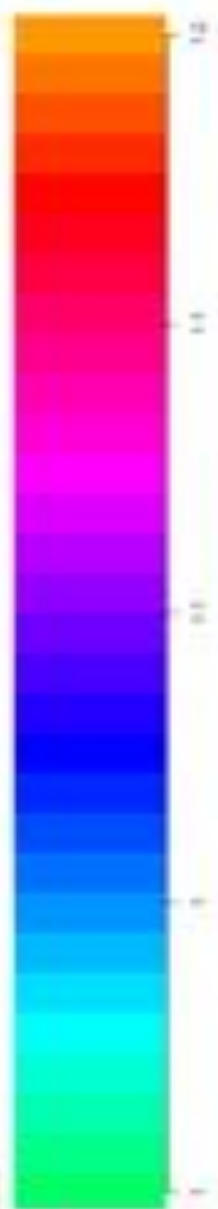
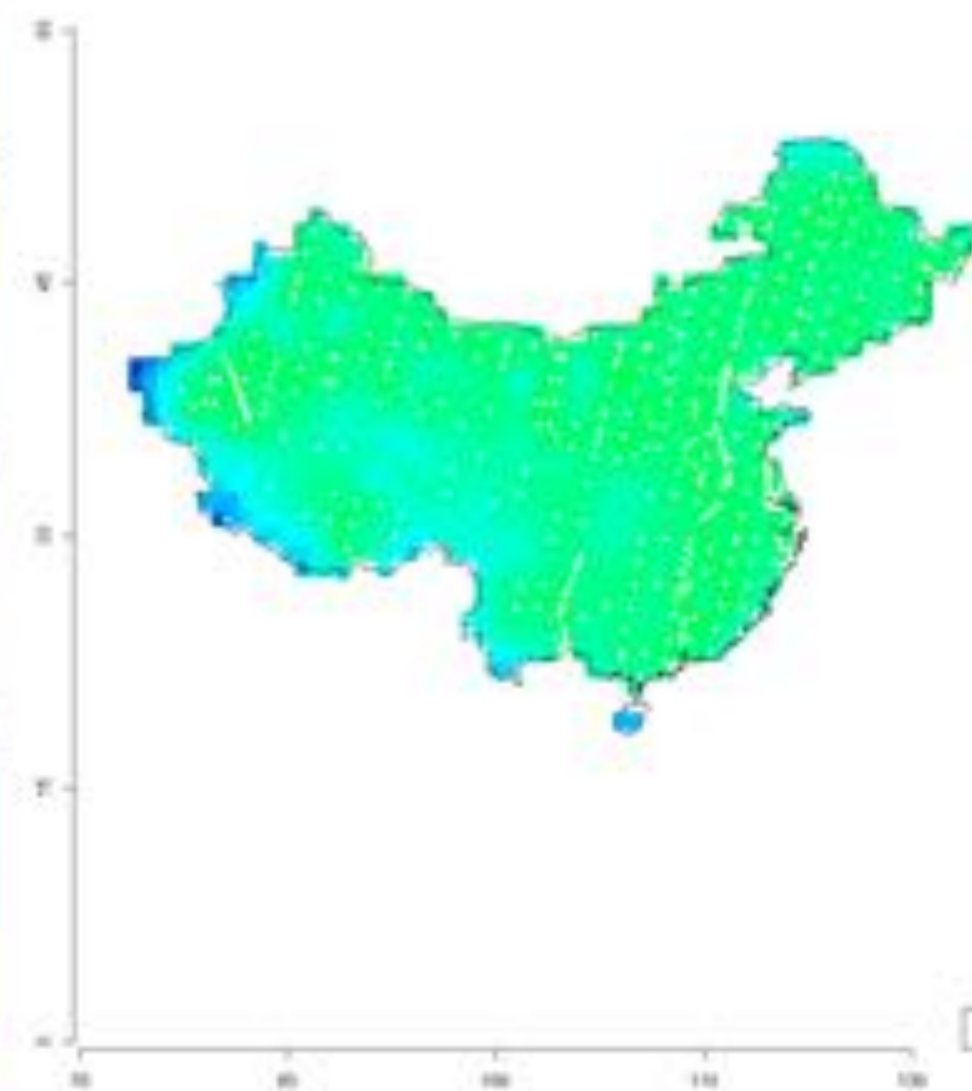
Vw_ao2_100_2014



Pre0_ao3_00_2000

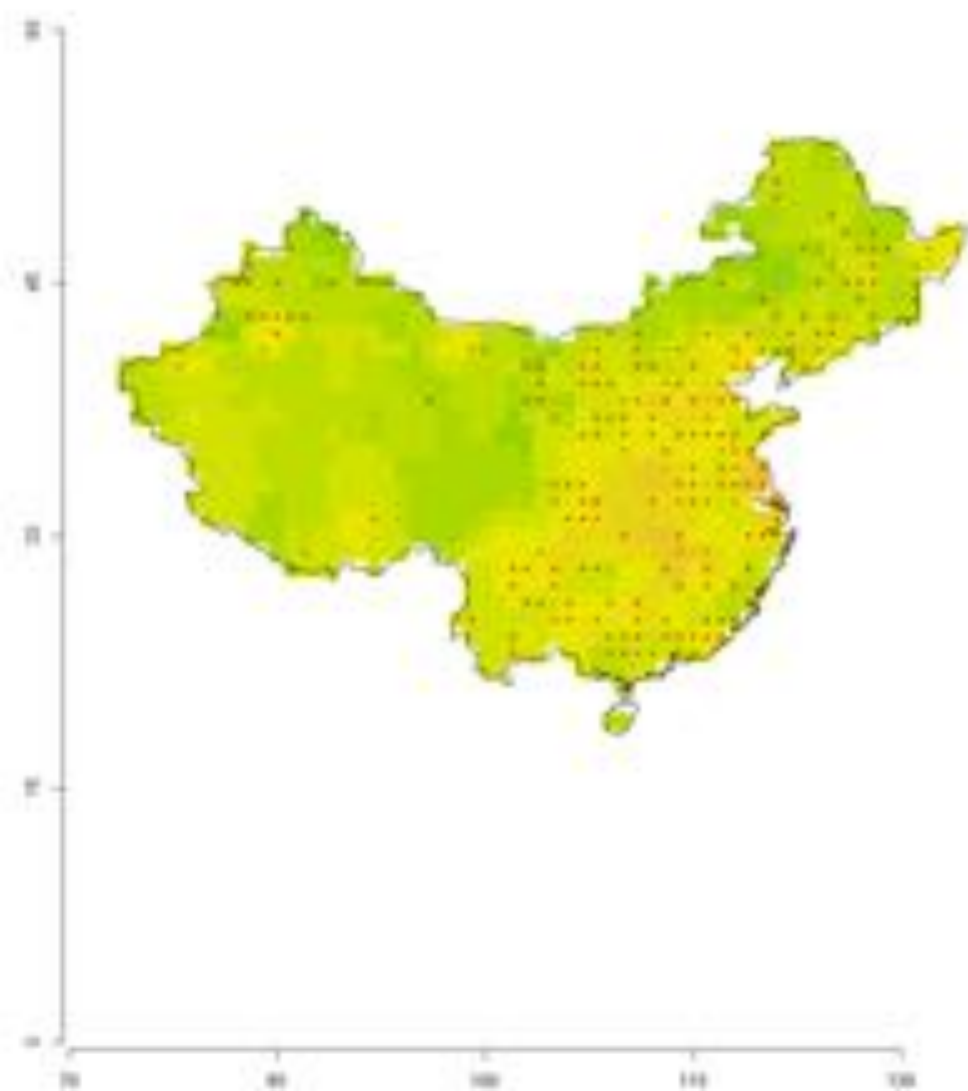


Vw_ao3_00_2000

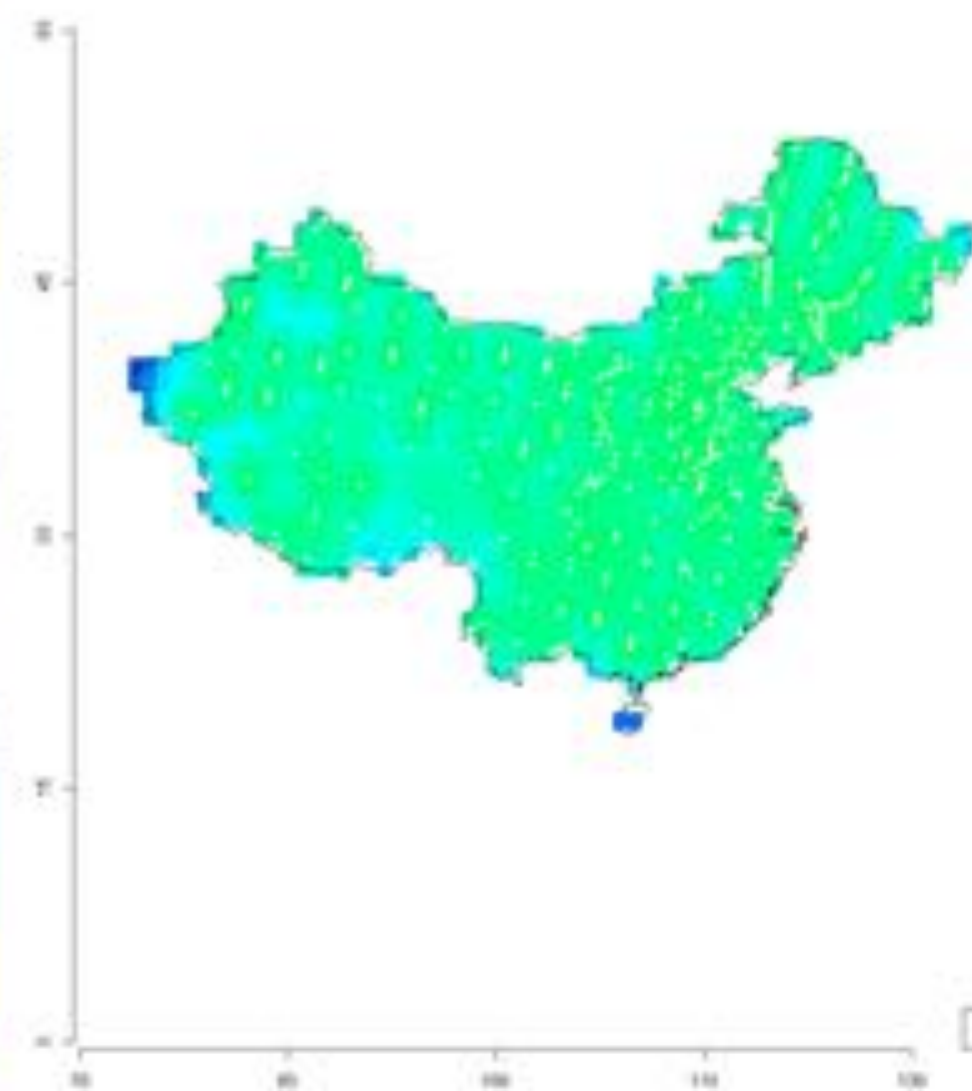


0-110

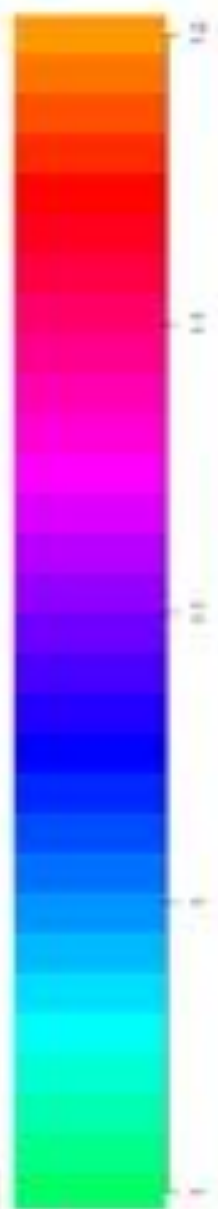
Pre0_ao3_100_2010



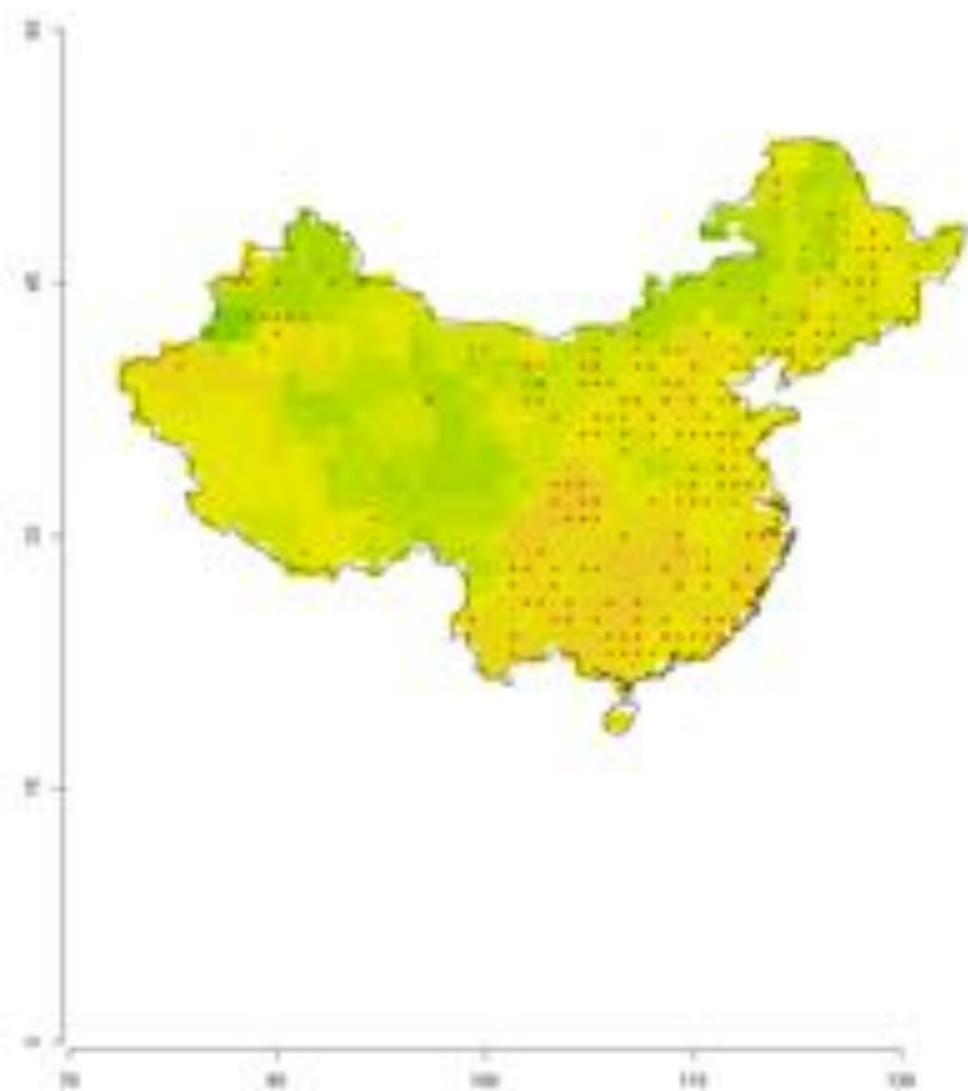
Vw_ao3_100_2010



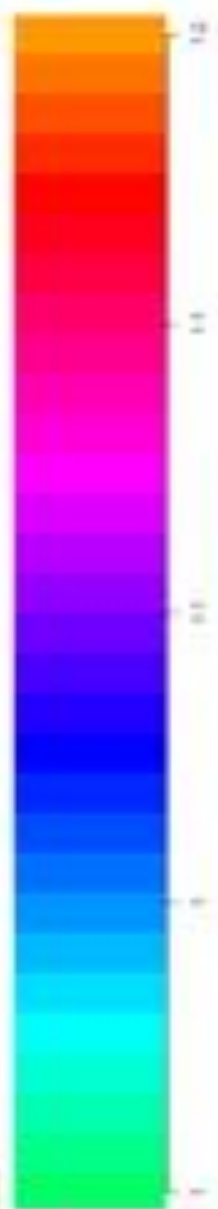
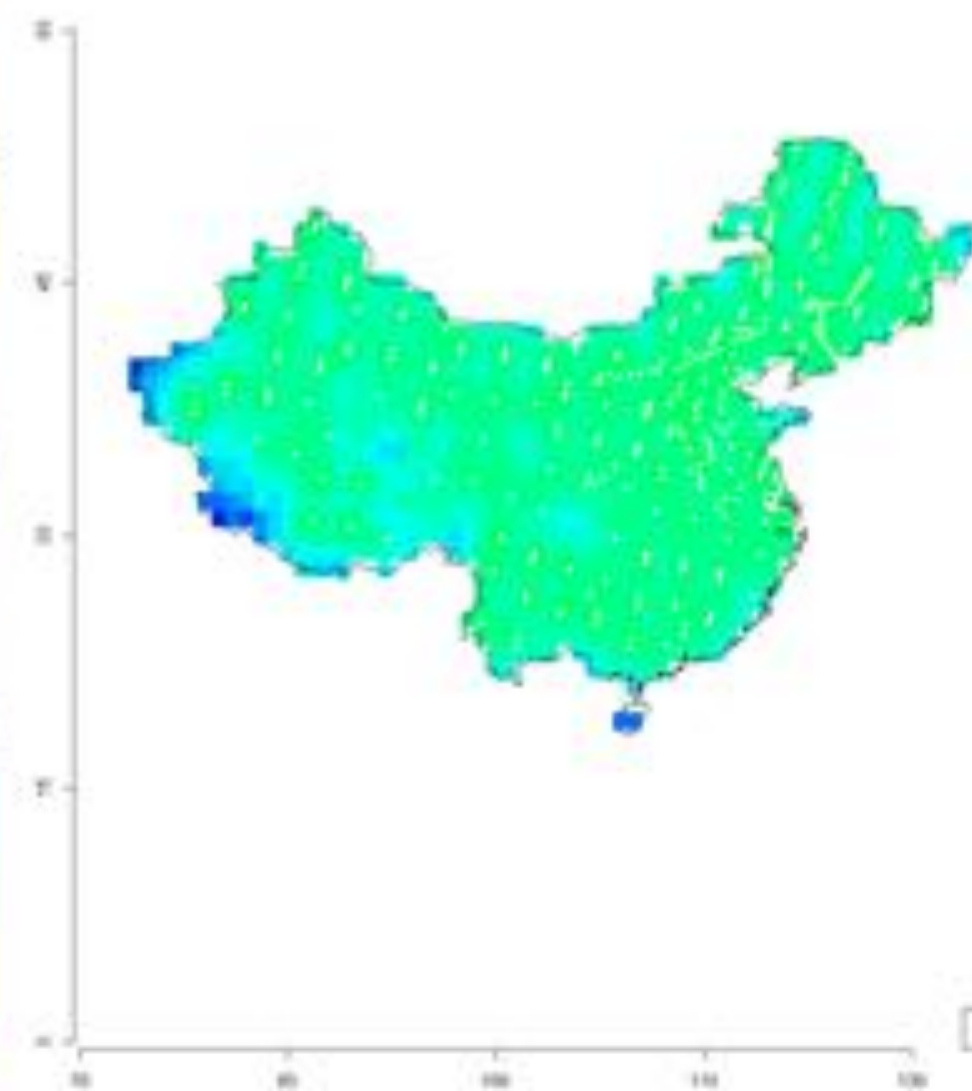
0.0001



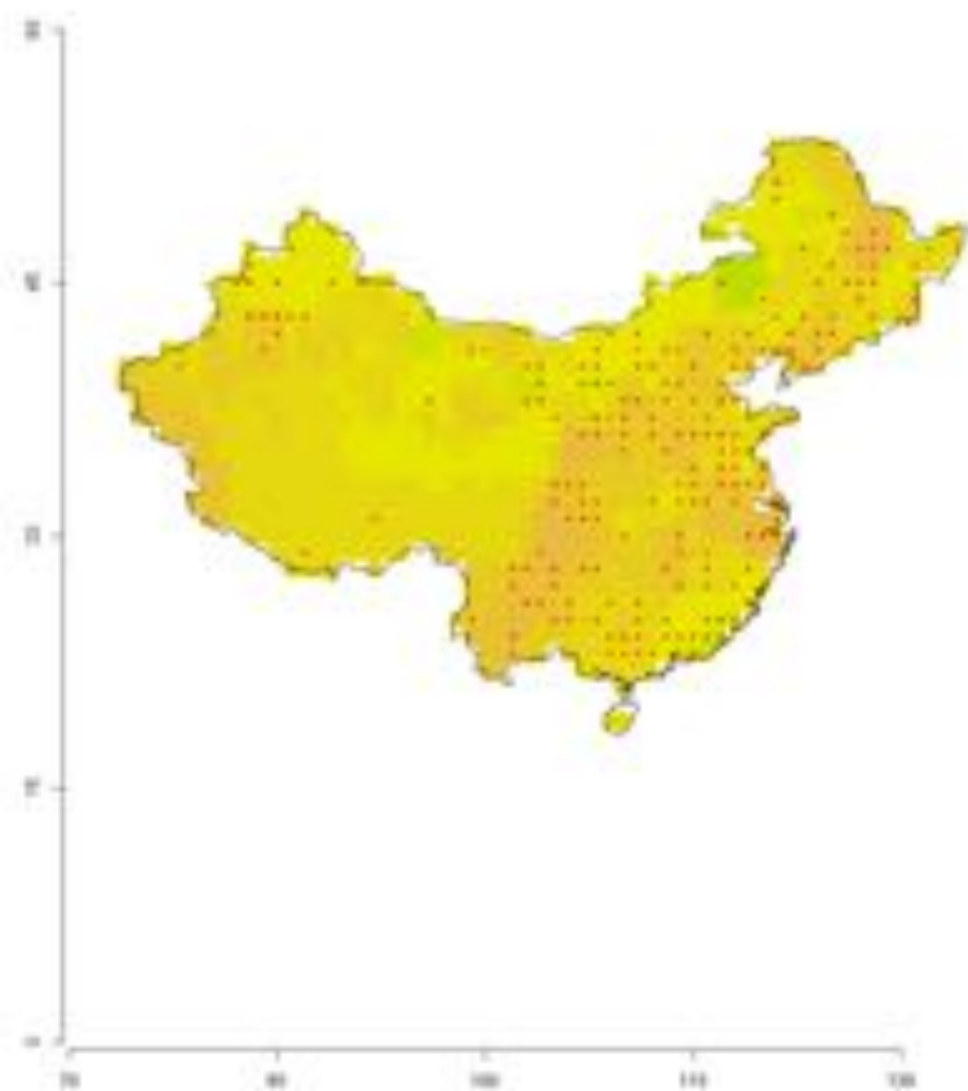
Pre0_ao3_2011



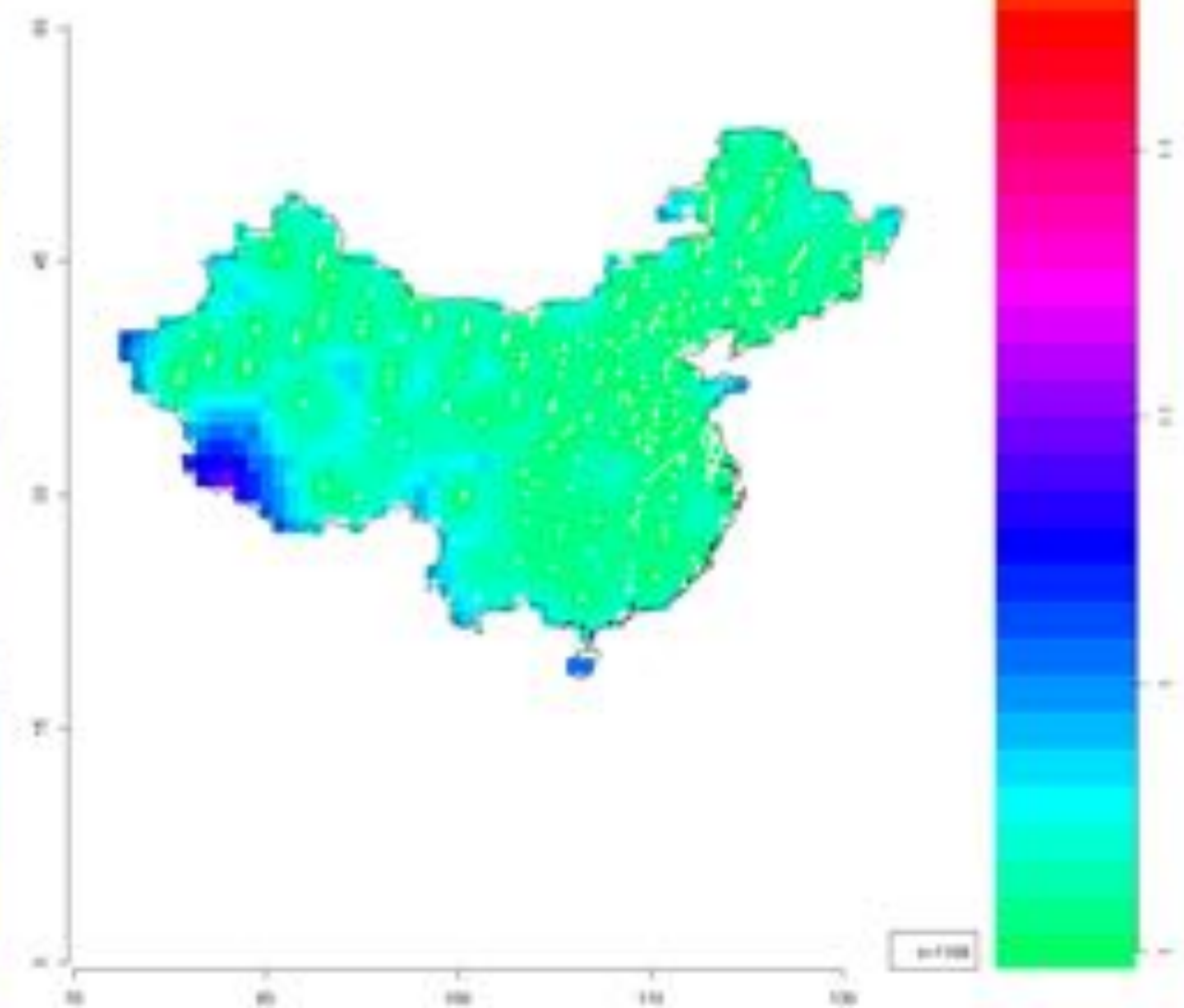
Nw_ao3_2011



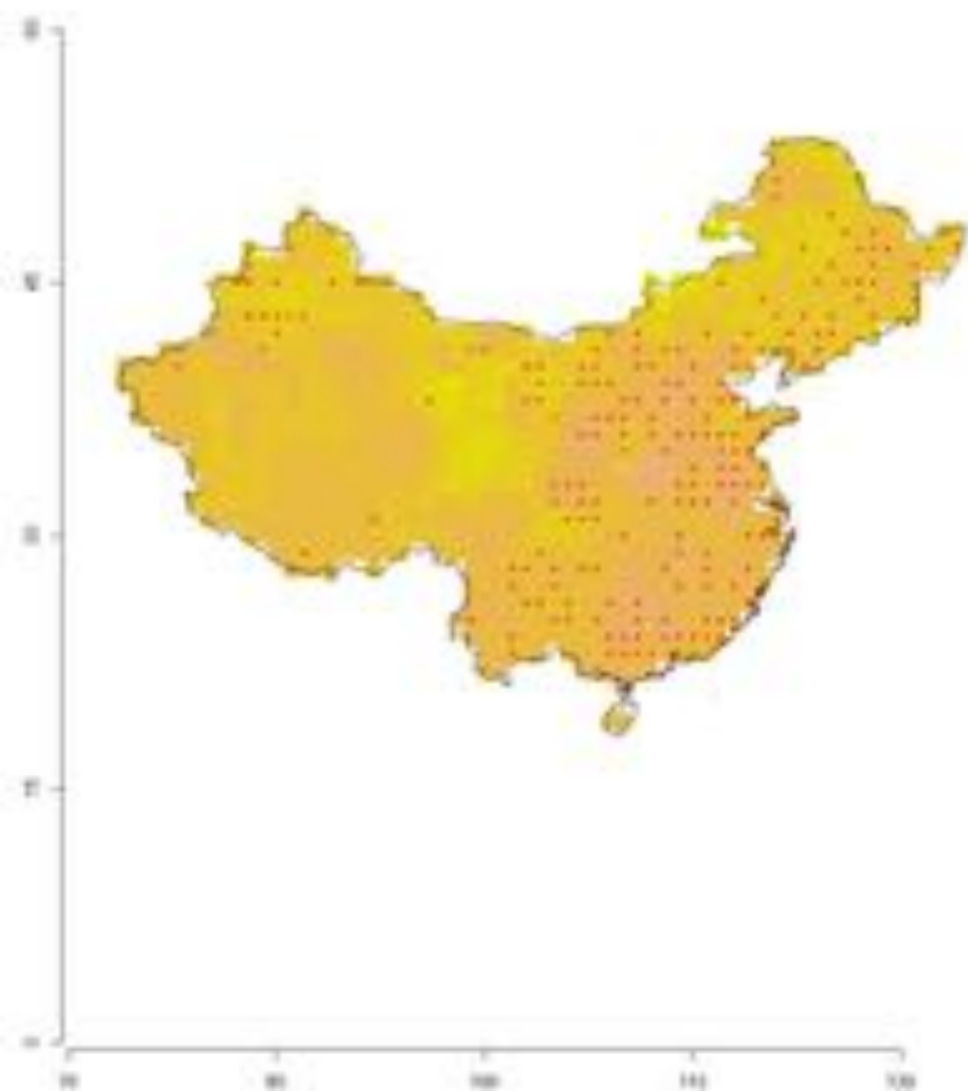
Pre0_000_000_2012



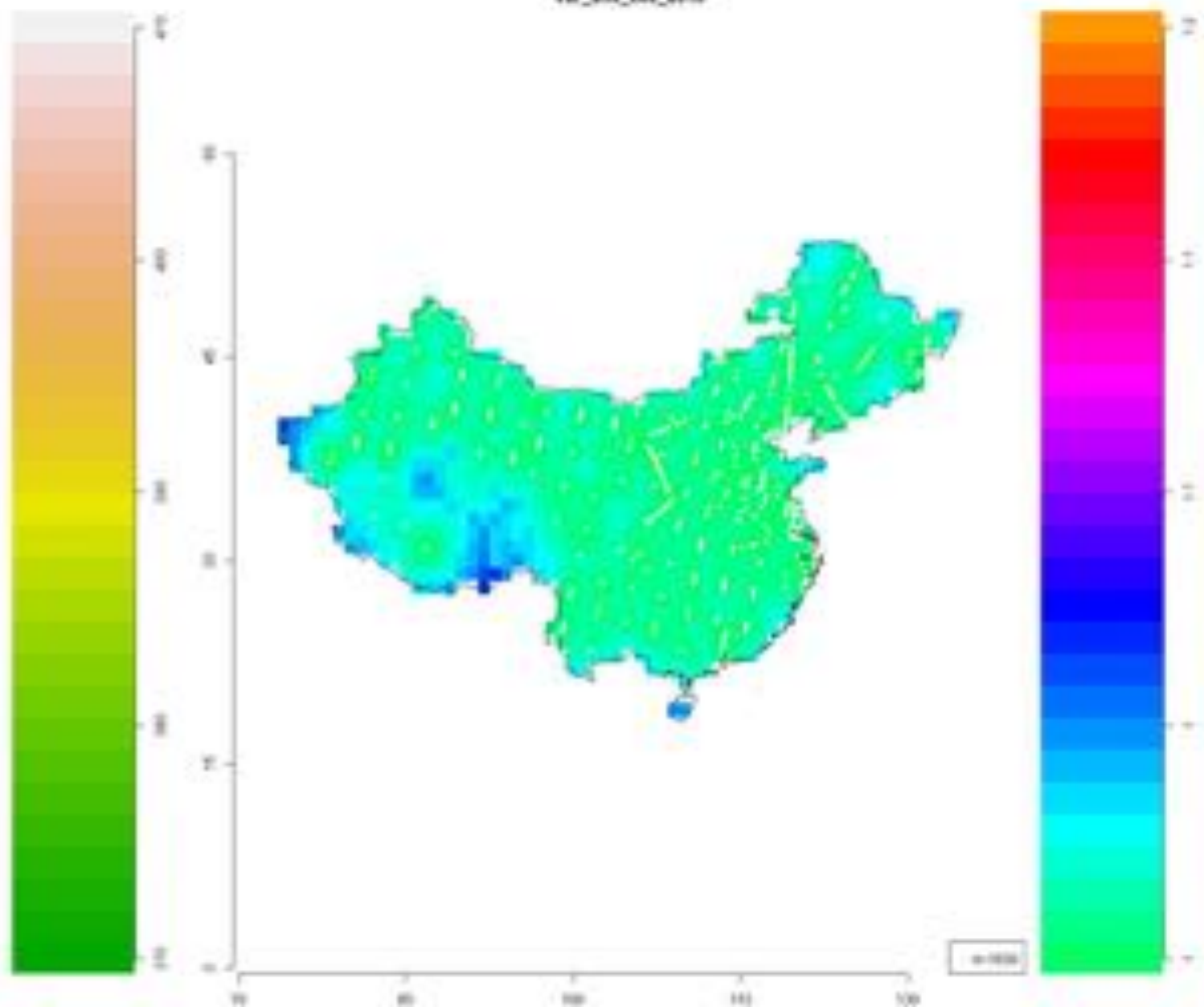
Nw_000_000_2012



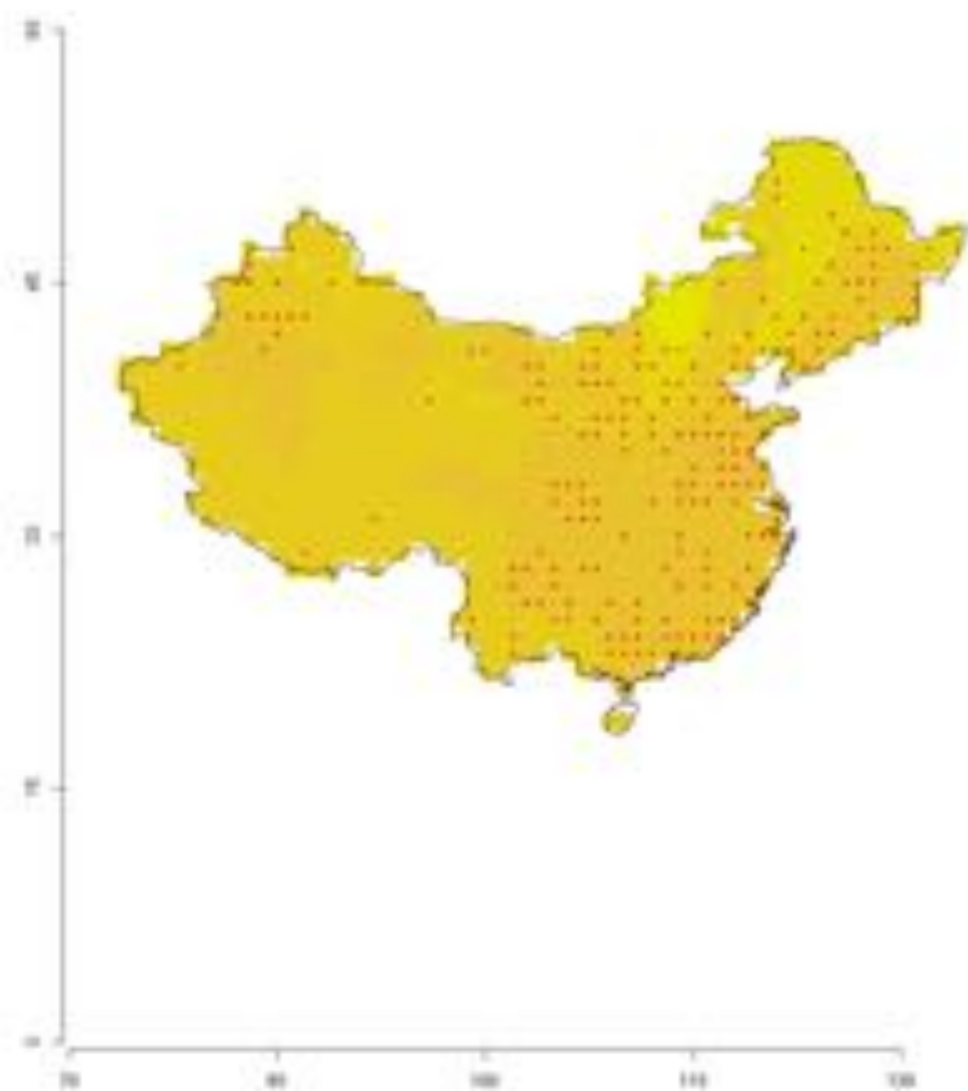
Pind_642_c00_2013



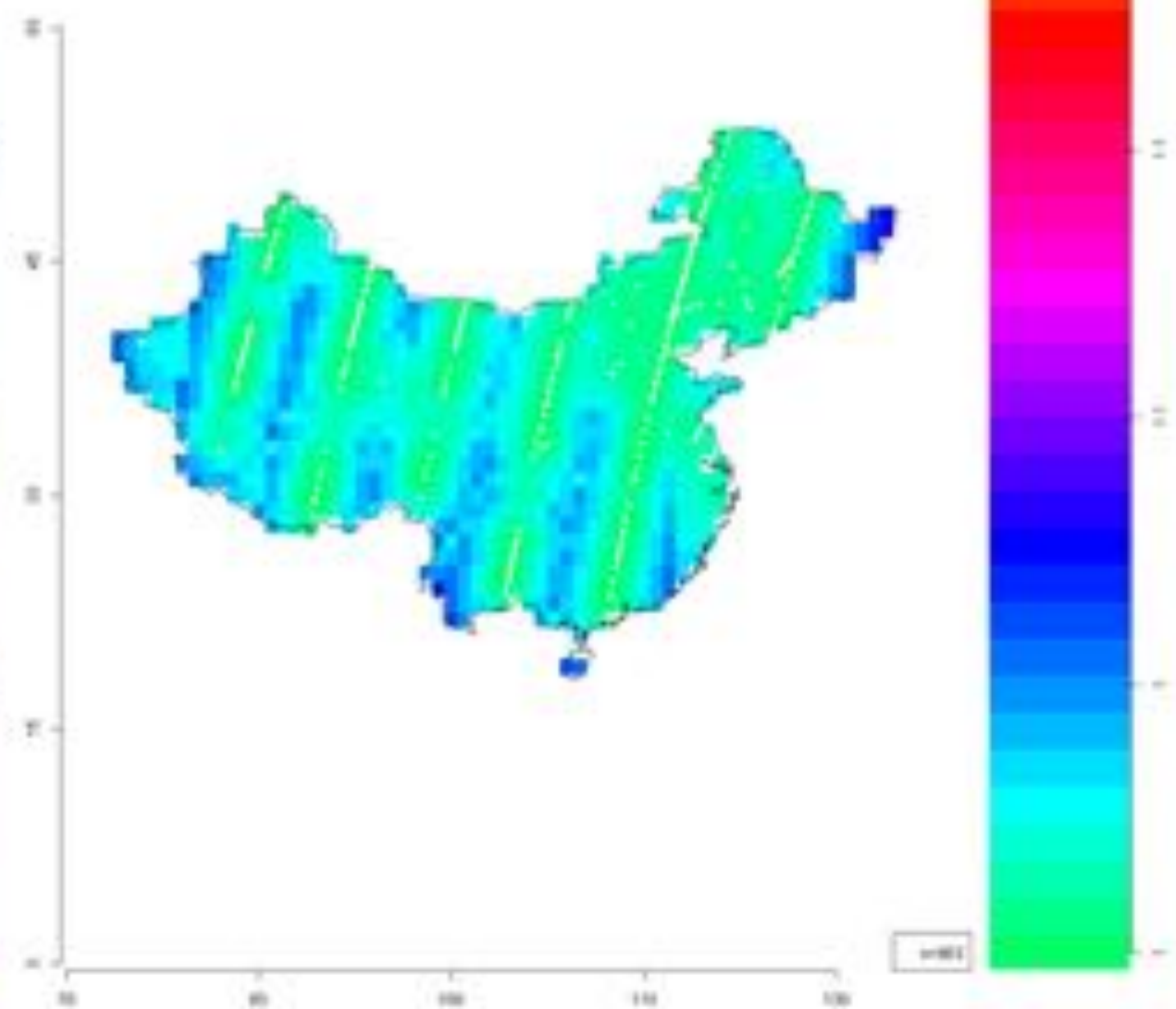
Vw_642_c00_2013



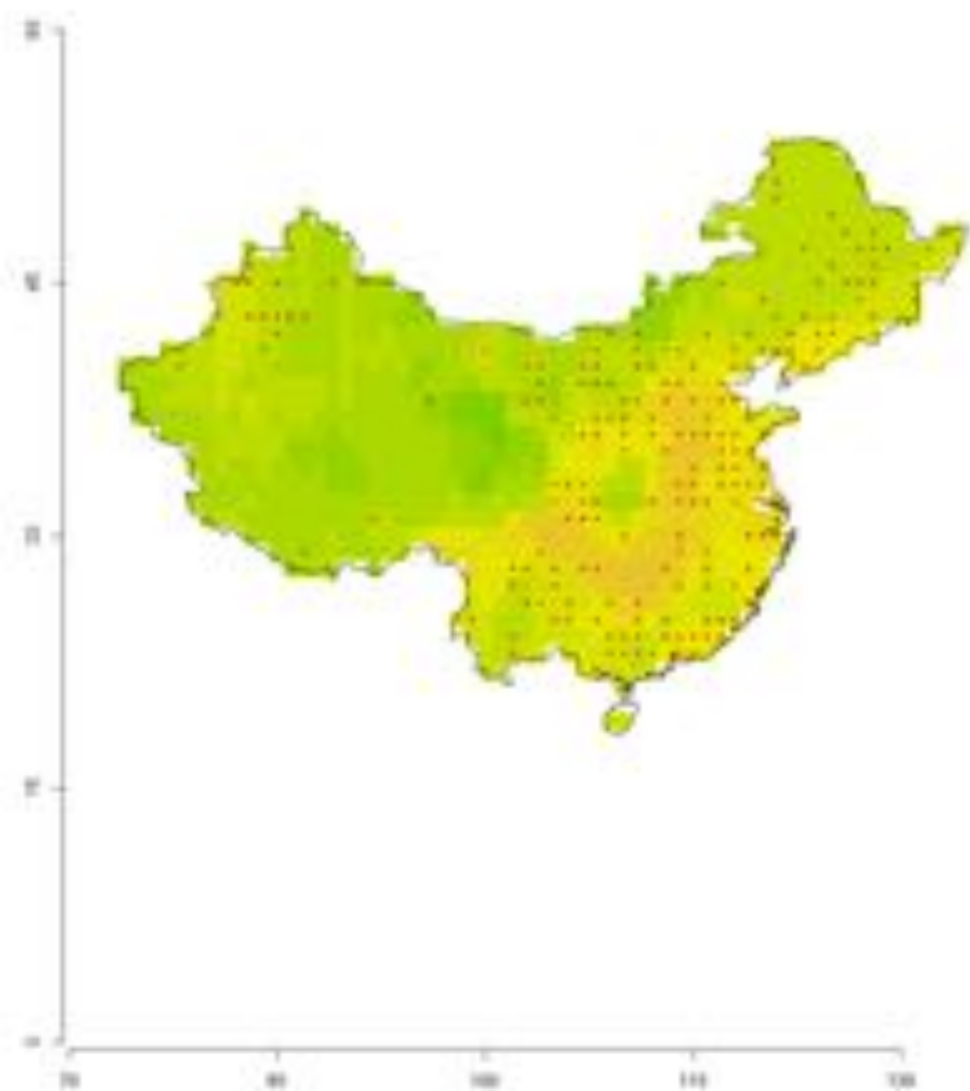
Pre0_ao3_2014



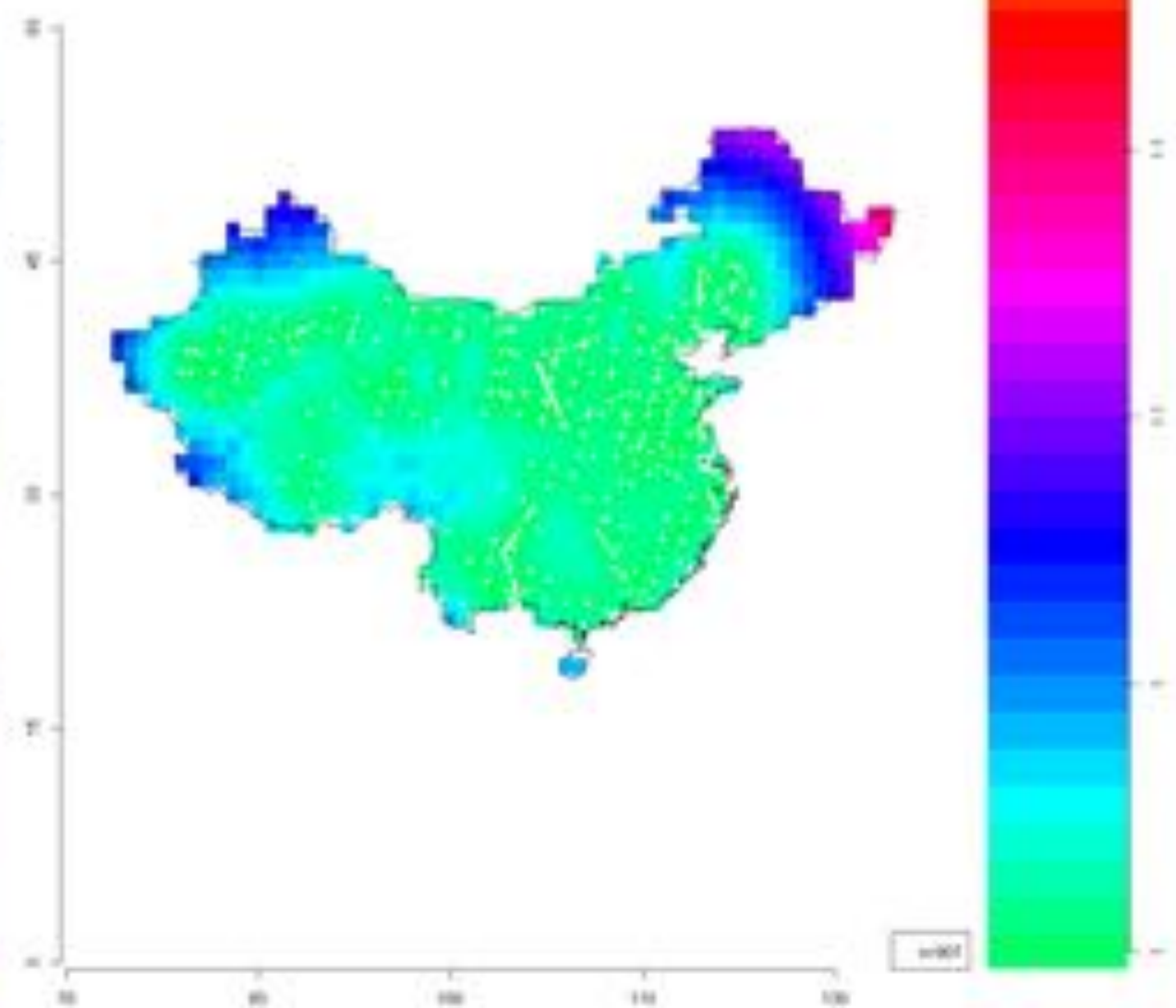
Vw_ao3_2014



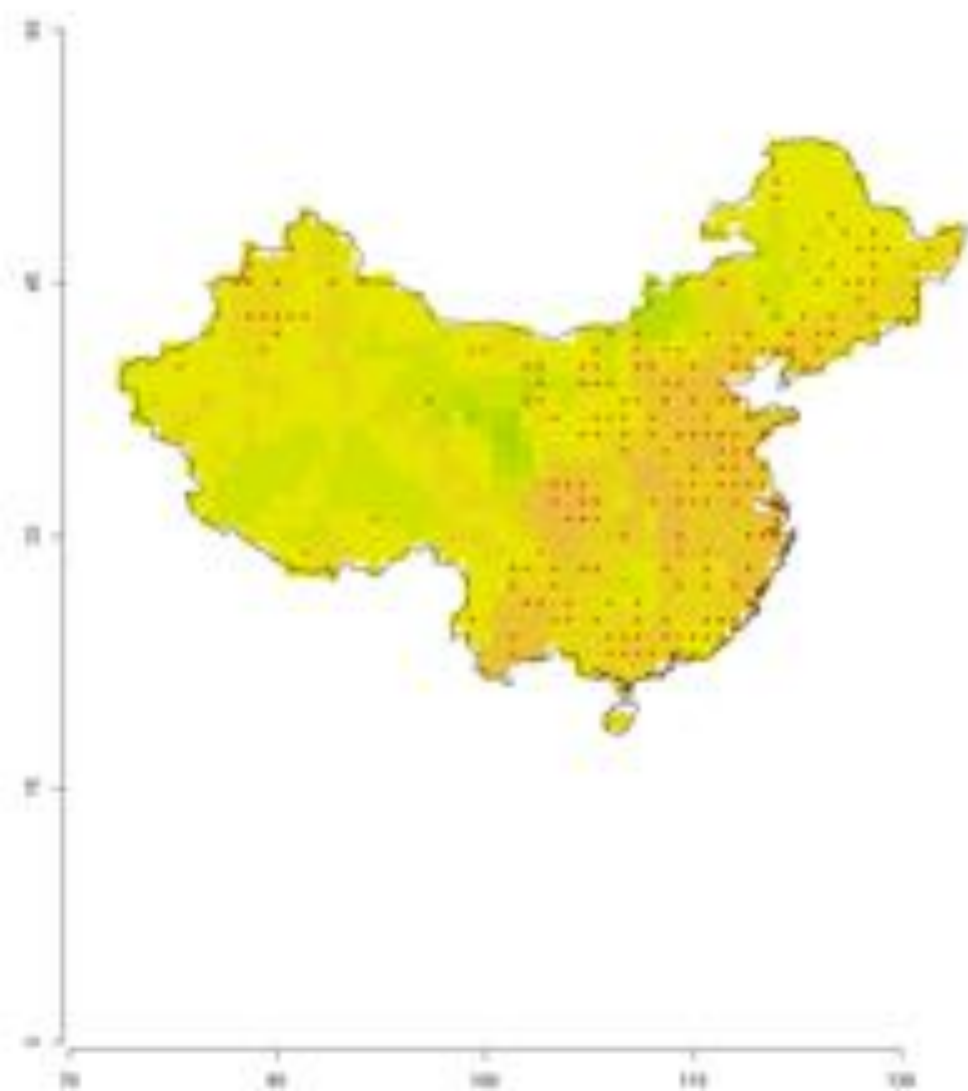
Pred_sml_s30_2008



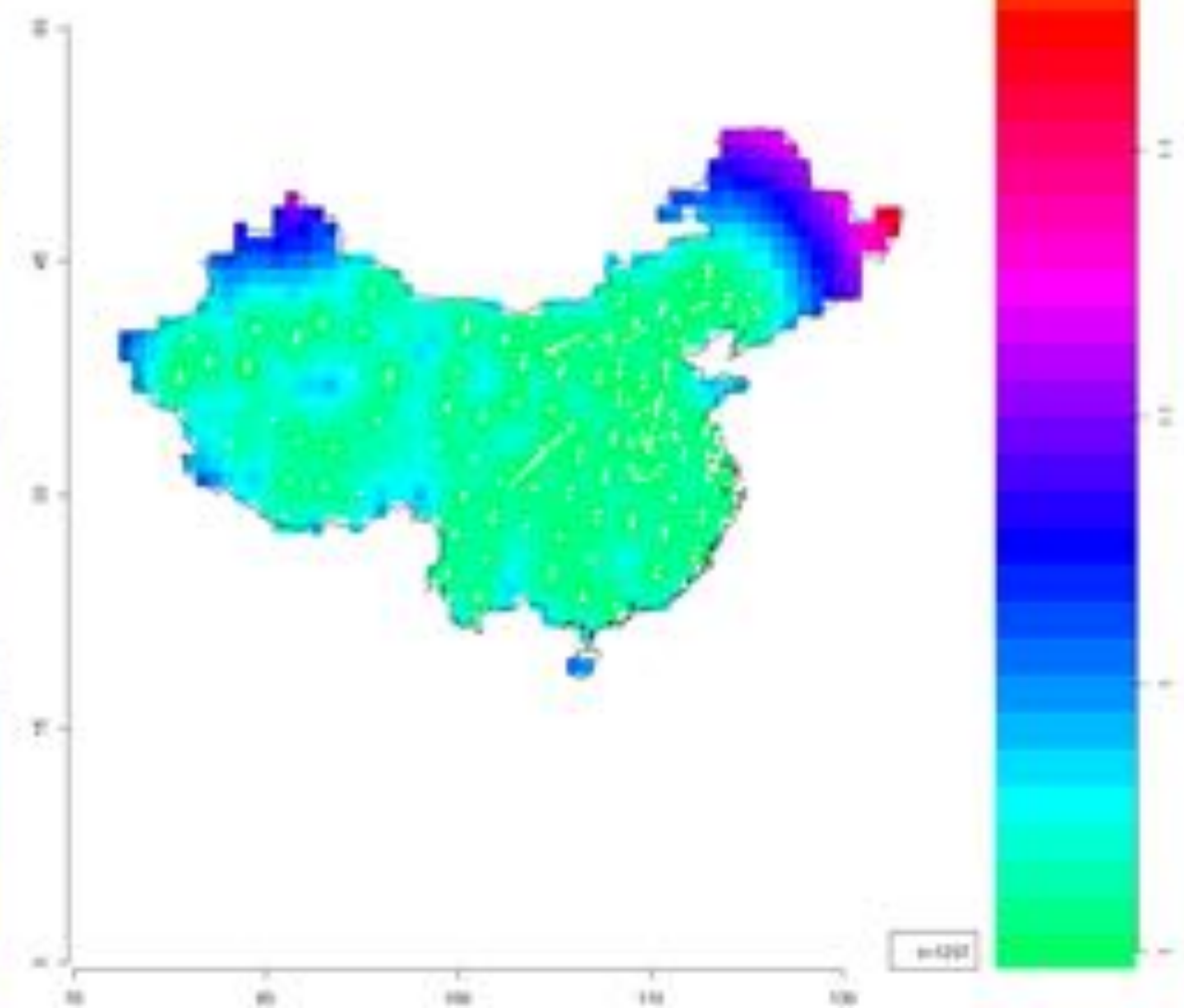
Vw_sml_s30_2008



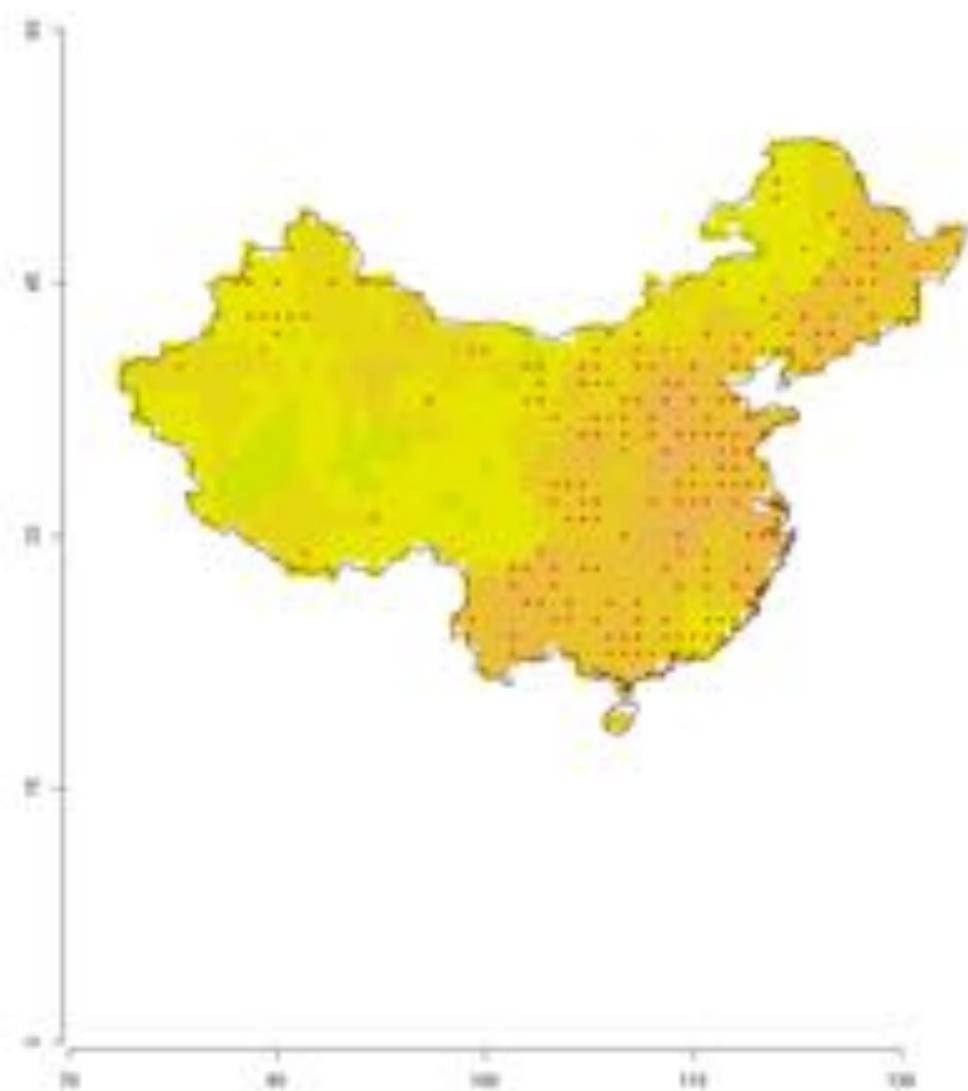
Prod_sml_s30_2010



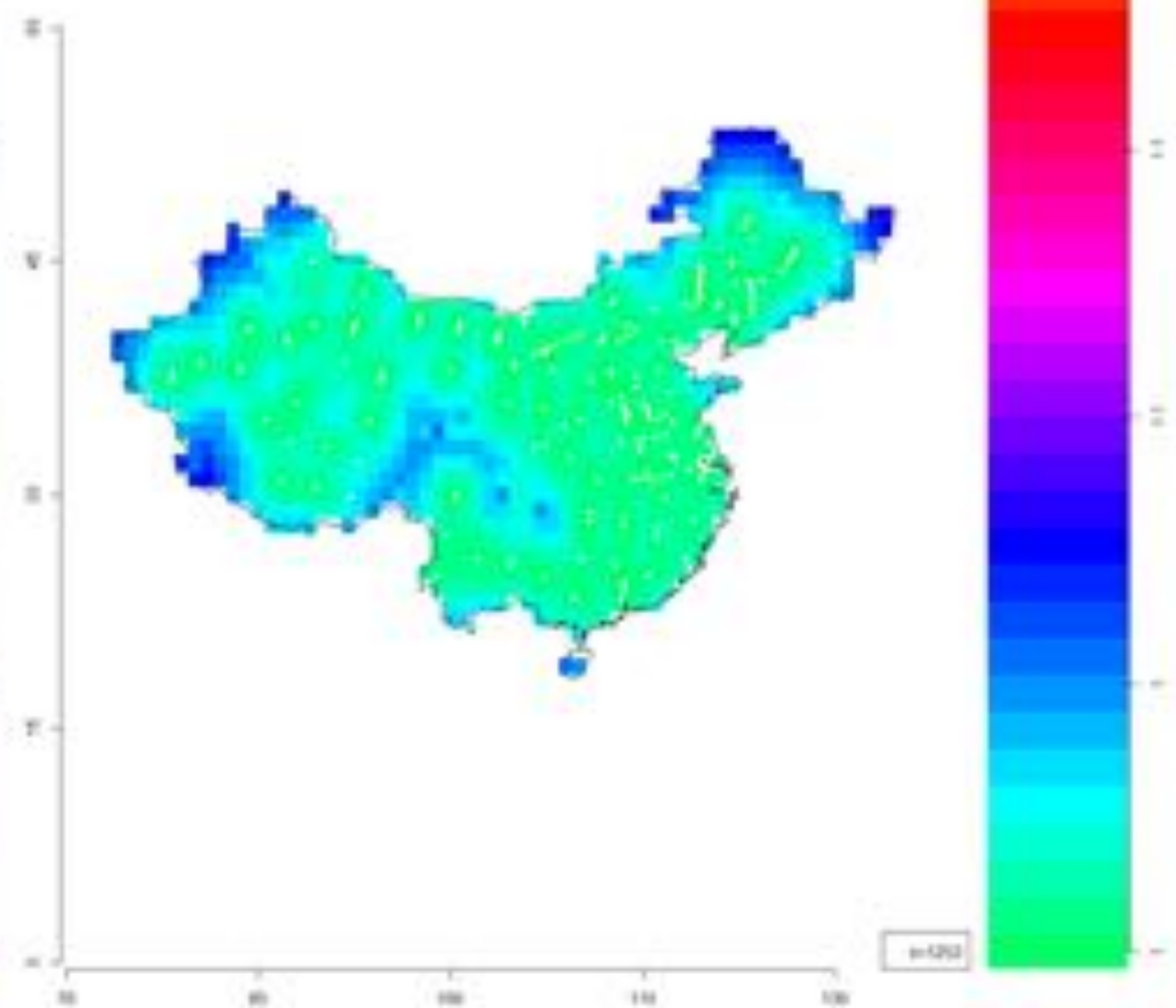
Nw_sml_s30_2010

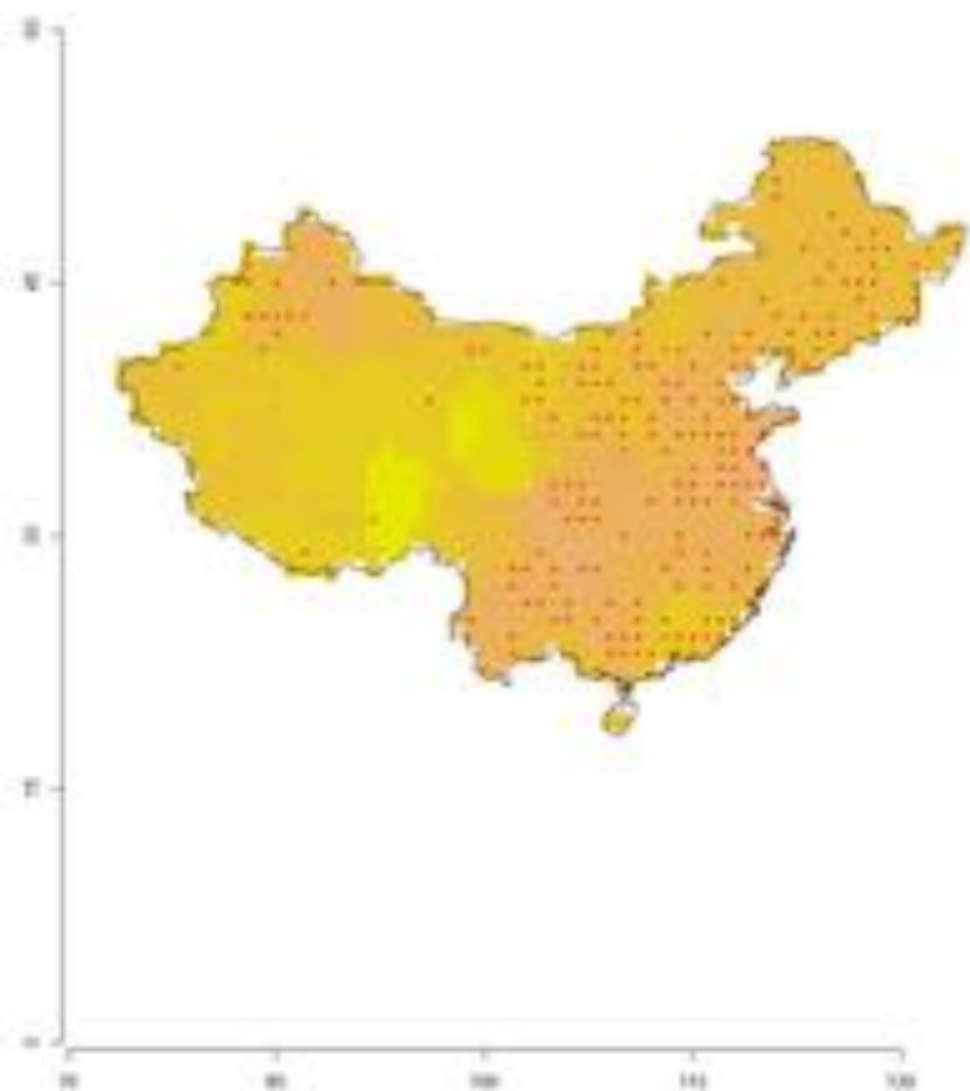


Pred_sml_s30_2011

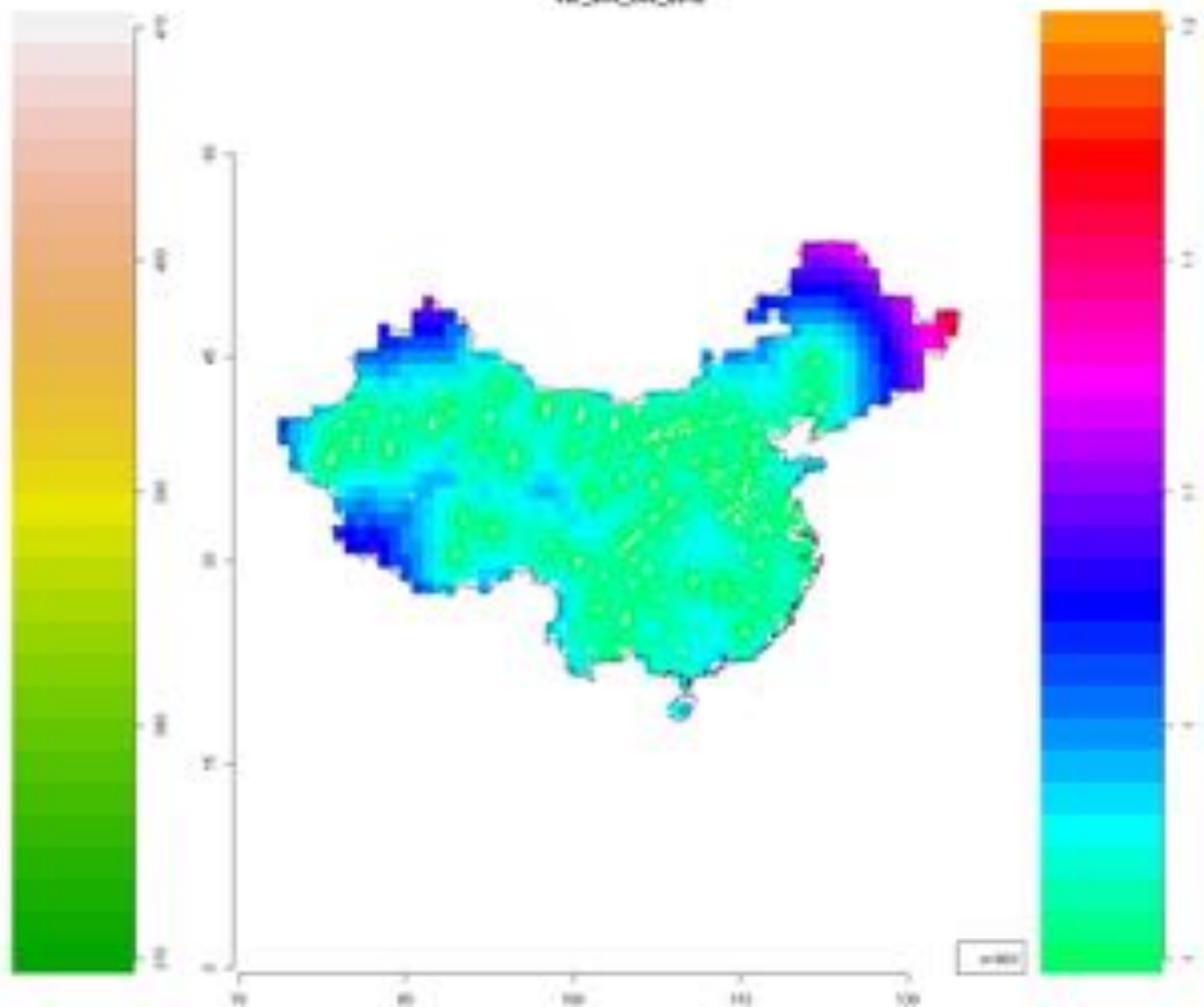


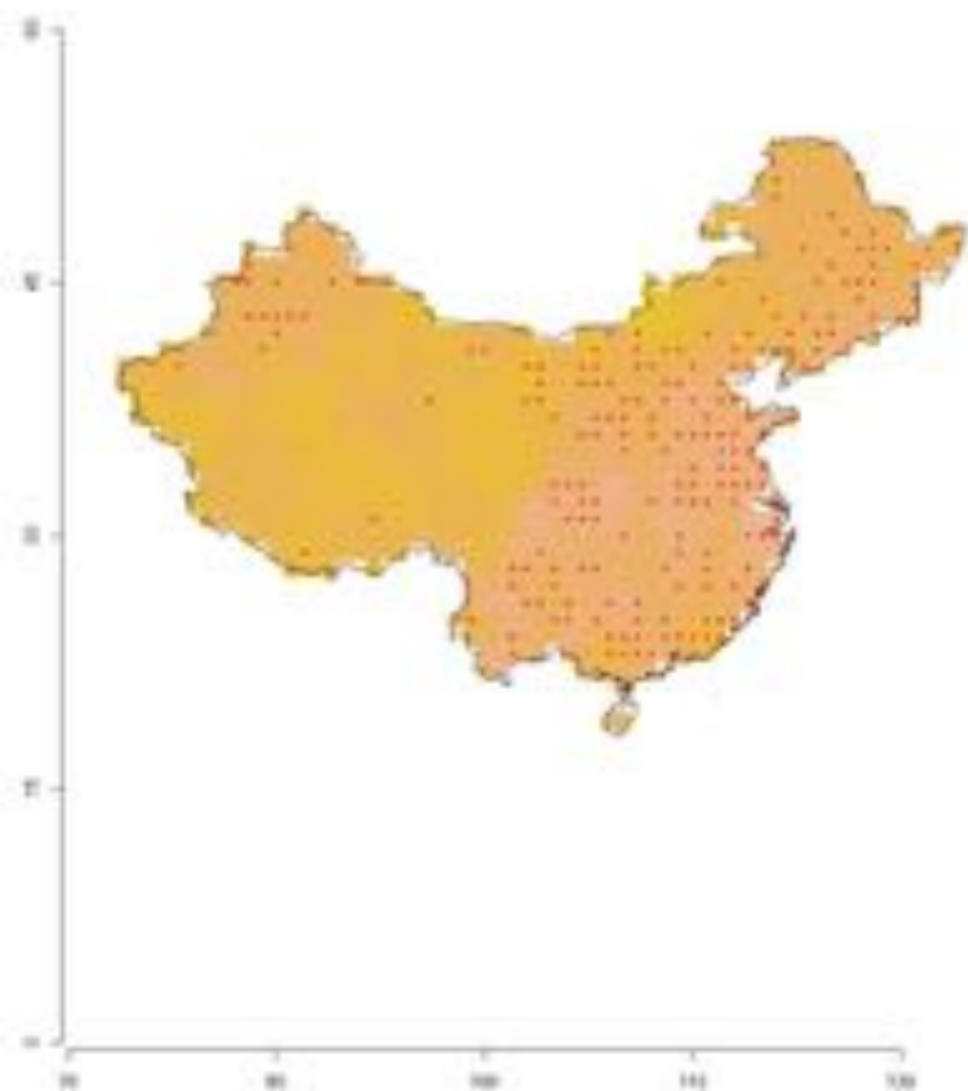
Vw_sml_s30_2011



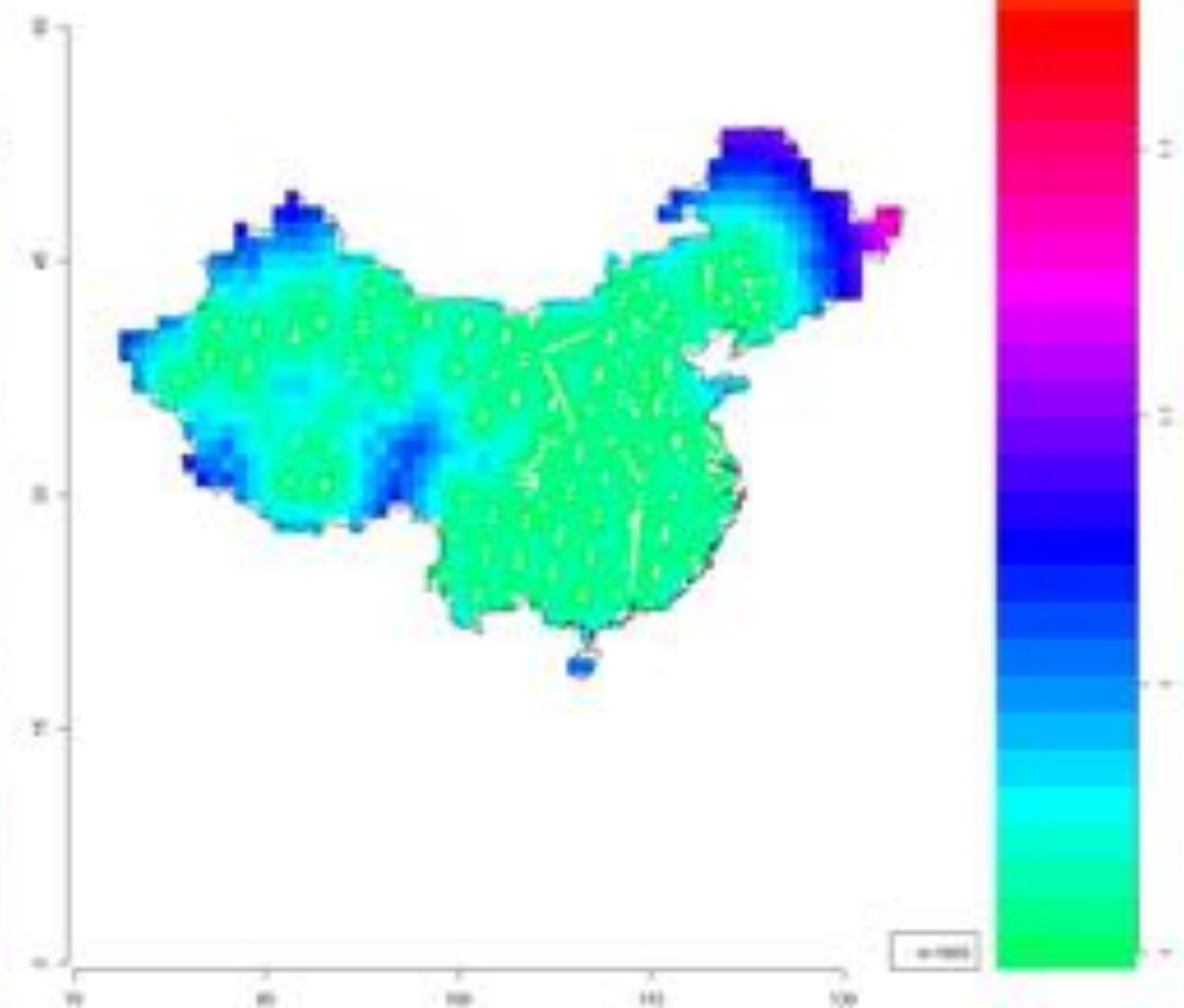
PM_{2.5}_AHE_C00_2012

Vw_AHE_C00_2012

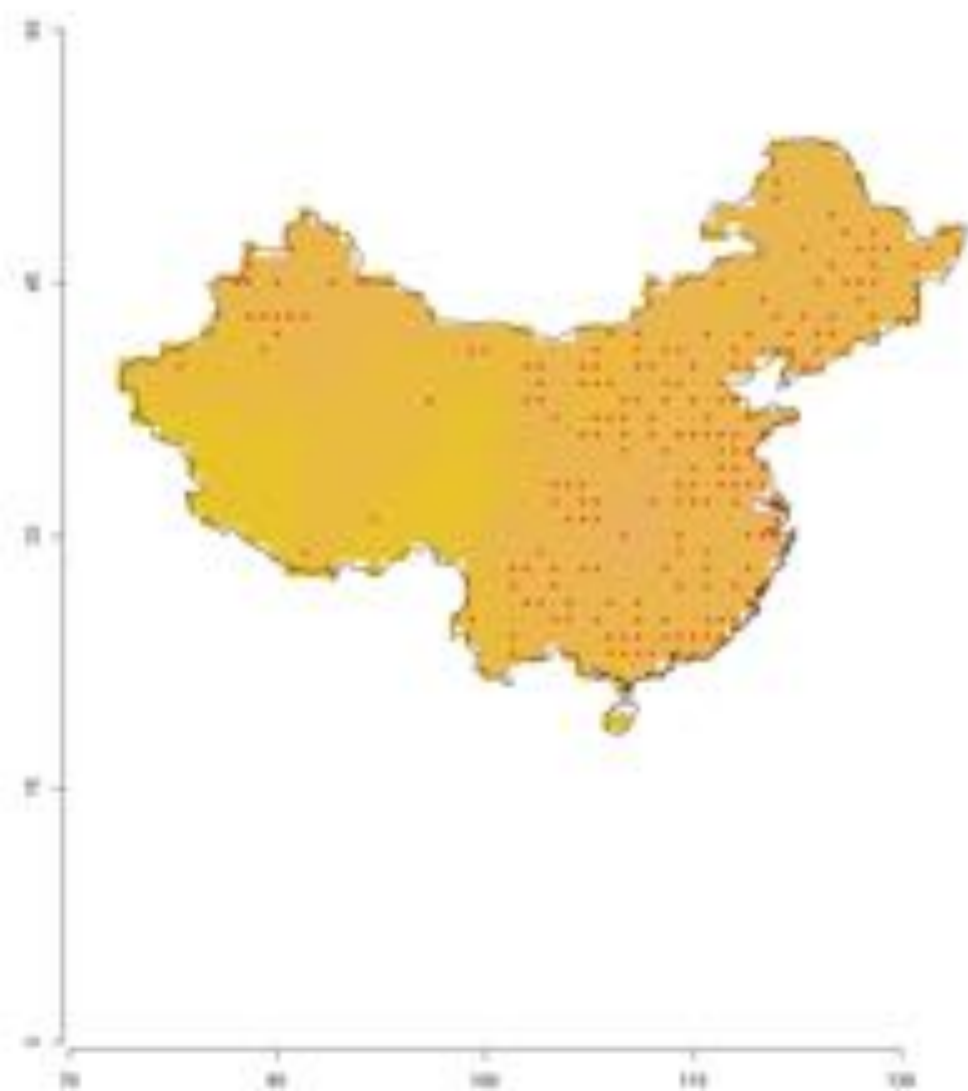


PM_{2.5}_AHE_C30_2013

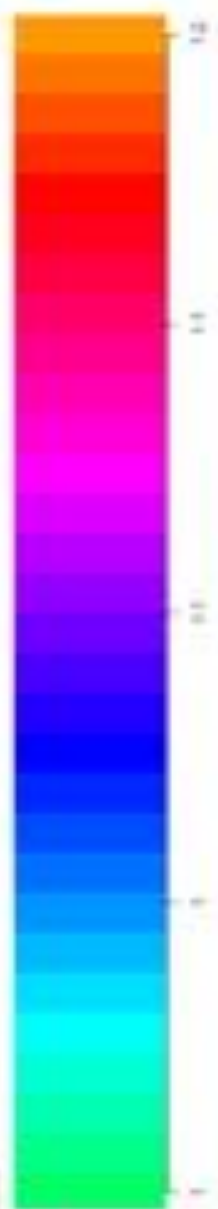
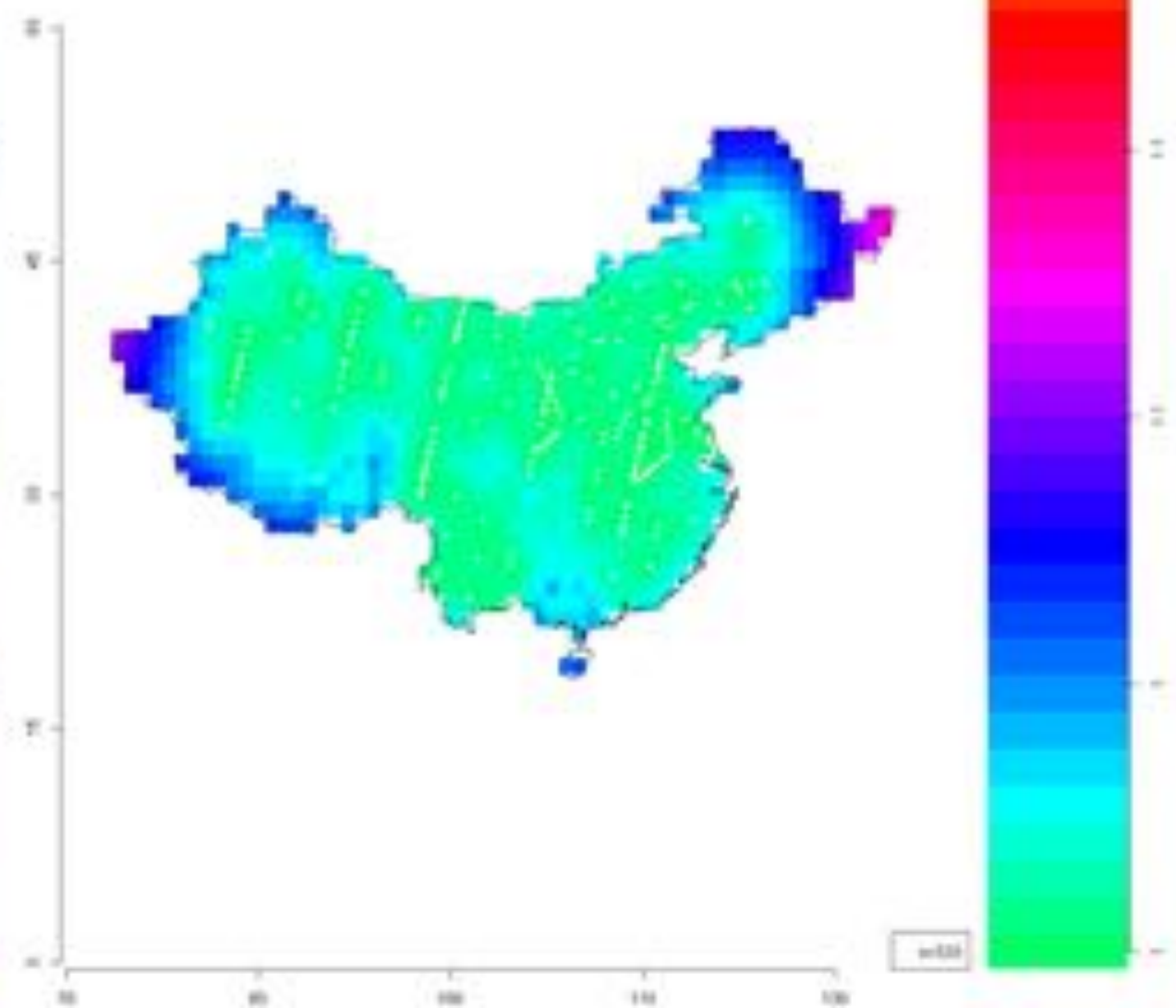
Vw_AHE_C30_2013



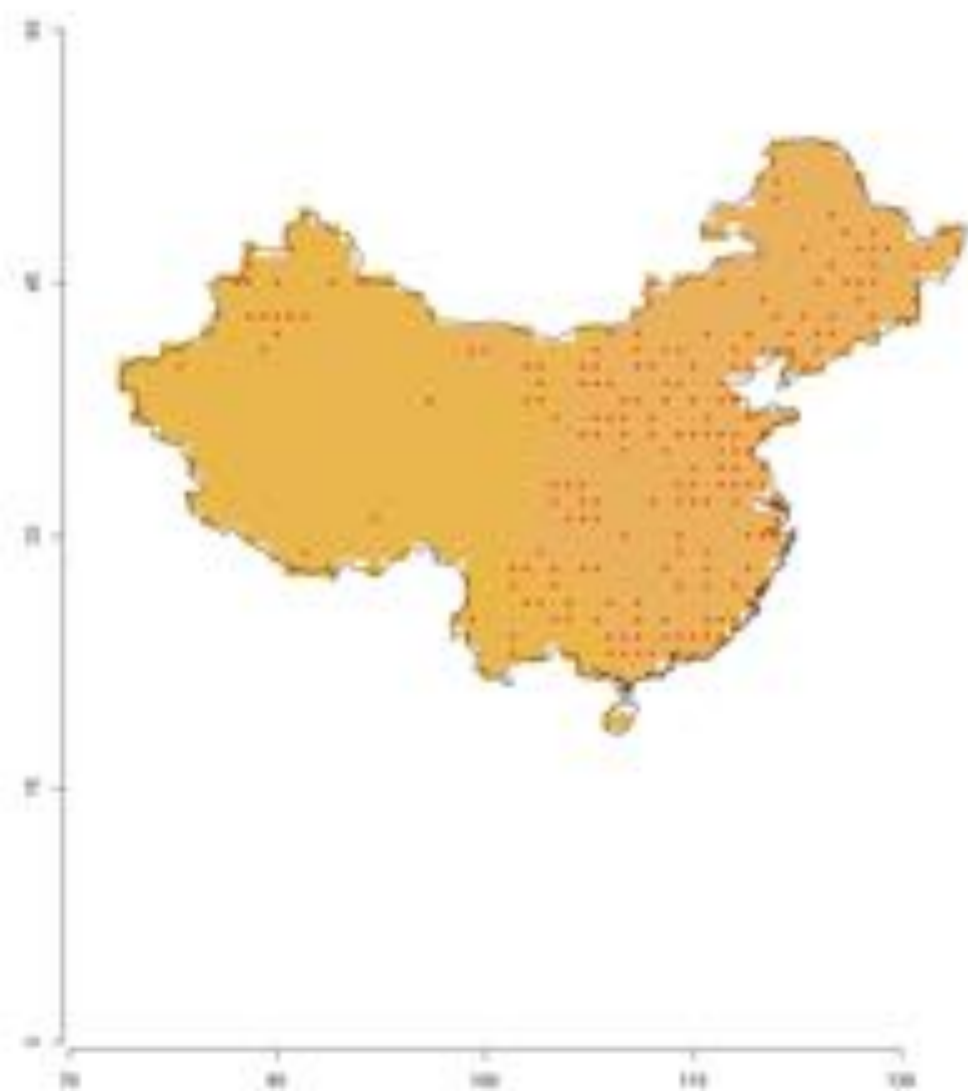
Pred_sml_c30_2014



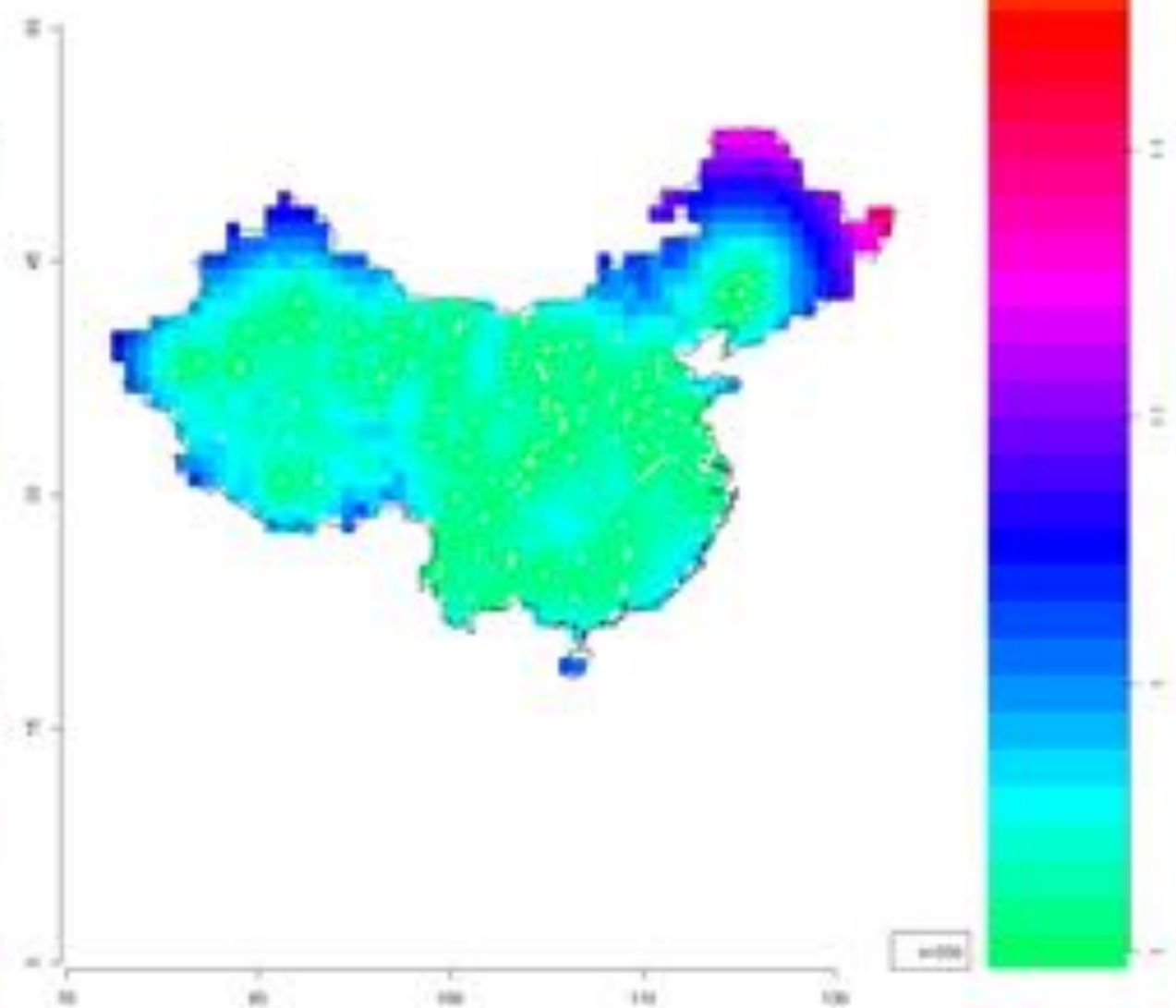
Vw_sml_c30_2014



Pred_sml_s30_2010



Vw_sml_s30_2010



Conclusions

- XCO₂ shows an increasing trend since 2009.
- XCO₂ are highest in spring (April or May) and lowest in summer (July or August).
- Influence range of XCO₂ is approximately 1200 km.
- Areas of higher XCO₂ in China are roughly consistent with areas of higher population densities.

參考文獻

- **GOSAT/IBUKI Data Users Handbook, 2011, Japan Aerospace Exploration Agency, National Institute for Environment Studies, Ministry of the Environment.**
- **Kimberly, B. 2013. Nighttime Lights Compositing Using the VIIRS Day-Night Band: Preliminary Results**
- **Zhu Liu, 2015, Carbon Emissions Report 2015, Associate, Energy Technology Innovation Policy research group, China.**

